Modes of fitness increase during the aggregative multicellular development program of *Myxococcus xanthus*

A thesis submitted to attain the degree of

DOCTOR OF SCIENCES
(Dr. sc. ETH Zürich)

presented by

Sarah M. Cossey

MSc, ETH Zürich

born on 01.08.1993

accepted on the recommendation of

Prof. Dr. Gregory J. Velicer, ETH Zürich (supervisor)

Prof. Dr. Rolf Kümmerli, University of Zürich (co-examiner)

Dr. Yuen-Tsu Nicco Yu, ETH Zürich (co-examiner)

2024

Table of contents

Abstract

In nature, environmental conditions are in constant flux. Organisms must dynamically respond and adapt to the presence of other biological entities as well as abiotic factors in order to survive and reproduce. Both cooperative and competitive interactions between organisms are common. Cooperation involves the expression of a trait that enhances the fitness of other individuals, and usually is costly to express. Conflict arises when the evolutionary interests of interacting individuals do not align, such as when some individuals benefit from a cooperative action without contributing to its expression. The fitness advantage of such social defectors can allow them to increase in frequency, and if their frequency increase is not controlled they can be disruptive to cooperation. Conflict can therefore have devastating effects on cooperative systems and there is much interest in understanding how cooperation is maintained despite the threat of its exploitation.

Abiotic pressures such as fluctuations in resource availability or temperature can also affect the evolutionary trajectory of a population. Many organisms, including microbes, can respond to fluctuating environments by evolving bet-hedging strategies. These can either be conservative, where an organism expresses a 'safe' trait value, or diversifying, where multiple phenotypes are produced as a risk-spreading strategy. Both forms of bet-hedging ensure survival in an unpredictable environment, which can make them appear maladaptive when observed in isolation or over short time scales and without environmental fluctuations.

Myxococcus xanthus is a model system for studying the genetics of bacterial development. Its aggregative multicellular lifestyle and cooperative behaviors also make it an attractive system to study the evolution of social behavior. One of the most prominent features of the *M. xanthus* lifecycle is the cooperative formation of multicellular fruiting-body structures, a development program initiated in response to starvation. Conflict between interacting individuals of different genotypes, evidenced by (sometimes extreme) fitness asymmetries

during chimeric fruiting-body formation in *M. xanthus*, is not uncommon. The mechanisms responsible for increased fitness during multicellular development, however, are not well understood. The aim of this thesis is to further explore how fitness can be increased in response to biotic and abiotic selective pressures during *M. xanthus* social behaviors, particularly during cooperative fruiting-body formation.

In the first chapter I investigate how biotic interactions, namely the presence of competitors, influences the ways that fitness increases can be gained by evolving a nearly-saturated mutant library under conditions that select for genotypes with high spore production in chimera, *i.e.* in developmental groups composed of multiple genotypes. I then characterize the range of different strategies that *M. xanthus* can use to gain a relative fitness advantage during chimeric development. The results show that evolved populations can be composed of multiple distinct competitors and that several qualitatively distinct strategies result in fitness gains during chimeric development.

Conflict during social interactions can be dampened by preferentially interacting with highly related individuals. One mechanism that promotes high relatedness is kin discrimination. In the second chapter, I investigate the role of TraA/B-mediated outer membrane exchange (OME) as a potential driver of colony merger incompatibilities (CMIs) between swarming groups of *M. xanthus*. CMIs are a form of microbial kin discrimination and are known to reduce the level of chimeric fruiting-body formation at the interface of two swarms in *M. xanthus*. I test whether disrupting TraA functionality influences CMI phenotypes or strong antagonisms during chimeric development between natural strains. The results show that kin discriminatory behaviors in *M. xanthus* are complex and likely multifactorial, which is in line with what is known about kin discrimination in other bacterial species.

Two differentiated cell types produced during *M. xanthus* development, stress-resistant spores and viable rod cells (peripheral rods), have the potential to survive and resume growth after nutrients become replete. In the final chapter of this thesis, I investigate

how selection in environments that vary in the length of starvation can influence cell-type partitioning during multicellular development. Specifically, I test for a potential contribution of peripheral rod cells to group-level fitness during starvation-induced development. I show that the relative benefit of producing different developmental cell types (spores versus viable rods) changes in response to how quickly nutrients are replenished after starvation initiation. Therefore, another path to increased fitness during multicellular development could involve altered investment in developmental cell types.

Zusammenfassung

In der Natur sind die Umweltbedingungen in ständigem Wandel. Um zu überleben und sich fortzupflanzen, müssen Organismen dynamisch auf die Anwesenheit anderer biologischer Einheiten sowie auf abiotische Faktoren reagieren und sich anpassen. Sowohl kooperative als auch kompetitive Interaktionen zwischen Organismen sind üblich. Kooperation erfordert die Ausprägung eines Merkmals, das die Fitness anderer Individuen verbessert, und ist in der Regel mit hohen Kosten verbunden. Ein Konflikt entsteht, wenn die evolutionären Interessen der interagierenden Individuen nicht übereinstimmen, z. B. wenn einige Individuen von einer kooperativen Handlung profitieren, ohne zu deren Ausprägung beizutragen. Der Fitnessvorteil solcher sozialer Abtrünniger kann dazu führen, dass ihre relative Häufigkeit zunimmt, und wenn ihre Häufigkeitszunahme nicht kontrolliert wird, können sie die Zusammenarbeit stören. Konflikte können daher verheerende Auswirkungen auf kooperative Systeme haben, und es besteht ein grosses Interesse daran zu verstehen, wie Kooperation trotz der Gefahr der Ausbeutung aufrechterhalten wird.

Abiotische Einflüsse wie Schwankungen bei der Verfügbarkeit von Ressourcen oder der Temperatur können sich ebenfalls auf die Evolutionsverlauf einer Population auswirken. Viele Organismen, darunter auch Mikroben, können auf schwankende Umweltbedingungen reagieren, indem sie Strategien zur Absicherung entwickeln. Dabei kann es sich entweder um konservative Strategien handeln, bei denen ein Organismus einen "sicheren" Merkmalswert ausprägt, oder um diversifizierende Strategien, bei denen mehrere Phänotypen als Risikostreuung produziert werden. Beide Formen der Absicherung gewährleisten das Überleben in einer unvorhersehbaren Umwelt, was sie bei isolierter Betrachtung oder über kurze Zeiträume und ohne Umweltschwankungen als unangepasst erscheinen lassen kann.

Myxococcus xanthus ist ein Modellsystem für die Untersuchung der Genetik der bakteriellen Entwicklung. Seine aggregative, multizelluläre Lebensweise und sein

kooperatives Verhalten machen ihn auch zu einem attraktiven System für die Untersuchung der Evolution des Sozialverhaltens. Eines der auffallendsten Merkmale des Lebenszyklus von *M. xanthus* ist die kooperative Bildung von mehrzelligen Fruchtkörperstrukturen, ein Entwicklungsprogramm, das als Reaktion auf Nährstoffmangel eingeleitet wird. Konflikte zwischen interagierenden Individuen unterschiedlicher Genotypen, die sich in (manchmal extremen) Asymmetrien der Fitness während der Bildung chimärer Fruchtkörper bei *M. xanthus* zeigen, sind nicht ungewöhnlich. Die Mechanismen, die für die erhöhte Fitness während der mehrzelligen Entwicklung verantwortlich sind, sind jedoch nicht gut verstanden. Ziel dieser Arbeit ist es, weiter zu erforschen, wie die Fitness als Reaktion auf biotischen und abiotischen Selektionsdruck während des Sozialverhaltens von *M. xanthus*, insbesondere während der kooperativen Fruchtkörperbildung, gesteigert werden kann.

Im ersten Kapitel untersuche ich, wie biotische Interaktionen, insbesondere die Anwesenheit von Konkurrenten, die Art und Weise beeinflussen, in der Fitnesssteigerungen durch die Evolution einer nahezu gesättigten Mutantenbibliothek unter Bedingungen erzielt werden können, die für Genotypen mit hoher Sporenproduktion in Chimären, d. h. in Entwicklungsgruppen, die aus mehreren Genotypen bestehen, selektieren. Anschliessend charakterisiere ich das Spektrum der verschiedenen Strategien, die *M. xanthus* anwenden kann, um einen relativen Fitnessvorteil während der chimären Entwicklung zu erlangen. Die Ergebnisse zeigen, dass sich entwickelte Populationen aus mehreren unterschiedlichen Konkurrenten zusammensetzen können und dass mehrere qualitativ unterschiedliche Strategien zu Fitnessgewinnen während der chimären Entwicklung führen.

Konflikte bei sozialen Interaktionen können durch die bevorzugte Interaktion mit nahverwandten Individuen gedämpft werden. Ein Mechanismus, der eine hohe Verwandtschaft fördert, ist die Verwandtendiskriminierung. Im zweiten Kapitel untersuche ich die Rolle des TraA/B-vermittelten Aussenmembranaustauschs (OME) als potenzieller Antrieb von Koloniefusionsinkompatibilitäten (CMIs) zwischen schwärmenden Gruppen von *M.*

xanthus. CMIs sind eine Form der mikrobiellen Verwandtendiskriminierung und reduzieren bekanntermassen die Bildung chimärer Fruchtkörper an der Schnittstelle zweier Schwärme von *M. xanthus*. Ich teste, ob die Unterbrechung der TraA-Funktionalität CMI-Phänotypen oder starke Antagonismen während der chimären Entwicklung zwischen natürlichen Stämmen beeinflusst. Die Ergebnisse zeigen, dass das Verhalten zur Unterscheidung von Verwandten bei *M. xanthus* komplex und wahrscheinlich multifaktoriell ist, was im Einklang mit dem steht, was über die Unterscheidung von Verwandten bei anderen Bakterienarten bekannt ist.

Zwei differenzierte Zelltypen, die während der Entwicklung von *M. xanthus* entstehen, nämlich stressresistente Sporen und lebensfähige Stäbchenzellen (periphere Stäbchenzellen), haben das Potenzial, zu überleben und das Wachstum erneut aufzunehmen, wenn die Nährstoffe wieder ausreichend vorhanden sind. Im letzten Kapitel dieser Arbeit untersuche ich, wie die Selektion in Umgebungen, die sich in der Dauer des Nährstoffmangels unterscheiden, die Verteilung der Zelltypen während der mehrzelligen Entwicklung beeinflussen kann. Insbesondere untersuche ich, ob periphere Stäbchenzellen während der nährstoffmangel-induzierten Entwicklung einen potenziellen Beitrag zur Fitness auf Gruppenebene leisten. Ich zeige, dass sich der relative Vorteil der Produktion verschiedener Entwicklungszelltypen (Sporen gegenüber lebensfähigen Stäbchen) in Abhängigkeit davon ändert, wie schnell die Nährstoffe nach Beginn des Mangels wieder aufgefüllt werden. Daher könnte ein weiterer Weg zur Steigerung der Fitness während der mehrzelligen Entwicklung eine veränderte Investition in Entwicklungszelltypen beinhalten.

General Introduction

Microbes, once considered solitary organisms, are now known to have complex social lives (Crespi 2001; Velicer 2003). Group-living is pervasive in microbes and ranges from single- and multi-species biofilms (Hall-Stoodley et al. 2004; Flemming and Wuertz 2019) to the complex communities that make up the gut microbiota (Coyte et al. 2015) or colonize human teeth (Kolenbrander et al. 2002). Due to the proximity of cells within these populations, cell-cell interactions are inevitable. These interactions set the stage for cooperation when the interests of individual cells align or conflict when they do not (Strassmann et al. 2000), and the appreciation of the importance of these interactions has led to the flourishing research field of sociomicrobiology.

Living in groups makes having efficient forms of communication or means of gaining information about the social environment important. For example, being able to adjust the expression level of a costly trait as a function of the composition of the social environment is likely to be important (Kümmerli et al. 2009b; Allen et al. 2016). Quorum sensing is one form of bacterial cell-cell communication which generally involves the production of extracellular signaling molecules that induce changes in the behavior of recipient cells (Papenfort and Bassler 2016). Quorum sensing is often used as a mechanism to coordinate the behaviors of groups of cells (Popat et al. 2015) although it is not exclusively associated with that function (Li et al. 2001; Heurlier et al. 2005). The expression of some traits in isolation is costly and results in limited benefits for an individual cell but if the population density is sufficiently high and the expression of the trait is coordinated, its expression can be beneficial (Diggle et al. 2007; Sandoz et al. 2007; Darch et al. 2012). For example, coordinated expression of bioluminescence enzymes (Nealson et al. 1970; Greenberg et al. 1979), virulence factors (Passador et al. 1993; Harrison et al. 2006; McNally and Brown 2015), biofilm structural components (Davies et al. 1998; Hammer and Bassler 2003), multicellular development and

sporulation (Velicer and Vos 2009; Strassmann and Queller 2011), antibiotic and anti-competitor toxin production (Chao and Levin 1981; Bainton et al. 1992), digestive exoenzymes (Rosenberg et al. 1977; Greig and Travisano 2004; Diggle et al. 2007), and biosurfactants (Pearson et al. 1997; Xavier et al. 2011) can all occur in response to quorum sensing molecules.

Many coordinated group behaviors in bacteria are cooperative. Cooperative behaviors are beneficial to an individual other than the expressing cell (recipient) and are often costly to the individual expressing the behavior (actor). The costs associated with cooperation limit the scenarios under which it can evolve. Cooperative behaviors can be classified with respect to the combination of effects they have on the actor and the recipient (West et al. 2007b):

-Mutually beneficial cooperation occurs when both the actor and recipient benefit from a behavior.

-Altruism is defined as a behavior that has negative fitness consequences for the actor but benefits the recipient.

The evolution of mutually beneficial cooperation can be readily explained because the actor gains a fitness benefit and therefore natural selection can act to maximize fitness at the individual level (Sachs et al. 2004; Lehmann and Keller 2006). The evolution of altruism, however, poses conceptual difficulties due to the negative fitness consequences for the actor. Two major conceptual frameworks are frequently used to explain the evolution of altruism and cooperation in general: kin-selection theory and multilevel-selection theory.

The inclusive-fitness theory (Hamilton 1964), often referred to as kin-selection theory (Smith 1964), states that cooperative or altruistic traits can be selected for if the cost (c) to the actor is outweighed by the benefits (b) of that action to its recipient, modulated by the degree of relatedness (r) between interactants. The benefits gained by related individuals are referred to as indirect fitness benefits. A higher degree of relatedness between the actor and the

recipient results in greater indirect fitness gains for the actor. Hamilton's rule (Hamilton 1964) summarizes this concept as a simple inequality:

$$rb - c > 0$$

This formalized the concept of inclusive fitness, or the combination of direct and indirect fitness, and provided a new way to understand how natural selection can favor the evolution of altruistic cooperation, namely by maximizing the inclusive fitness of an individual. Hamilton's rule is not limited to explaining the evolution of altruism but can also be extended to explain the evolution of other social behaviors including mutually beneficial cooperation, selfishness (positive effect on actor and negative effect on recipient), and spite (net negative fitness for actor and recipient) (Gardner et al. 2011). Hamilton's rule and kin-selection theory has been reworked over the decades resulting in a more general framework (Queller 1992) that also accommodates different ways of defining relatedness (Frank 2013). As a result, it has become the dominant theory for explaining the evolution of cooperation.

Multilevel selection theory differs primarily in how it conceptualizes the biological levels of organization at which natural selection can act (Okasha 2006). In this perspective, more productive cooperative groups can have a competitive advantage over groups composed of both cooperators and cheaters, allowing altruism to evolve through selection between groups even when selfish behaviors are favored between individuals within the group. Although the extent to which this is the case is debated (West et al. 2008). Many researchers consider multilevel selection and kin selection frameworks to be mathematically equivalent (Lehmann et al. 2007; Marshall 2011) and despite the differences between them, they both converge on the same requirement for the evolution of cooperation/altruism: populations should be structured in a way so that cooperators/altruists are more likely to interact with other cooperators/altruists (assortment) (Débarre et al. 2014). Despite this, the existence of two conceptual frameworks to explain the evolution of cooperation has resulted in much debate that is still ongoing (Kramer and Meunier 2016).

Microbial cooperation often involves the production of 'public goods', molecules which are available to the producer but also to any neighboring cells, making them particularly susceptible to exploitation by non-producing genotypes (often referred to as cheaters). Cooperators therefore pay the cost associated with expressing a cooperative trait while non-producing genotypes, resulting from mutation or migration, benefit from the trait expression without paying the cost; this is referred to as the problem of cooperation (West et al. 2007a). In this scenario, cooperators are at a selective disadvantage and non-producers should be able to produce more progeny and become overrepresented in the population over time. This can have detrimental effects on population-level fitness if the frequency of cheater genotypes goes unchecked (Fiegna and Velicer 2003; Rainey and Rainey 2003; Greig and Travisano 2004; Griffin et al. 2004; Diggle et al. 2007; Ross-Gillespie et al. 2007; Sandoz et al. 2007; Jiricny et al. 2010; Popat et al. 2012). Cheaters, however, are often self-limiting due to negative frequency dependence of their cheating-derived fitness advantage, which can result in an equilibrium frequency of cooperators and cheaters (Velicer et al. 2000; Fiegna and Velicer 2003; Ross-Gillespie et al. 2007; Chuang et al. 2009). Further, populations of only cooperators are often more productive than populations of cooperators and cheaters (cheating load), which can result in cooperative groups outcompeting mixed cooperator/cheater groups when the scale of competition is more global (Velicer et al. 2000; Fiegna and Velicer 2003; Griffin et al. 2004; Gilbert et al. 2007; Velicer and Vos 2009). The effects that cheaters can have on population productivity and their within-group advantage over cooperators have prompted many theoretical and experimental studies investigating the potential mechanisms that microbes use to stabilize cooperation over evolutionary time.

Social evolution theory predicts that positive assortment is important for the stabilization of cooperation, and a mechanism as simple as limited dispersal, which results in structured populations where related individuals are more likely to interact with each other, can achieve this (Griffin et al. 2004; Kreft 2004; Gilbert et al. 2007; Xavier and Foster 2007;

MacLean and Brandon 2008; Nadell et al. 2008; Kümmerli et al. 2009a; Drescher et al. 2014).

More active mechanisms such as kin discrimination, where non-kin are recognized and prevented from benefiting from cooperative acts as much as kin do, can have the same assortative effect (Gilbert et al. 2007; Gibbs et al. 2008; Ostrowski et al. 2008; Vos and Velicer 2009; Strassmann et al. 2011; Lyons et al. 2016). A third mechanism, known as the greenbeard effect (Gardner and West 2010) does not rely on genealogical relatedness but on relatedness only at the cooperative locus. Greenbeard alleles (either a single allele or group of statistically associated alleles) encode both the cooperative behavior and a mechanism that causes cooperators to associate (Gardner and West 2010). Being able to recognize and direct altruistic or cooperative behaviors exclusively toward other cooperators ensures that the actor will gain indirect fitness benefits from cooperation resulting in the stabilization of cooperation. Few examples of greenbeards have been discovered (Queller et al. 2003; Smukalla et al. 2008; Gruenheit et al. 2017). This in combination with the potential for 'falsebeards' that express the assortative behavior but not the cooperative trait suggest that this mechanism has limited potential for the stabilization of cooperation.

Other mechanisms such as pleiotropy (Foster et al. 2004), metabolic incentives to cooperate (Dandekar et al. 2012), metabolic prudence where a public good is only produced when its cost is minimal (Xavier et al. 2011), and 'policing' of cheating mutants (Manhes and Velicer 2011) can all prevent cheaters from displacing cooperators. Environments where more than one cooperative trait is required can also lead to an equilibrium frequency of cheaters because a cheater for one trait can be a cooperator for another trait (Özkaya et al. 2018). Diversity in social groups may also promote cooperation in some situations and can result in higher group-level productivity and reduced susceptibility to invasion by cheats (Brockhurst et al. 2006). Mechanisms that reduce competition between individuals, such as randomized reproductive success, can also stabilize cooperation without relying on high genetic relatedness (Frank 2003; Kümmerli et al. 2010)

Group living not only sets the stage for cooperation but also competition. Competitive bacterial interactions can be broadly classified as either resource or interference competition. Resource competition (also referred to as exploitative competition) involves a cell increasing their access to nutrients, usually by altering their metabolism (Vulić and Kolter 2001; MacLean and Gudelj 2006) or producing exoproducts that enhance their access to nutrients (Diggle et al. 2007; Leinweber et al. 2018). Many of these exoproducts can be considered public goods and are therefore exploitable by non-producing cells. Some species can even produce molecules that cause competitors to perform fitness reducing behaviors that benefit the manipulating cells (Egland et al. 2004). Interference competition is typified by the production of compounds such as antibiotics or toxins that are either released into the environment or directly transferred into other cells resulting in growth inhibition or cell death (Hood et al. 2010; Ruhe et al. 2018; Westhoff et al. 2020; Serapio-Palacios et al. 2022; Teschler et al. 2022). Both forms of competition can ultimately result in the displacement of competitors, which increases access to nutrients and space for the winner.

Competition can occur between genetically identical kin cells, genetically distinct strains of a single bacterial species, or between distinct bacterial species. Both intra- and interspecific competition have important implications during evolution and can affect the evolution and stabilization of cooperation (Griffin et al. 2004; Brockhurst et al. 2006; Harrison et al. 2006). Further, any process that results in fitness asymmetries during otherwise cooperative social behaviors can result in conflict (Velicer and Vos 2009). This is exemplified in one of the model species for studying cooperative behaviors in bacteria, *Myxococcus xanthus*, where antagonistic interaction are frequently observed between genetically distinct strains (Fiegna and Velicer 2005; Vos and Velicer 2009; Rendueles et al. 2015a) and clones isolated from a single fruiting body can vary in their abilities to perform social traits such as group motility and sporulation when in pure culture (Kraemer et al. 2010; Kraemer and Velicer 2011, 2014). Evolution in mixture with antagonistic strains can also result in the loss of fruiting-

body formation, demonstrating the potential for fitness asymmetries to select against cooperation (La Fortezza and Velicer 2021).

Myxococcus xanthus as a model for studying bacterial development and the evolution of social behaviors

The Myxobacteria are a group of gram-negative, deltaproteobacteria that are well known for their social behaviors, which include group motility, predation, and the formation of multicellular fruiting-body structures (Kaiser 2004; Zusman et al. 2007). Coordination of the various group behaviors requires communication between cells and the signaling pathways responsible for initiating multicellular development and group motility are relatively well-understood (Zusman et al. 2007; Bretl and Kirby 2016).

The lifecycle of _Myxococcus xanthus_ can be separated into the vegetative growth phase and the starvation-induced multicellular development phase (Figure 1). During vegetative growth cells can scavenge nutrients from their environment. Before macromolecules can be taken up, cells must release enzymes for their extracellular digestion which often occurs in a cell-density dependent manner (Rosenberg et al. 1977). The extracellular enzymes can be considered public goods because the products of digestion are available to cells other than the producer. _M. xanthus_ is also a predator that feeds on other microbes in the soil (Reichenbach 1999) and the killing of prey cells can occur via contact dependent or contact independent mechanisms (Thiery and Kaimer 2020; Arend et al. 2021). Contact independent killing can occur through diffusible molecules, such as antibiotics (Xiao et al. 2011) and lytic proteins (Hart and Zahler 1966; Sudo and Dworkin 1972) that can potentially benefit other cells in the vicinity.

17
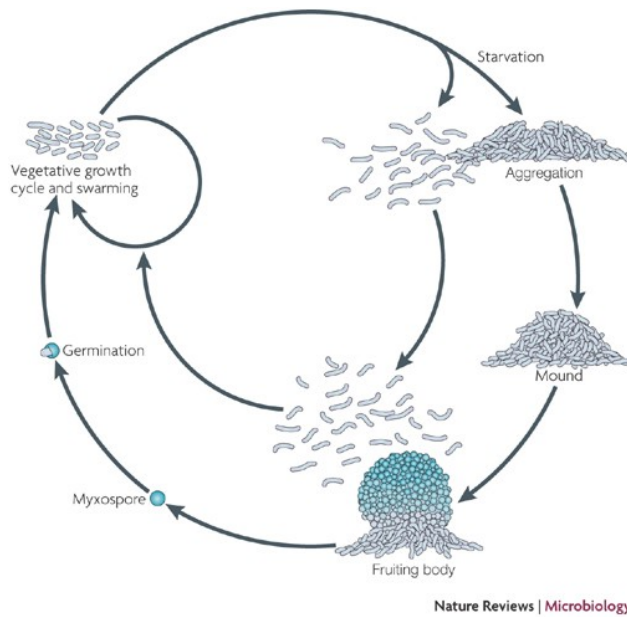
Figure 1. The lifecycle of Myxococcus xanthus. When nutrients and prey are present, groups of cells grow vegetatively and swarm outward in search of additional nutrients. When nutrients become limiting, cells begin to aggregate and form mounds then mature fruiting bodies. Within the fruiting body, cells differentiate into stress-resistant spores which can germinate when nutrients reappear and resume vegetative growth. Peripheral-rod cells are pictured as the cells that do not aggregate to form fruiting bodies. These cells can survive starvation and resume vegetative growth if nutrients become replete relatively quickly. Figure from (Zusman et al. 2007)

When swarming groups of cells run out of nutrients/prey, the multicellular development program is initiated. As in other bacteria (Gaca et al. 2015) starvation triggers the stringent response resulting in the production of the alarmone, (p)ppGpp. Production of (p)ppGpp initiates the production of the A signal (Figure 2). The A signal is a set of amino acids, generated by extracellular proteolysis, that function as a quorum sensing system, with the extracellular concentration of A signal being proportional to the cell density (Kuspa et al. 1992). The combination of (p)ppGpp production (starvation sensing) and detection of sufficient concentrations of A signal (assessment of population density) initiate the expression of early genes of the multicellular development program (Kaiser 2004). Given that A signal is a quorum sensing molecule, starving *M. xanthus* cells are able to sense their social environment and alter their gene expression patterns accordingly. If nutrients are becoming scarce ((p)ppGpp production in the cell) but the population density is insufficient for multicellular development (low extracellular A signal concentrations), cells will alter their growth rates and enter

stationary phase rather than initiate development (Kaiser 2004). If population density is high,

the high level of A signal in the environment initiates a signaling cascade that culminates in

multicellular fruiting-body formation and sporulation of a fraction of the population.
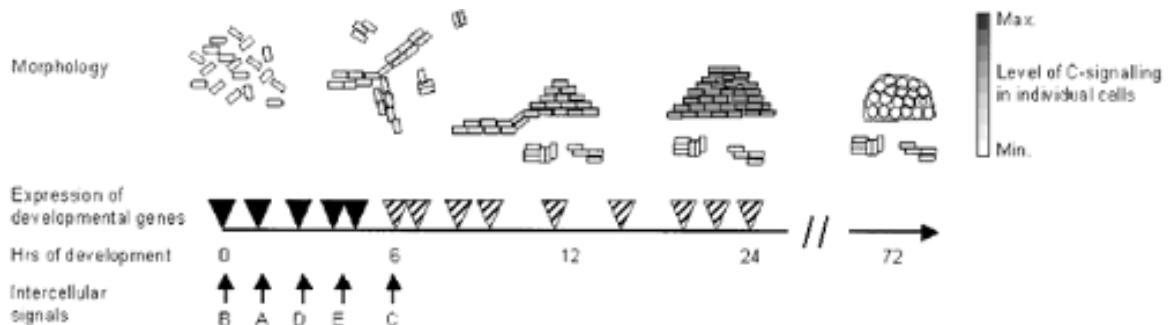
Figure 2. Fruiting-body morphogenesis and timeline of developmental signals. The morphological
progression of groups of cells during fruiting-body formation is shown above the developmental gene-
expression timeline. The grey-scale intensity of the cells represents the level of C signaling.
Developmental gene expression (timeline) is initiated by the intercellular signaling (arrows below the
timeline). Black triangles on the timeline show the expression of developmental genes in all cells before
the initiation of C signaling. Hatched triangles show the expression of C-signal dependent genes that
are only expressed in sporulating cells. Figure from (Søgaard-Andersen et al. 2003)

The C signal, encoded by the *csgA* gene is also an extracellular signaling molecule

which is important for fruiting-body morphogenesis and sporulation, the precise nature of

which has not been resolved (Bretl and Kirby 2016). CsgA is present in vegetatively growing

cells but starvation triggers a five-fold increase in its production (Crawford and Shimkets 2000;

Kruse et al. 2001). Increasing levels of C signal are important for the expression of different

behaviors such as aggregation (Jelsbak and Søgaard-Andersen 2002; Stevens and Søgaard-

Andersen 2005) and high levels of C signal, such as those found in fruiting bodies where cell

density is high, induce sporulation (Figure 2) (Søgaard-Andersen 2004). One model proposes

that the C-signal is a membrane associated protein that undergoes extracellular proteolytic

cleavage resulting in the functional 17kDa CsgA protein (Konovalova et al. 2012). Under this

model, activation of C-signal-dependent gene expression requires cell contact and alignment

in order for C-signal receptors to bind CsgA on neighboring cells (Kim and Kaiser 1990). The

putative receptor has yet to be identified however. A competing model suggests that the

enzymatic activity of the full length (25kDa) CsgA protein is important for C-signaling (Lee et

al. 1995). Strains expressing *csgA* with mutations in the phospholipase domain are defective in development, further lipid extracts of *csgA*^{+} cells can complement the developmental defect of *csgA* mutants (Boynton and Shimkets 2015). Interestingly, sporulation can also occur outside of fruiting bodies (Kruse et al. 2001) and some selective conditions can result in the evolution of fruiting-body-defective but sporulation-proficient evolved populations (La Fortezza and Velicer 2021).

Other classes of developmental signals are not as well understood, but mutants of these signaling classes are defective to varying degrees during development and arrest their developmental programs at distinct developmental stages (Shimkets 1999). When environmental conditions improve, the spores germinate and resume the vegetative stage of the *M. xanthus* lifecycle. Interestingly, germination also appears to be cooperative (Pande et al. 2020). Not only spores have the potential to resume growth after nutrients become replete. Peripheral rod cells are an additional differentiated cell type that do not get incorporated into fruiting bodies but instead remain metabolically active and motile (O'Connor and Zusman 1991b). The role of peripheral rods during starvation induced development is unknown but they may function as bet-hedging strategy against the rapid return of nutrients or exposure to low nutrient levels sufficient to fuel rod growth but insufficient to induce spore germination (O'Connor and Zusman 1991a)

M. xanthus is also a model for studying the evolution of social behavior in bacteria and there is a growing literature of experimental evolution experiments that investigate a variety of ecological and evolutionary questions (Velicer et al. 1998; Fiegna and Velicer 2003; Velicer and Yu 2003; Hillesland et al. 2009; Manhes and Velicer 2011; Nair et al. 2019; La Fortezza and Velicer 2021). *M. xanthus* has an aggregative multicellular lifestyle making it particularly susceptible to conflict during cooperative behaviors. Indeed, *M. xanthus* is known to form chimeric fruiting bodies under laboratory conditions (Fiegna and Velicer 2003, 2005; Vos and Velicer 2009; Rendueles et al. 2015a) and in nature (Kraemer and Velicer 2011). Fitness, as

measured by the production of heat-resistant spores, can be determined for each genotype during chimeric development. The social environment can have dramatic effects on the fitness of strains during chimeric development and on group-level productivity (Fiegna and Velicer 2005; Vos and Velicer 2009; Pande and Velicer 2018). Further, kin discrimination by colony-merger incompatibility can prevent chimeric fruiting-body formation between strains that are known to be antagonistic in pairwise mixes (Rendueles et al. 2015b). This leads to the interesting questions of how *M. xanthus* discerns between kin and non-kin and how antagonisms between strains are manifested.

The aim of this thesis is to further explore the how fitness can be increased during *M. xanthus* social behaviors, particularly during cooperative fruiting-body formation. In the first chapter, I evolved a transposon-mutant library under conditions that favored genotypes that became overrepresented in the spore population during chimeric development with their non-evolving cooperative ancestor. I found that the evolved populations tended to be developmentally proficient in pure culture and showed signatures of facultative exploitation during chimeric development with the ancestor. I also found that the evolved populations were composed of phenotypically distinct clones that could be classified as different competitive types based on their sporulation in pure culture and in mixture with the ancestor. Among the evolved clones that had a relative fitness advantage in chimera, facultative exploitation, cheating and increased intrinsic sporulation were common.

In the second chapter, I investigated the role of TraA/B-mediated outer membrane exchange (OME) as a potential mechanism of kin discrimination. First, I examined the role of OME on the generation of colony-merger incompatibilities at the interface of swarms using *traA* mutants constructed in natural isolate backgrounds. After finding no reduction in the incompatibility phenotypes I tested for the reduced ability of the mutants to antagonize during mixed swarming assays and mixed development assays. When the mutations, again, did not reduce the antagonisms between strains I investigated the role of Type 6 secretion system

21

(T6SS) mediated antagonisms during swarming and found that T6SS mutants do show reduced killing during mixed swarming. Together these results show that kin discriminatory behaviors in *M. xanthus* are complex and likely multifactorial, as has been shown in other bacterial species. The apparent limits of OME for kin discrimination leave open the question of what adaptive benefits result from exchanging large portions of cellular material with neighboring cells.

During multicellular development in the laboratory, the fitness of a genotype is typically assigned based on its sporulation efficiency. This measure of fitness is not necessarily reflective of the natural ecology of *M. xanthus*. Specifically, it does not take into consideration the peripheral-rod developmental fate. In the final chapter of this thesis, I describe an evolution experiment designed to test whether the different cell types present during *M. xanthus* development each have a distinct selective advantage in different environments. The results provide evidence for the existence of cell-type bet hedging and show that peripheral rods cells are an evolutionarily important cell type that represent an under-studied fitness component during multicellular development.

References

Allen RC, McNally L, Popat R, Brown SP. Quorum sensing protects bacterial co-operation from exploitation by cheats. Isme J. 2016;10(7):1706–16.

Arend KI, Schmidt JJ, Bentler T, Lüchtefeld C, Eggerichs D, Hexamer HM, et al. Myxococcus xanthus Predation of Gram-Positive or Gram-Negative Bacteria Is Mediated by Different Bacteriolytic Mechanisms. Appl Environ Microbiol. 2021;87(5).

Bainton NJ, Bycroft BW, Chhabra SR, Stead P, Gledhill L, Hill PJ, et al. A general role for the lux autoinducer in bacterial cell signalling: control of antibiotic biosynthesis in Erwinia. Gene. 1992;116(1):87–91.

Boynton TO, Shimkets LJ. Myxococcus CsgA, Drosophila Sniffer, and human HSD10 are cardiolipin phospholipases. Genes Dev [Internet]. 2015 Sep 15;29(18):1903–14. Available from: message:%3C7946019C-63CF-4406-B8BD-A45021FBE0F8@env.ethz.ch%3E

Bretl DJ, Kirby JR. Molecular Mechanisms of Signaling in Myxococcus xanthus Development. J Mol Biol. 2016;428(19):3805–30.

Brockhurst MA, Hochberg ME, Bell T, Buckling A. Character Displacement Promotes Cooperation in Bacterial Biofilms. Curr Biol. 2006;16(20):2030–4.

Chao L, Levin BR. Structured habitats and the evolution of anticompetitor toxins in bacteria. Proc Natl Acad Sci USA. 1981;78(10):6324–8.

Chuang JS, Rivoire O, Leibler S. Simpson's Paradox in a Synthetic Microbial System. Science. 2009;323(5911):272–5.

Coyte KZ, Schluter J, Foster KR. The ecology of the microbiome: Networks, competition, and stability. Science. 2015;350(6261):663–6.

Crawford EW, Shimkets LJ. The Myxococcus xanthus socE and csgA genes are regulated by the stringent response. Mol Microbiol. 2000;37(4):788–99.

Crespi BJ. The evolution of social behavior in microorganisms. Trends Ecol Evol. 2001;16(4):178–83.

Dandekar AA, Chugani S, Greenberg EP. Bacterial Quorum Sensing and Metabolic Incentives to Cooperate. Science. 2012;338(6104):264–6.

Darch SE, West SA, Winzer K, Diggle SP. Density-dependent fitness benefits in quorum-sensing bacterial populations. Proc Natl Acad Sci USA. 2012;109(21):8259–63.

Davies DG, Parsek MR, Pearson JP, Iglewski BH, Costerton JW, Greenberg EP. The Involvement of Cell-to-Cell Signals in the Development of a Bacterial Biofilm. Science. 1998;280(5361):295–8.

Débarre F, Hauert C, Doebeli M. Social evolution in structured populations. Nat Commun. 2014;5(1):3409.

Diggle SP, Griffin AS, Campbell GS, West SA. Cooperation and conflict in quorum-sensing bacterial populations. Nature. 2007;450(7168):411–4.

Drescher K, Nadell CD, Stone HA, Wingreen NS, Bassler BL. Solutions to the Public Goods Dilemma in Bacterial Biofilms. Curr Biol. 2014;24(1):50–5.

Egland PG, Palmer RJ, Kolenbrander PE. Interspecies communication in Streptococcus gordonii–Veillonella atypica biofilms: Signaling in flow conditions requires juxtaposition. Proc Natl Acad Sci USA. 2004;101(48):16917–22.

Fiegna F, Velicer GJ. Competitive fates of bacterial social parasites: persistence and selfinduced extinction of Myxococcus xanthus cheaters. Proc Biol Sci. 2003;270(1523):1527–34.

Fiegna F, Velicer GJ. Exploitative and Hierarchical Antagonism in a Cooperative Bacterium. Plos Biol. 2005;3(11):e370.

Flemming HC, Wuertz S. Bacteria and archaea on Earth and their abundance in biofilms. Nat Rev Microbiol. 2019;17(4):247–60.

Fortezza ML, Velicer GJ. Social selection within aggregative multicellular development drives morphological evolution. Proc Biol Sci. 2021;288(1963):20211522.

Foster KR, Shaulsky G, Strassmann JE, Queller DC, Thompson CRL. Pleiotropy as a mechanism to stabilize cooperation. Nature. 2004;431(7009):693–6.

Frank SA. Perspective: repression of competition and the evolution of cooperation. Evolution. 2003;57(4):693–705.

Frank SA. Natural selection. VII. History and interpretation of kin selection theory. J Evol Biol. 2013;26(6):1151–84.

Gaca AO, Colomer-Winter C, Lemos JA. Many Means to a Common End: the Intricacies of (p)ppGpp Metabolism and Its Control of Bacterial Homeostasis. J Bacteriol. 2015;197(7):1146–56.

Gardner A, West SA. Greenbeards. Evolution. 2010;64(1):25–38.

Gardner A, West SA, Wild G. The genetical theory of kin selection. J Evol Biol. 2011;24(5):1020–43.

Gibbs KA, Urbanowski ML, Greenberg EP. Genetic Determinants of Self Identity and Social Recognition in Bacteria. Science. 2008;321(5886):256–9.

Gilbert OM, Foster KR, Mehdiabadi NJ, Strassmann JE, Queller DC. High relatedness maintains multicellular cooperation in a social amoeba by controlling cheater mutants. Proc Natl Acad Sci USA. 2007;104(21):8913–7.

Greenberg EP, Hastings JW, Ulitzur S. Induction of luciferase synthesis in Beneckea harveyi by other marine bacteria. Arch Microbiol. 1979;120(2):87–91.

Greig D, Travisano M. The Prisoner's Dilemma and polymorphism in yeast SUC genes. Proc Biol Sci. 2004;271(suppl_3):S25–6.

Griffin AS, West SA, Buckling A. Cooperation and competition in pathogenic bacteria. Nature. 2004;430(7003):1024–7.

Gruenheit N, Parkinson K, Stewart B, Howie JA, Wolf JB, Thompson CRL. A polychromatic 'greenbeard' locus determines patterns of cooperation in a social amoeba. Nat Commun. 2017;8(1):14171.

Hall-Stoodley L, Costerton JW, Stoodley P. Bacterial biofilms: from the Natural environment to infectious diseases. Nat Rev Microbiol. 2004;2(2):95–108.

Hamilton WD. The genetical evolution of social behaviour. I. J Theor Biol. 1964;7(1):1–16.

Hammer BK, Bassler BL. Quorum sensing controls biofilm formation in Vibrio cholerae. Mol Microbiol. 2003;50(1):101–4.

Harrison F, Browning LE, Vos M, Buckling A. Cooperation and virulence in acute Pseudomonas aeruginosa infections. BMC Biol. 2006;4(1):21.

Hart BA, Zahler SA. Lytic Enzyme Produced by Myxococcus xanthus. J Bacteriol. 1966;92(6):1632–7.

Heurlier K, Dénervaud V, Haenni M, Guy L, Krishnapillai V, Haas D. Quorum-Sensing-Negative (lasR) Mutants of Pseudomonas aeruginosa Avoid Cell Lysis and Death. J Bacteriol. 2005;187(14):4875–83.

Hillesland KL, Velicer GJ, Lenski RE. Experimental evolution of a microbial predator's ability to find prey. Proc Biol Sci. 2009;276(1656):459–67.

Hood RD, Singh P, Hsu F, Güvener T, Carl MA, Trinidad RRS, et al. A Type VI Secretion System of Pseudomonas aeruginosa Targets a Toxin to Bacteria. Cell Host Microbe. 2010;7(1):25–37.

Jelsbak L, Søgaard-Andersen L. Pattern formation by a cell surface-associated morphogen in Myxococcus xanthus. Proc Natl Acad Sci USA. 2002;99(4):2032–7.

Jiricny N, Diggle SP, West SA, Evans BA, Ballantyne G, Ross-Gillespie A, et al. Fitness correlates with the extent of cheating in a bacterium. J Evol Biol. 2010;23(4):738–47.

Kaiser D. Signaling in Myxobacteria. Annu Rev Microbiol. 2004;58(1):75–98.

Kim SK, Kaiser D. Cell Alignment Required in Differentiation of Myxococcus xanthus. Science. 1990;249(4971):926–8.

Kolenbrander PE, Andersen RN, Blehert DS, Egland PG, Foster JS, Palmer RJ. Communication among Oral Bacteria. Microbiol Mol Biol Rev. 2002;66(3):486–505.

Konovalova A, Wegener-Feldbrügge S, Søgaard-Andersen L. Two intercellular signals required for fruiting body formation in Myxococcus xanthus act sequentially but non-hierarchically. Mol Microbiol. 2012;86(1):65–81.

Kraemer SA, Toups MA, Velicer GJ. Natural variation in developmental life-history traits of the bacterium Myxococcus xanthus. FEMS Microbiol Ecol. 2010;73(2):226–33.

Kraemer SA, Velicer GJ. Endemic social diversity within natural kin groups of a cooperative bacterium. Proc National Acad Sci USA. 2011;108(supplement_2):10823–30.

Kraemer SA, Velicer GJ. Social complementation and growth advantages promote socially defective bacterial isolates. Proc Biol Sci. 2014;281(1781):20140036.

Kramer J, Meunier J. Kin and multilevel selection in social evolution: a never-ending controversy? F1000Res. 2016;5:F1000 Faculty Rev-776.

Kreft JU. Biofilms promote altruism. Microbiology (Reading). 2004;150(8):2751–60.

Kruse T, Lobedanz S, Berthelsen NMS, Søgaard-Andersen L. C-signal: a cell surface-associated morphogen that induces and co-ordinates multicellular fruiting body morphogenesis and sporulation in Myxococcus xanthus. Mol Microbiol. 2001;40(1):156–68.

Kümmerli R, Berg P van den, Griffin AS, West SA, Gardner A. Repression of competition favours cooperation: experimental evidence from bacteria. J Evol Biol. 2010;23(4):699–706.

Kümmerli R, Griffin AS, West SA, Buckling A, Harrison F. Viscous medium promotes cooperation in the pathogenic bacterium Pseudomonas aeruginosa. Proc Biol Sci. 2009a;276(1672):3531–8.

Kümmerli R, Jiricny N, Clarke LS, West SA, Griffin AS. Phenotypic plasticity of a cooperative behaviour in bacteria. J Evol Biol. 2009b;22(3):589–98.

Kuspa A, Plamann L, Kaiser D. A-signalling and the cell density requirement for Myxococcus xanthus development. J Bacteriol. 1992;174(22):7360–9.

Lee BU, Lee K, Mendez J, Shimkets LJ. A tactile sensory system of Myxococcus xanthus involves an extracellular NAD(P)(+)-containing protein. Genes Dev. 1995;9(23):2964–73.

Lehmann L, Keller L. The evolution of cooperation and altruism – a general framework and a classification of models. J Evol Biol. 2006;19(5):1365–76.

Lehmann L, Keller L, West S, Roze D. Group selection and kin selection: Two concepts but one process. Proc Natl Acad Sci USA. 2007;104(16):6736–9.

Leinweber A, Weigert M, Kümmerli R. The bacterium Pseudomonas aeruginosa senses and gradually responds to inter-specific competition for iron. Evolution. 2018;72(7):1515–28.

Li YH, Lau PCY, Lee JH, Ellen RP, Cvitkovitch DG. Natural Genetic Transformation of Streptococcus mutans Growing in Biofilms. J Bacteriol. 2001;183(3):897–908.

Lyons NA, Kraigher B, Stefanic P, Mandic-Mulec I, Kolter R. A Combinatorial Kin Discrimination System in Bacillus subtilis. Curr Biol. 2016;26(6):733–42.

MacLean RC, Brandon C. Stable public goods cooperation and dynamic social interactions in yeast. J Evol Biol. 2008;21(6):1836–43.

MacLean RC, Gudelj I. Resource competition and social conflict in experimental populations of yeast. Nature. 2006;441(7092):498–501.

Manhes P, Velicer GJ. Experimental evolution of selfish policing in social bacteria. P Natl Acad Sci USA. 2011;108(20):8357–62.

Marshall JAR. Group selection and kin selection: formally equivalent approaches. Trends Ecol Evol. 2011;26(7):325–32.

McNally L, Brown SP. Building the microbiome in health and disease: niche construction and social conflict in bacteria. Philos Trans R Soc Lond B Biol Sci. 2015;370(1675):20140298.

Nadell CD, Xavier JB, Levin SA, Foster KR. The Evolution of Quorum Sensing in Bacterial Biofilms. PLoS Biol. 2008;6(1):e14.

Nair RR, Vasse M, Wielgoss S, Sun L, Yu YTN, Velicer GJ. Bacterial predator-prey coevolution accelerates genome evolution and selects on virulence-associated prey defences. Nat Commun. 2019;10(1):4301.

Nealson KH, Platt T, Hastings JW. Cellular Control of the Synthesis and Activity of the Bacterial Luminescent System. J Bacteriol. 1970;104(1):313–22.

O'Connor KA, Zusman DR. Behavior of peripheral rods and their role in the life cycle of Myxococcus xanthus. J Bacteriol. 1991a;173(11):3342–55.

O'Connor KA, Zusman DR. Development in Myxococcus xanthus involves differentiation into two cell types, peripheral rods and spores. J Bacteriol. 1991b;173(11):3318–33.

Okasha S, Okasha S. Evolution and the Levels of Selection. Oxford University Press; 2006.

Ostrowski EA, Katoh M, Shaulsky G, Queller DC, Strassmann JE. Kin Discrimination Increases with Genetic Distance in a Social Amoeba. Plos Biol. 2008;6(11):e287.

Özkaya Ö, Balbontín R, Gordo I, Xavier KB. Cheating on Cheaters Stabilizes Cooperation in Pseudomonas aeruginosa. Curr Biol. 2018;28(13):2070-2080.e6.

Pande S, Escriva PP, Yu YTN, Sauer U, Velicer GJ. Cooperation and Cheating among Germinating Spores. Curr Biol. 2020;30(23):4745-4752.e4.

Pande S, Velicer GJ. Chimeric Synergy in Natural Social Groups of a Cooperative Microbe. Curr Biol. 2018;28(2):262-267.e3.

Papenfort K, Bassler BL. Quorum sensing signal–response systems in Gram-negative bacteria. Nat Rev Microbiol. 2016;14(9):576–88.

Passador L, Cook JM, Gambello MJ, Rust L, Iglewski BH. Expression of Pseudomonas aeruginosa Virulence Genes Requires Cell-to-Cell Communication. Science. 1993;260(5111):1127–30.

Pearson JP, Pesci EC, Iglewski BH. Roles of Pseudomonas aeruginosa las and rhl quorum-sensing systems in control of elastase and rhamnolipid biosynthesis genes. J Bacteriol. 1997;179(18):5756–67.

Popat R, Cornforth DM, McNally L, Brown SP. Collective sensing and collective responses in quorum-sensing bacteria. J R Soc Interface. 2015;12(103):20140882.

Popat R, Crusz SA, Messina M, Williams P, West SA, Diggle SP. Quorum-sensing and cheating in bacterial biofilms. Proc Biol Sci. 2012;279(1748):4765–71.

Queller DC. A General Model for Kin Selection. Evolution. 1992;46(2):376–80.

Queller DC, Ponte E, Bozzaro S, Strassmann JE. Single-Gene Greenbeard Effects in the Social Amoeba Dictyostelium discoideum. Science. 2003;299(5603):105–6.

Rainey PB, Rainey K. Evolution of cooperation and conflict in experimental bacterial populations. Nature. 2003;425(6953):72–4.

Reichenbach H. The ecology of the myxobacteria. Environ Microbiol. 1999;1(1):15–21.

Rendueles O, Amherd M, Velicer GJ. Positively Frequency-Dependent Interference Competition Maintains Diversity and Pervades a Natural Population of Cooperative Microbes. Curr Biol. 2015a;25(13):1673–81.

Rendueles O, Zee PC, Dinkelacker I, Amherd M, Wielgoss S, Velicer GJ. Rapid and widespread de novo evolution of kin discrimination. Proc Natl Acad Sci USA. 2015b;112(29):9076–81.

Rosenberg E, Keller KH, Dworkin M. Cell density-dependent growth of Myxococcus xanthus on casein. J Bacteriol. 1977;129(2):770–7.

Ross-Gillespie A, Gardner A, West SA, Griffin AS. Frequency Dependence and Cooperation: Theory and a Test with Bacteria. Am Nat. 2007;170(3):331–42.

Ruhe ZC, Subramanian P, Song K, Nguyen JY, Stevens TA, Low DA, et al. Programmed Secretion Arrest and Receptor-Triggered Toxin Export during Antibacterial Contact-Dependent Growth Inhibition. Cell. 2018;175(4):921-933.e14.

Sachs JL, Mueller UG, Wilcox TP, Bull JJ. The Evolution of Cooperation. Q Rev Biol. 2004;79(2):135–60.

Sandoz KM, Mitzimberg SM, Schuster M. Social cheating in Pseudomonas aeruginosa quorum sensing. Proc National Acad Sci USA. 2007;104(40):15876–81.

Serapio-Palacios A, Woodward SE, Vogt SL, Deng W, Creus-Cuadros A, Huus KE, et al. Type VI secretion systems of pathogenic and commensal bacteria mediate niche occupancy in the gut. Cell Rep. 2022;39(4):110731.

Shimkets LJ. Intercellular signaling during fruiting-body development of Myxococcus xanthus. Annu Rev Microbiol. 1999;53(1):525–49.

Smith JM. Group Selection and Kin Selection. Nature. 1964;201(4924):1145–7.

Smukalla S, Caldara M, Pochet N, Beauvais A, Guadagnini S, Yan C, et al. FLO1 Is a Variable Green Beard Gene that Drives Biofilm-like Cooperation in Budding Yeast. Cell. 2008;135(4):726–37.

Søgaard-Andersen L. Cell polarity, intercellular signalling and morphogenetic cell movements in Myxococcus xanthus. Curr Opin Microbiol. 2004;7(6):587–93.

Søgaard-Andersen L, Overgaard M, Lobedanz S, Ellehauge E, Jelsbak L, Rasmussen AAa. Coupling gene expression and multicellular morphogenesis during fruiting body formation in Myxococcus xanthus. Mol Microbiol. 2003;48(1):1–8.

Stevens A, Søgaard-Andersen L. Making waves: pattern formation by a cell-surface-associated signal. Trends Microbiol. 2005;13(6):249–52.

Strassmann JE, Gilbert OM, Queller DC. Kin Discrimination and Cooperation in Microbes. Annu Rev Microbiol. 2011;65(1):349–67.

Strassmann JE, Queller DC. Evolution of cooperation and control of cheating in a social microbe. Proc National Acad Sci USA. 2011;108(Supplement 2):10855–62.

Strassmann JE, Zhu Y, Queller DC. Altruism and social cheating in the social amoeba Dictyostelium discoideum. Nature. 2000;408(6815):965–7.

Sudo S, Dworkin M. Bacteriolytic Enzymes Produced by Myxococcus xanthus. J Bacteriol. 1972;110(1):236–45.

Teschler JK, Jiménez-Siebert E, Jeckel H, Singh PK, Park JH, Pukatzki S, et al. VxrB Influences Antagonism within Biofilms by Controlling Competition through Extracellular Matrix Production and Type 6 Secretion. mBio. 2022;13(4):e01885-22.

Thiery S, Kaimer C. The Predation Strategy of Myxococcus xanthus. Front Microbiol. 2020;11:2.

Velicer GJ. Social strife in the microbial world. Trends Microbiol. 2003;11(7):330–7.

Velicer GJ, Kroos L, Lenski RE. Loss of social behaviors by Myxococcus xanthus during evolution in an unstructured habitat. Proc National Acad Sci USA. 1998;95(21):12376–80.

Velicer GJ, Kroos L, Lenski RE. Developmental cheating in the social bacterium Myxococcus xanthus. Nature. 2000;404(6778):598–601.

Velicer GJ, Vos M. Sociobiology of the Myxobacteria. Annu Rev Microbiol. 2009;63(1):599–623.

Velicer GJ, Yu YTN. Evolution of novel cooperative swarming in the bacterium Myxococcus xanthus. Nature. 2003;425(6953):75–8.

Vos M, Velicer GJ. Social Conflict in Centimeter-and Global-Scale Populations of the Bacterium Myxococcus xanthus. Curr Biol. 2009;19(20):1763–7.

Vulić M, Kolter R. Evolutionary Cheating in Escherichia coli Stationary Phase Cultures. Genetics. 2001;158(2):519–26.

West SA, Griffin AS, Gardner A. Evolutionary Explanations for Cooperation. Curr Biol. 2007a;17(16):R661–72.

West SA, Griffin AS, Gardner A. Social semantics: altruism, cooperation, mutualism, strong reciprocity and group selection. J Evol Biol. 2007b;20(2):415–32.

WEST SA, GRIFFIN AS, GARDNER A. Social semantics: how useful has group selection been? J Evol Biol. 2008;21(1):374–85.

Westhoff S, Otto SB, Swinkels A, Bode B, Wezel GP van, Rosen DE. Spatial structure increases the benefits of antibiotic production in Streptomyces* | Evolution | Oxford Academic. Evolution. 2020;

Xavier JB, Foster KR. Cooperation and conflict in microbial biofilms. Proc National Acad Sci USA. 2007;104(3):876–81.

Xavier JB, Kim W, Foster KR. A molecular mechanism that stabilizes cooperative secretions in Pseudomonas aeruginosa. Mol Microbiol. 2011;79(1):166–79.

Xiao Y, Wei X, Ebright R, Wall D. Antibiotic Production by Myxobacteria Plays a Role in Predation. J Bacteriol. 2011;193(18):4626–33.

Zusman DR, Scott AE, Yang Z, Kirby JR. Chemosensory pathways, motility and development in Myxococcus xanthus. Nat Rev Microbiol. 2007;5(11):862–72.

Chapter 1

Chimeric interactions during multicellular development select for a variety of competitive types in the bacterium *Myxococcus xanthus*

Sarah M. Cossey, Marie Vasse, Yuen-Tsu Nicco Yu, Gregory Velicer

Abstract

Behaviors that provide a benefit to individuals other than the actor can be considered cooperative. Cooperative behaviors can be favored by selection when they improve the fitness of related individuals. Many cooperative microbes have an aggregative multicellular lifestyle, where individual cells come together to perform a cooperative behavior despite having potentially low relatedness. Conflict can arise in populations with relatively low relatedness between individuals, which can have a destabilizing effect on cooperation. Here, we investigated the types of competitive strategies that can evolve in an aggregative multicellular form of cooperation. To do this we evolved a nearly saturated mutant library during chimeric interactions with a non-evolving cooperative ancestor in the social bacterium *Myxococcus xanthus*. From post-evolution assays with samples of whole evolved populations, we found that the evolved populations remained developmentally proficient when assayed in the absence of their ancestor but increased their absolute fitness during chimeric development, a fitness pattern known as facultative exploitation. However, only 43% of the clones isolated from evolved populations and then examined separately had a relative fitness advantage during pairwise interactions with the ancestor. Developmental cheating, facultative exploitation, and increased intrinsic sporulation were all common strategies among the competitive winners. The remaining clones did not have a clear competitive advantage during pairwise interactions with the ancestor, suggesting that interactions between mutants were also important in determining which phenotypes increased in frequency. Overall, we show that fitness in chimera can improve as a result of multiple strategies and that no one strategy clearly dominates.

Introduction

Microbes often live at high density and in complex polymicrobial communities (Mitri and Foster 2013; Ghoul and Mitri 2016). Interactions between cells and cell groups are inevitable under these conditions and can involve competition for space and resources (Freilich et al. 2011; Palmer and Foster 2022), but can also be cooperative. A cooperative behavior is beneficial to other cells and is often costly for the expressing cell. Metabolically costly behaviors such as the production of extracellular polymers and enzymes, expression of virulence factors, siderophore production, and multicellular fruiting-body formation can result in increased fitness when their expression is coordinated and performed as a group (Velicer 2003; West et al. 2007).

High relatedness is important for the maintenance of cooperation in many systems (Hamilton 1964a; Strassmann et al. 2011; Medina et al. 2019; Ostrowski 2019). However, cells in microbial groups within which cooperative interactions occur are often genetically diverse, which generates the potential for genetic conflict within groups. Such within-group competition can have a destabilizing effect on cooperation even when relatedness is high (Frank 1998; Griffin et al. 2004).

Cells within microbial populations can increase their fitness by engaging in resource competition (also known as exploitation competition), in which cells compete for resources without interacting directly. Adaptations for resource competition include metabolic alterations that allow for faster nutrient acquisition in *Saccharomyces cerevisiae* and *Escherichia coli* (Vulić and Kolter 2001; MacLean and Gudelj 2006), or the production of extracellular enzymes, such as elastase (Diggle et al. 2007) that allow the uptake of otherwise inaccessible nutrients. Nutrients, such as iron, can also be sequestered through the production of iron-chelating molecules (Griffin et al. 2004) resulting in a reduction in their availability to competitors. Genotypes can also gain an advantage over others by engaging in interference competition, *i.e.* by directly harming competitors. In bacteria, for example, many species secret

bacteriocins/antibiotics (Slattery et al. 2001; Riley and Wertz 2002) to antagonize susceptible genotypes or use secretion systems such as the Type VI secretion system (T6SS) to transfer toxins to neighboring cells (Sana et al. 2016). In T6SS interactions, cells that are closely related to the toxin-producer often express the cognate antitoxin and survive the interaction while more distantly related cells are killed (Basler et al. 2013).

In microbial social environments in which some cells cooperatively produce molecules that benefit others (many of which are referred to as public goods), capitalizing on such molecules while avoiding the metabolic cost of their production is another way to gain a fitness advantage. Non-producer genotypes that advantageously exploit social molecules produced by other genotypes are often referred to as cheaters. Cheaters are readily evolvable under laboratory conditions (Velicer et al. 2000; Sandoz et al. 2007; Harrison et al. 2008; Katzianer et al. 2015) and are also found in nature and clinically relevant settings (Strassmann et al. 2000; Smith et al. 2006; Bruce et al. 2017; Butaitė et al. 2017). At least for obligate non-producers, cheater fitness is highest when their frequency in the population is low because the frequency of cooperators can impact population growth and more cooperators provide more opportunities for a given non-producer to cheat (Velicer et al. 2000; Fiegna and Velicer 2003; Diggle et al. 2007; Ross-Gillespie et al. 2007). Their fitness advantage allows cheaters to increase in frequency within their local population in the short run, but such increase can become self-limiting in two ways. Cheaters can lose their within-group advantage upon reaching a threshold frequency or can reduce population-level fitness (Fiegna and Velicer 2003; Rainey and Rainey 2003; Özkaya et al. 2018) sometimes even driving populations to extinction (Fiegna and Velicer 2003; Fiegna et al. 2006). Lowered group productivity from cheating – 'cheating load' – reduces the competitiveness of populations with high cheater frequencies compared to populations with fewer cheaters, resulting in cooperative populations having a selective advantage (Griffin et al. 2004; Travisano and Velicer 2004; Gilbert et al. 2007; Chuang et al. 2009; Velicer and Vos 2009).

Despite the potentially devastating effects of cheating on the fate of cooperative lineages and group productivity, cooperation is prevalent in many microbial species (Strassmann et al. 2000, 2011; Velicer 2003; Griffin et al. 2004; Lenz et al. 2004; West et al. 2007; Pollitt et al. 2014). Mechanisms that stabilize cooperation – *i.e.* prevent non-cooperators from driving cooperators to extinction – have received much attention across diverse systems (Travisano and Velicer 2004). Population structure, which can occur passively as a result of limited dispersal, is thought to be important for the evolution and stability of cooperation because it can allow cooperative acts to be directed towards more highly related individuals on average (Griffin et al. 2004; Kreft 2004; Gilbert et al. 2007; Xavier and Foster 2007; Kümmerli et al. 2009a), thereby increasing the inclusive fitness of cooperators (Hamilton 1963, 1964a, 1964b). Cooperative traits can also be stabilized if they become pleiotropically linked to the expression of other traits important for fitness. For example, in *Dictyostelium discoidium,* mutants that under-invest in sterile stalk cells and are over-represented in the prespore zone early during chimeric development – an intermediate development fate that might be expected to result in a cheating outcome – are in fact out-competed later in development and end up under-represented in the spore population (Foster et al. 2004). The ability to respond to and produce quorum-sensing signaling molecules can also be linked to the production of cellular enzymes, resulting in a metabolic incentive to cooperate (Dandekar et al. 2012). The expression of cooperative traits can also be adjusted in response to changes in the social environment, for example as seen in *Pseudomonas aeruginosa* (Kümmerli et al. 2009b). Potentially more costly mechanisms of stabilizing cooperation involve "policing" cheater cells. *Myxococcus xanthus*, for example, evolved mechanisms to reduce the fitness advantage of specific cheaters during chimeric development in a laboratory evolution experiment (Manhes and Velicer 2011), demonstrating that cheater-control strategies can be favored by selection.

Given the importance of high relatedness for stabilizing cooperation in many cooperative systems, it is interesting that many cooperative microbes, such as the

dictyostelids and myxobacteria, engage in aggregative multicellularity (La Fortezza et al. 2022). Aggregative multicellular organisms come together to perform tasks as a group despite the potential for individual aggregating cells to have low relatedness. Aggregating into a genetic chimera can be advantageous, despite the associated potential for within-group conflict, if benefits of increasing total local cell density collectively outweigh negative effects of such conflict (Foster et al. 2002; Medina et al. 2019; Ostrowski 2019). Both *Myxococcus* and *Dictyostelium* form fruiting bodies composed of genetically distinct cells, both in nature (Gilbert et al. 2007; Kraemer et al. 2010; Sathe et al. 2010; Kraemer and Velicer 2011) and under laboratory conditions (Strassmann et al. 2000; Fiegna and Velicer 2005; Santorelli et al. 2008; Buttery et al. 2010; Rendueles et al. 2015; Pande and Velicer 2018) This chimerism can sometimes result in synergisms (Pande and Velicer 2018), but often results in competitive interactions between genotypes (Foster et al. 2002; Fortunato et al. 2003; Fiegna and Velicer 2005; Vos and Velicer 2009; Mendes-Soares et al. 2014; Rendueles et al. 2015; La Fortezza and Velicer 2021). Complex social interactions govern spore production in chimeric mixes in both species (Fiegna and Velicer 2005; Buttery et al. 2009, 2010), but little is known about the molecular mechanisms contributing to fitness in chimeras in the myxobacteria.

During chimeric multicellular development there are multiple strategies that can enhance a competitor's relative fitness. Mutations that increase the intrinsic sporulation efficiency of a genotype may translate into increased relative fitness during chimeric development (Strassmann et al. 2000; Velicer and Vos 2009). Coordinated group behaviors, like multicellular development, often rely on cell-cell communication through quorum sensing. Development in *M. xanthus*, for example, is initiated by the extracellular A signal, which accumulates in a cell-density-dependent manner and triggers expression of developmental genes when a threshold level of A signal is reached (Kuspa et al. 1992). Cells with altered responses to such developmental signals might gain relative-fitness advantages during chimeric development by entering the developmental program more quickly. However, a study

that examined this hypothesis in *M. xanthus* suggested that fast developers are not generally more fit than slower developers in chimeric groups (Nair et al. 2018). Developmental cheating can result in fitness asymmetries that are attributable to unequal metabolic investment in the production of signaling molecules or response to those molecules. Cells that invest less in signaling may be able to invest more in sporulation (Velicer et al. 2000; Fiegna and Velicer 2003). A more metabolically costly strategy may involve harming competing cells by producing antibiotics or toxins resulting in fewer competitor cells that can differentiate into spores. Strong antagonisms occur during chimeric development in *M. xanthus* (Fiegna and Velicer 2005; Vos and Velicer 2009; Rendueles et al. 2015) although the mechanisms resulting in those antagonisms have not been determined. The optimal competitive strategy likely depends on the social context, for example whether a cell is surrounded by primarily highly related, cooperative clonemates or by more genetically distant cells that may be antagonistic.

Using a nearly-saturated transposon mutant library of *Myxococcus xanthus*, we ask which mutations result in increased fitness during starvation-induced development when the spatial structure of evolving populations is repeatedly randomized. To do this, we enriched for genotypes that were proficient in spore production in chimeric mixes with their non-evolving ancestor over the course of eight cycles of growth and development in which spatial population structure was randomized by sonication after development. We also investigate the level of genetic diversity present in the evolved populations and whether population-level phenotypes are consistent with the phenotypes of clones isolated from those populations. Finally, we characterize the types of competitive strategies that result in increased fitness in the evolved populations and analyze their distribution among mutants that rose in frequency over the course of our evolution experiment.

Materials and Methods

Transposon-mutant library construction

The laboratory reference strain GJV1 is a derivative of DK1622 that differs by only a few mutations (Kaiser 1979; Velicer et al. 2006). GJV1 was electroporated with pMiniHimar in a protocol similar to that of (Chen et al. 2019). Based on previous repeated estimates of transformation efficiency, electroporated cell cultures were subdivided immediately after electroporation, before transformed cells could divide, into 40 separate pools estimated to each contain ~500 independent transposon mutants on average, so that all mutant pools would be fully non-overlapping (excepting any rare identical independent mutations that might have occurred). After subdivision, pool cultures of transformants were grown in CTT liquid with kanamycin (40 μg/mL) to high density prior to being stored frozen with 20% glycerol. DK1622 is currently estimated to have a 9.14 Mb genome containing 7,373 genes (NC_008095.1). With a library size of 19,500 mutants, we estimate to have a mutation in ~93% of the genes, assuming ever gene is nonessential and equally likely to be hit (Jacobs et al. 2003)

Experimental evolution

We designed a selection experiment to favor transposon-mutant genotypes with a relative within-group advantage at sporulation during starvation-induced multicellular development in mixture with their sporulation-proficient ancestor (GJV1). We first grew the non-evolving ancestor and 39 (one of the mutant pools was lost) transposon-mutant pools from freezer stock in CTT liquid medium (Bretscher and Kaiser 1978) at 32 °C and 300 rpm shaking. After all cultures reached turbidity but were still in log-phase growth, we centrifuged them at 12,000 rpm for five minutes, removed the supernatant and resuspended them to a density of ~5 x 10^9 cells/mL in TPM buffer (Bretscher and Kaiser 1978). The high-density transposon cultures were each mixed as a 25% minority with the non-evolving ancestor. 50

μL of the chimeric populations (total population size of ~2.5 x 10^8) were then spotted onto to TPM 1.5% agar plates and allowed to dry completely before being incubated at 32 °C and 90% relative humidity (rH) for five days. After five days of starvation, cell populations were harvested using a sterile scalpel and resuspended in 1 mL of sterile double-distilled water, incubated at 50 °C for two hours, and sonicated to disperse the spores. Since non-spore cells do not survive the heat and sonication treatment and because only a fraction of the population entering development becomes spores, the selection pressure in this experiment was very stringent. 200 μL of the dispersed spore suspensions were used to quantify the spore production of the total chimeric population and the kanamycin-resistant subpopulation by dilution plating into liquid-phase CTT 0.5% agar with and without 40 μg/mL kanamycin, respectively. Dilution plates were incubated at 32 °C and 90% rH for six days to allow spores to germinate and grow to a clearly visible colony size for counting. The remaining cell suspensions were transferred to fresh CTT liquid medium supplemented with 40 μg/mL kanamycin allowing only the kanamycin-resistant transposon mutants to grow. We repeated these steps for eight selection cycles.

Competition assays

We performed developmental competition assays with evolved transposon-mutant populations from the end of cycle 4 as well as with clones selected from the final cycle (cycle 8) of the evolution experiment. As in the evolution experiment, whole populations or clones as well as GJV1 were grown to turbidity from freezer stock in CTT liquid at 32 °C with 300 rpm shaking. All cultures were resuspended to ~5 x 10^9 cells/mL in TPM buffer and the transposon-mutant populations or clones were mixed with the ancestor as a 25% minority. Pure-culture sporulation assays were also performed in parallel. Chimeric populations and pure cultures were starved at 32 °C and 90% rH for five days, after which we measured the spore production

of the chimeric populations and the fraction of spores contributed by the transposon-mutant

populations or clones as well as the pure-culture spore production of all strains.

Sporulation parameters

Spore counts were analyzed as in (Fiegna and Velicer 2005). The pure-culture

sporulation efficiency (proportion of cells that survived development as spores) is calculated

as the parameter *D* for a given strain *i* as follows:

$$D_{i} = N_i(t_5)/N_i(t_0)$$

where $N_i(t_5)$ represents the number of spores counted after five days of development

and $N_i(t_0)$ is the number of cells that entered development (2.5×10^8 for pure culture assays).

The sporulation efficiency of strain *i* when mixed with strain *j* is then:

$$D_i(j) = N_i(j, t_5)/N_i(j, t_0)$$

The one-way mixing effect is the effect of mixing strains *i* and *j* on the sporulation

efficiency of strain *i:*

$$C_i(j) = \log(D_i[j]) - \log(D_i)$$

A positive $C_i(j)$ value indicates that strain *i* sporulates more efficiently in presence of

strain *j* than in pure culture while a negative value indicates that strain *i* sporulates less

efficiently in presence of strain *j*. The relative sporulation efficiency of two strains during

chimeric development is calculated as:

$$W_{ij} = \log(D_i[j]) - \log(D_j[i])$$

When the W_{ij} parameter is positive, then the focal strain *i* produces more spores per a

given number of input cells than strain *j*. When W_{ij} is negative, then strain *j* is converts more

cells into spores than strain *i*.

The bidirectional effect of mixing shows the impact of chimeric development on total

group spore production. It is calculated as the total number of spores produced during chimeric

development relative to the total number of spores produced by the strains in pure culture (corrected for their mixing frequency, *e.g.* strain *i* mixed at 75% and strain *j* at 25%).

$$B_{ij} = \log ([N_i(j, t_5) + N_j(i, t_5)]/[N_i(t_5) * 0.75 + N_j(t_5) * 0.25])$$

If chimeric development has no effect on group-level spore production, B_{ij} is zero; negative B_{ij} values result from pure-culture spore production of the mixed strains being greater than chimeric spore production and positive values indicate increased total spore productivity in chimera.

Statistical methods

Analyses were performed using R version 4.3.0 and Rstudio version 2023.03.1+446 (Team 2023; team 2023). We fitted a mixed linear model using the lmer() function from the lme4 R package (Bates et al. 2015) to our dataset of log-transformed sporulation data with the interaction between evolution state (ancestor or cycle-4 evolved) and chimeric treatment (pure culture spores, total chimeric spores or transposon-derived chimeric spores) as a fixed effect and replicate nested into strain as a random effect. The model was followed by type III ANOVA using the car R package (Fox and Weisberg 2019) and comparisons of the marginal means of the ancestral mutant pools vs the evolved mutant pools within each chimeric treatment category (corrected for multiple testing with the Tukey method) using the emmeans R package (Length 2023). A similar analysis was done on the calculated sporulation parameter data and in cases where sporulation parameters were compared to zero a Benjamini & Hochberg correction was used. The clone level data was similarly analyzed with a mixed linear model with the sporulation parameter as a fixed effect and replicate nested into clone nested into strain as a random effect, followed by type III ANOVA and comparison of the marginal mean of each sporulation parameter versus zero (corrected for multiple testing using the Benjamini & Hochberg method).

Results

Evolution with a non-evolving ancestor resulted in increased relative fitness of the transposon-mutant pools

We designed an evolution experiment aimed at enriching for transposon mutants with increased relative fitness during chimeric development with their ancestor (GJV1). We evolved 39 populations, each composed of ~500 independent transposon mutants on average, in cycles of starvation-induced multicellular development where they competed in the minority (25%) against their non-evolving ancestor GJV1. Kanamycin-resistant spores then germinated and grew vegetatively in selective growth medium (Figure S1). The spores produced by the ancestor are kanamycin-sensitive and therefore did not compete with the spores from the transposon populations during vegetative growth. We ran the experiment for a total of eight selection cycles.

In the first, second and third cycles of development, the transposon-mutant subpopulations collectively increased from 25% at the onset of each development phase to ~38%, ~55%, and ~87%, on average, among heat-resistant spores at the end of each cycle, respectively. In the subsequent cycles, the degree of increase from 25% leveled off after a dip in the fourth cycle, remaining relatively constant over the last four cycles (Figure S2). Not only did the frequency of transposon mutants increase over the course of evolution but so did the absolute number of transposon spores (Figure S2). Chimeric interactions can result in changes in group-level productivity, absolute fitness changes in one or more interactants, and fitness asymmetries between interacting individuals (Vos and Velicer 2009). In order to distinguish between potential competitive strategies used during chimeric development, pure-culture spore production data is necessary.

One potential way to increase relative fitness during chimeric interactions is by reducing investment in costly cooperative behaviors and capitalizing on their expression by

other cells (cheating). Developmental cheaters have increased relative fitness in mixture with cooperators, but if the frequency of cheaters becomes too high the total group productivity may decline (Velicer et al. 2000; Fiegna and Velicer 2003; Diggle et al. 2007). By analyzing the trends in kanamycin-resistant spore production (transposon-mutant-derived spores) for each individual population in mixture with the ancestor combined with the spore productivity of the chimeric group, we could identify three evolved populations that show spore-production patterns suggestive of developmental cheating. Populations Tn14, Tn27, and Tn29 increased their frequencies beyond the 25% initial mixing frequency and appear to impose a chimeric load (reduced spore production of the chimeric group), which is consistent with the trends expected of developmental cheaters (Figure S3).

Evolved transposon populations show sporulation trends consistent with facultative exploitation

To further characterize the competitive strategies of the evolved populations, we measured the spore production of a subset of 18 transposon populations both in pure culture and in chimeric mixes with GJV1 (1:3 initial ratio) both for the ancestral transposon-mutant pools and their descendent populations after cycle 4 of the experiment. Pure-culture spore production of the ancestral mutant pools was not significantly different from that of GJV1 despite the genetic diversity resulting from the coexistence of many mutants (Figure 1A, mixed linear model: evolution state x chimeric treatment interaction, $Chi^2 = 24.095$, $p < 0.0001$, Tukey contrasts on mutant pool marginal means vs GJV1: ancestral vs GJV1 $t_{37.8} = -0.652$, $p = 0.792$, cycle-4 vs GJV1 $t_{37.8} = -1.022$, $p = 0.568$). The evolved populations also did not significantly increase or decrease in their pure-culture spore production compared to that the ancestral mutant pools (Figure 1A, mixed linear model: evolution state x chimeric treatment interaction, $Chi^2 = 24.0952$, $p < 0.0001$, Tukey contrasts on ancestral vs evolved marginal means $t_{271.9} = 1.272$, $p = 0.413$). This indicates that if developmentally-defective cheaters are present in the

evolved populations, they are present at frequencies not detectably detrimental to population

productivity in pure culture.
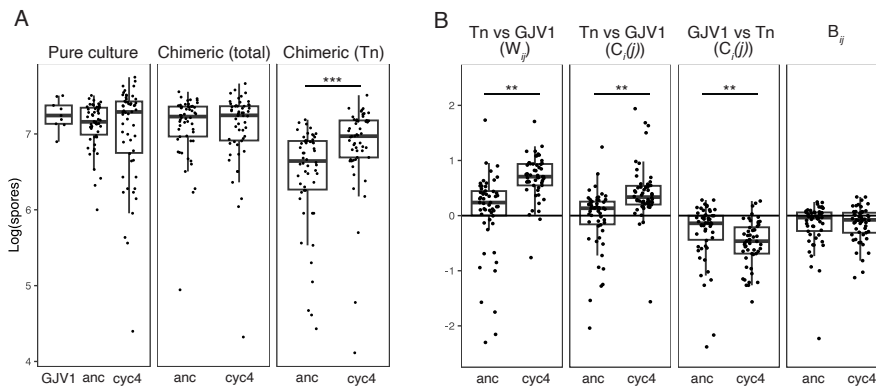
Figure 1. Evolved transposon-mutant pools are more competitive during chimeric development with GJV1 than their ancestral pools. A) Comparison of the pure-culture spore production of GJV1, ancestral, and evolved (cycle 4) transposon mutant pools (left); total spore production (chimeric) of the ancestral and evolved transposon mutant pools in mixture with the GJV1 (middle); and the number of spores produced by the transposon (Tn) mutant pools during chimeric development with GJV1 (right). *** indicates significant difference with $p < 0.0001$ after fitting a mixed linear model: evolution state (anc or cyc4) x chimeric treatment, $Chi^2 = 24.095$, $p < 0.0001$; and performing Tukey contrasts on ancestral vs evolved marginal means. **B**) Relative fitness (W_{ij}) of the transposon-mutant pools during chimeric development with GJV1; one-way effect of mixing ($C_i(j)$) with GJV1 on the spore production of the transposon-mutant pools; one-way effect of mixing ($C_i(j)$) with the transposon-mutant pools, either ancestral or cycle-4 evolved, on the spore production of GJV1; and the bidirectional effect of mixing (B_{ij}) during chimeric development. The horizontal line at 0 shows the null expectation of no effect of mixing. Each point shows one biological replicate of one transposon mutant pool (18 pools in total). N = three biological replicates. ** indicates significant difference with $p = 0.005$ (or lower) after fitting a mixed linear model: evolution state (anc or cyc4) x sporulation parameter interaction, $Chi^2 = 41.97$, $p < 0.0001$, and performing Tukey contrasts on ancestral vs evolved marginal means.

Total spore production in chimeric mixtures with GJV1 was also not significantly

different between the ancestral mutant pools and the evolved populations (Figure 1A, mixed

linear model: evolution state x chimeric treatment interaction, $Chi^2 = 24.0952$, $p < 0.0001$,

Tukey contrasts on ancestral vs evolved marginal means $t_{271.9} = 0.321$, $p = 0.945$). However,

as expected from trends we observed during the evolution experiment (Figure S2), the number

of spores produced by the cycle-4 evolved populations in mixture with GJV1 was greater than

that of the ancestral pools (Figure 1A, mixed linear model: evolution state x chimeric treatment

interaction, $Chi^2 = 24.0952$, $p < 0.0001$, Tukey contrasts on ancestral vs evolved marginal

means $t_{271.9} = -5.165$, $p = < 0.0001$). Correspondingly, the fitness of the cycle-4 evolved

populations relative to their ancestor GJV1 (W_{ij}) significantly increased over the course of

evolution (Figure 1B, mixed linear model: evolution state x sporulation parameter interaction, Chi^2 = 41.97, p < 0.0001; Tukey contrasts on ancestral vs evolved marginal means t_{371} = -5.565, p < 0.0001).

That the increased fitness of cycle-4 evolved populations in mixture with their ancestor was not associated with either an increase or a decrease in their average pure-culture productivity suggested that the most common genotypes in those populations did not increase in fitness by either i) increasing their intrinsic sporulation level or ii) becoming developmentally-defective cheaters, respectively. A third possibility is that many populations evolved to increase their sporulation efficiency in response to being mixed with the ancestor without incurring major defects in pure-culture sporulation, a pattern of sporulation performance known as facultative exploitation (Fiegna and Velicer 2005). In a fourth possibility, populations might have evolved to decrease sporulation by their ancestor.

To begin testing between these modes of fitness increase, we calculated the one-way mixing effect $C_i(j)$ for both the 18 cycle-4 transposon-mutant populations and GJV1 in mixture. On average, although both the ancestral and evolved transposon populations benefited in the presence of GJV1 (Figure 1B), the average $C_i(j)$ among the transposon-mutant populations increased significantly over the course of evolution (mixed linear model: evolution state x mixing effect interaction, Chi^2 = 41.97, p < 0.0001; Tukey contrasts on ancestral vs evolved marginal means t_{371} = -3.439, p = 0.0007). Inversely, the transposon populations evolved to reduce the sporulation efficiency of GJV1 (mixed linear model: evolution state x mixing effect interaction, Chi^2 = 41.97, p < 0.0001; Tukey contrasts on ancestral vs evolved marginal means t_{371} = 2.806, p = 0.0053). Overall, these sporulation trends are consistent with the hypothesis that genotypes capable of facultative exploitation rose to high frequency in many of the transposon-mutant-derived evolved populations.

Due to the transposon-mutant populations always entering developmental competitions as a 25% minority, the likelihood of them significantly increasing or decreasing

the bidirectional effect of mixing parameter (B_{ij}) is low. Accordingly, we found that B_{ij} for competition mixes did not significantly change during evolution (Figure 1B, mixed linear model: evolution state x mixing effect interaction, Chi^2 = 41.97, p < 0.0001; Tukey contrasts on ancestral vs evolved marginal means t_{371} = 0.274, p = 0.78) and also is not significantly different from zero (Figure 1B, mixed linear model: evolution state x mixing effect interaction, Chi^2 = 41.97, p < 0.0001; Benjamini & Hochberg contrasts on ancestral and evolved marginal means vs 0, t_{424} = -1.730, p = 0.084 (ancestral), t_{424} = -2.115, p = 0.07 (evolved). This further confirms the pattern we observed during the evolution experiment where, on average, the transposon populations increased their fitness in mixture with the ancestor without negatively impacting total group productivity.

Evolved transposon populations are composed of phenotypically distinct clones

To further investigate the mechanisms responsible for the observed fitness increases, we isolated three clones from each evolved population after the 8th selection cycle for phenotyping. Analysis of the clones revealed that ~60% of the 3-clone sample sets are composed of phenotypically distinct clones, as measured by fruiting-body formation and pure-culture spore production (Figure S4 and S5), and that 31 of the 39 populations had at least one developmentally proficient clone present at high frequency (Figure S5).

As with the cycle-4 whole-population samples, we also performed developmental-competition experiments with mixes of the evolved clones (initially 25%) with GJV1 (initially 75%). Like in the whole-population experiments, we found that the average W_{ij} of the evolved clones was also significantly above zero (Figure 2, mixed linear model: sporulation parameters, Chi^2 = 55.438, p < 0.0001; Benjamini & Hochberg contrasts on W_{ij} marginal mean vs 0, t_{1007} = 5.362, p < 0.0001) showing that the evolved clones also had higher relative fitness during chimeric development. Also like the whole-population experiments, average spore production by the evolved clones was positively affected by the presence of GJV1, with $C_i(j)$

values being significantly greater than the null expectation of zero (Figure 2, mixed linear

model: sporulation parameters, Chi^2 = 55.438, p < 0.0001; Benjamini & Hochberg contrasts

on $C_i(j)$ marginal mean vs 0, t_{1007} = 8.111, p < 0.0001). The average B_{ij} value across all

ancestor/evolved clone mixes did not significantly differ from zero (mixed linear model:

sporulation parameters, Chi^2 = 55.438, p < 0.0001; Benjamini & Hochberg contrasts on B_{ij}

marginal mean vs 0, t_{1007} = -1.399, p = 0.162).
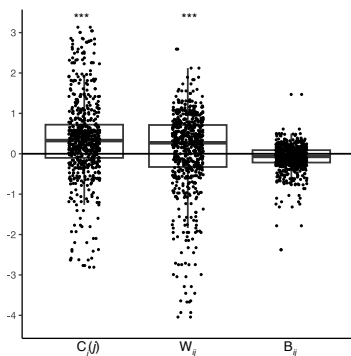
Figure 2. Evolved transposon-mutant clones are on average positively affected by chimeric development with GJV1. The calculated one-way mixing effect of GJV1 on all 116 transposon mutant clones is on average positive, as is the relative fitness of transposon clones in mixture with GJV1. The bidirectional effect of mixing is not significantly different from the null expectation of 0. Three clones were isolated from each of the 39 evolved populations after eight cycles of selection. Each point shows one biological replicate of one transposon mutant clone; three biological replicates were performed for each clone. Clones with sporulation parameters outside of the axis limits were included in the statistical analysis but are not shown in the plot. *** significant difference from the null with p < 0.0001 after fitting a linear mixed model: sporulation parameters, Chi^2 = 55.438, p < 0.0001, and performing Benjamini & Hochberg contrasts on the marginal means of each sporulation parameter versus 0.

Evolved clones exhibit diverse strategies in competition with their ancestor

Developmental competitions between the evolved clones and GJV1 revealed a range

of potential mechanisms used to become more developmentally competitive. We classified

each clone based on the pattern of parameter-value signs for its estimated pure-culture spore

production relative to its ancestor, and for both its one-way mixing effect ($C_i(j)$) and relative

fitness (W_{ij}) during chimeric development with GJV1 (Figure 3, Table 1, Table S2, Figures S5

and S6). Given the large number of comparisons for this dataset, our statistical power for

individual tests was limited and we therefore used consistency vs inconsistency of parameter-

value signs across replicates as our classification criteria. Specifically, we determined the

directionality (above or below the null expectation) of each data point, and if all three biological replicates were negative or all three were positive, a classification of either reduced or increased $C_i(j)$, W_{ij}, or pure-culture spore production was assigned, respectively. If the value signs were not consistent across all replicates, a clone was classified as having no difference in the measured value from the null expectation. This classification method is more stringent than simply using the sign of the mean of all replicates but less stringent than requiring statistically significant differences from zero for individual-mean comparisons after correcting for multiple testing. This approach allows us to analyze the general trends present in this large dataset despite having limited statistical power for individual tests. Further verification of the results, for example with additional competition replicates and through molecular analysis, will be important for drawing further conclusions in individual cases.

Table 1. *Performance classifications of the evolved transposon mutant clones.*

Classification	relative fitness of clone (W_{ij})	Pure culture	One-way mixing effect on clone ($C_i(j)$)	Number of clones in each category
Cheaters (Ch)	+	-	+	20
Facultative exploiters (E)	+	=	+	19
Increased pure-culture sporulators (P)	+	+	-/=	9
GJV1 sporulation suppressors	+	-	=	2
Disadvantaged cooperators (DC)	-	+/=	+/-/=	8
Disadvantaged defectors (DD)	-	-	+/-/=	16
Cooperator (Coop)	=	=	+/-/=	17
Complemented (Comp)	=	-	+/=	25

We first grouped clones based on the relative-fitness values and found that 50 out of the 116 clones had increased relative fitness in mixture with GJV1 (Table 1). Within this category, we could further group clones based on pure-culture spore production and one-way mixing effect $C_i(j)$. This resulted in four competitive strategies to increase relative fitness in chimera: cheating, facultative exploitation, increased intrinsic sporulation, and decreasing the sporulation of GJV1. Within the group of developmental winners, cheating was the most frequently evolved strategy (20 clones), but facultative exploitation (19 clones) and increased pure culture sporulation (9 clones) were not uncommon. Suppressing the spore production by GJV1 was not a commonly evolved strategy but did occur in two of the winning clones.
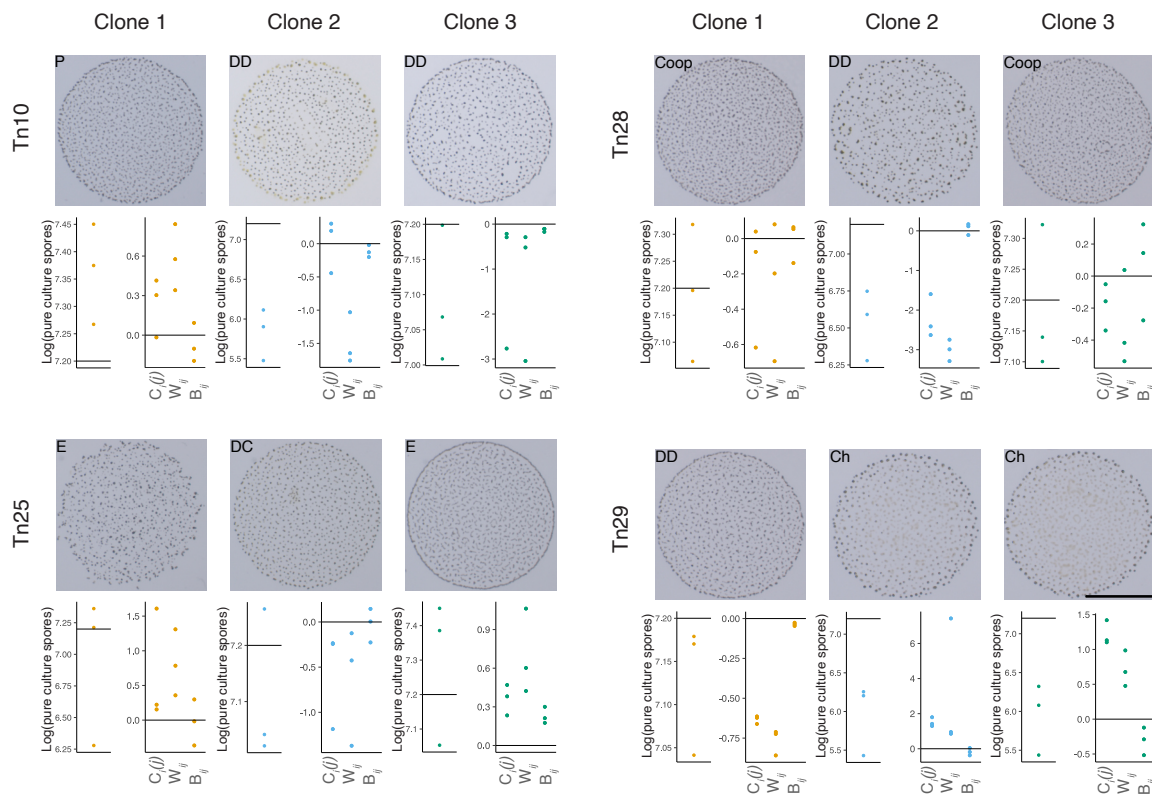
Figure 3. Clones isolated from the evolved transposon-mutant pools are phenotypically diverse, and these differences result in distinct competitor classifications. Images of pure-culture developmental plates after 5 days of starvation for all clones isolated from four of the mutant pools. The respective pure-culture spore production and $C_i(j)$, W_{ij}, and B_{ij} values in mixture with GJV1 are shown under each image. Competitor classifications assigned as outlined in Table 1 are printed at the top of the images. Scale bar is 0.5 cm. The horizontal line on the pure culture graphs shows the null expectation of no deviation from the average pure culture spore production of GJV1. The horizontal line at 0 shows the null expectations of no effects of mixing on clone and total-group spore productivity ($C_i(j)$ and B_{ij}, respectively) and of no fitness difference from the ancestor development. Three biological replicates were performed per clone per assay; each point represents a value from one replicate.

Twenty-four clones appear to have lower relative-fitness values during pairwise interactions with GJV1 (Table 1). Sixteen of the competitive losers were also found to be defective in pure culture, resulting in the classification of disadvantaged defectors (Velicer and Vos 2009). The final eight losers were deemed disadvantageous cooperators due to their pure-culture sporulation proficiency. Given that the design of the evolution experiment favored mutants with high spore production in mixtures with GJV1 present as 75% of the population at the start of each developmental phase, it is interesting to find genotypes that are likely present at high frequency in the evolved populations but have decreased fitness in pairwise mixes with GJV1. Due to their social defects and pairwise fitness disadvantages to GJV1, we would have expected such genotypes to be selected against. However, it is possible that other high-frequency transposon mutants can either partially or fully complement the disadvantageous defectors which is expected to slow their loss from a population (Velicer and Vos 2009).

The remaining 42 clones had W_{ij} values that did not differ from the null expectation based on our criterion of value-sign consistency and therefore there was no clear fitness asymmetry during chimeric development. Twenty-five of the equally fit clones had pure-culture sporulation defects and were therefore complemented in pairwise mixes with GJV1 (Table 1). The other 17 clones were sporulation proficient in pure culture and were classified as cooperators. Overall, we found that the evolved populations are composed of multiple clones likely present at high frequency, and these clones differ extensively in their performance patterns considering both pure-culture assays and competitiveness in pairwise mixes with GJV1.

Discussion

Competition in structured populations of social organisms can occur at different scales (*e.g.* more locally within groups versus more globally, including between groups) when

population structure is maintained across generations. The scale of competition and relatedness between individuals in a population can have implications for the evolution of cooperation (Frank 1998; Griffin et al. 2004). Here, we evolved a nearly saturated transposon mutant library under conditions that eliminated spatial structure after each selection cycle, thereby focusing on what forms of within-group adaptation can evolve in an aggregative-multicellular form of cooperation when there is no between-group component of selection. We found that the formation of multicellular fruiting bodies and spores was high in the ancestral mutant pools and remained high throughout the selection experiment at the population level. The elimination of spatial structure between selection cycles created a virtually equal chance of interaction with any other competitive genotype within each population during both vegetative growth and development. Under these conditions we found that the evolved populations were often comprised of multiple clones that differ in whether they have increased relative fitness during pairwise interactions with the non-evolving ancestor GJV1 and in their fitness patterns when both pure-culture and chimeric-competition outcomes are considered (Table 1).

A similar study that evolved mutant libraries of *D. discoideum* during chimeric development found 77.5% of isolated clones had a relative fitness advantage over their non-mutant ancestor. Among those developmental winners, both cheating by strains defective in pure culture and "facultative cheating" – defined in their study as a strain that is cooperative in pure culture winning over another strain in chimera – phenotypes were common. Facultative cheating phenotypes resulted from mutations in many genes comprising diverse molecular pathways (Santorelli et al. 2008), indicating that there are many genetic routes to improving fitness in chimeric groups without losing fitness in pure groups in *D. discoideum* (Santorelli et al. 2008). We similarly found that many *M. xanthus* strains evolved to outcompete their ancestor at spore production without incurring defects in pure-culture performance. This concordance of outcomes across systems suggests that aggregative multicellular organisms

in general often have many modes of increasing social competitiveness that do not trade off against intrinsic proficiency at within-genotype cooperation. We found that increased pure-culture sporulation was also a moderately common strategy, being associated with increased relative fitness in ~18% of the evolved clones. Thus, between the three major competitive strategies of facultative exploitation, cheating and increased pure-culture sporulation, no single strategy was clearly better or more easily evolved than the others in our experiment. This study differs from Santorelli *et al.* primarily in that we classify evolved clones not only based on their relative performance in chimera with the ancestor and pure-culture performance, but also based on whether their absolute spore production increases in response to mixing with the ancestor (*i.e.* whether their $C_i(j)$ values are positive). We find that most evolved competition winners (39/50, 78%) appear to have evolved to exploit GJV1 (*i.e.* positive $C_i(j)$ values), including both cheaters and facultative exploiters. This outcome suggests that there may be many genetic routes to evolving the ability to socially exploit other genotypes in *M. xanthus.*

We found that 29 out of the 39 evolved populations maintained at least one developmentally proficient clone at high frequency, and of the ten populations apparently composed of only developmentally defective clones, only one was composed of only cheaters. The frequency of cheaters therefore appears to have been limited within the majority of evolved populations. Socially defective genotypes can be controlled by negative frequency dependent selection (Velicer et al. 2000; Fiegna and Velicer 2003), however because the transposon populations were always mixed in the minority with their non-evolving ancestor, we would not expect negative frequency dependence to prevent socially defective cheaters from rising to high frequency. In theory, some of the social defectors, particularly the ones that do not have relative fitness advantages in mixture with GJV1, may somehow be able to cheat only when other mutants in their evolved population are present but not in pairwise mixes with only GJV1. In this case, negatively frequency-dependent fitness advantages of cheaters may

have resulted in their maintenance around an equilibrium frequency in the evolved populations. It is also possible that many of the strains classified as being complemented by GJV1 (pure culture defect and equal relative fitness) would be shifted to the cheater category if more replicates revealed that their W_{ij} values were above the null expectation. Similarly, some facultative exploiters may shift to the cheater category if more replicates clarify whether they have a pure culture defect. If that were to be the case, then there could more populations where cheaters went to fixation.

The limits of our competitor classification method have prompted us to explore alternative methods of analyzing the results of the clonal competition assays, such as a model-based clustering approach (Scrucca et al. 2023). We will then be able to determine whether our current classification method is a good representation of the data based on the level of agreement between our method and the model. Further work is also needed to identify the genes and molecular pathways that are important in generating the evolved competitive strategies described in this study. We are doing this with a combination of whole genome sequencing and manual transposon mapping (Chen et al. 2019). We will then construct mutants in the GJV1 background and test for effects of the mutations on the competitive phenotypes.

It will be interesting to learn whether the genes disrupted by transposon insertion are the primary determinants of the competitive phenotypes or whether spontaneous mutations that accumulated over the course of evolution are also important. Here, we used a transposon-mutant library to investigate the range of genetic innovations that can be generated by transposon insertions that can result in a relative fitness advantage during chimeric development. However, the types of spontaneous mutations that are favored by selection in *M. xanthus* may differ. A comparison of spontaneously evolved competitive strategies would therefore also be informative and may better recapitulate what happens in natural populations.
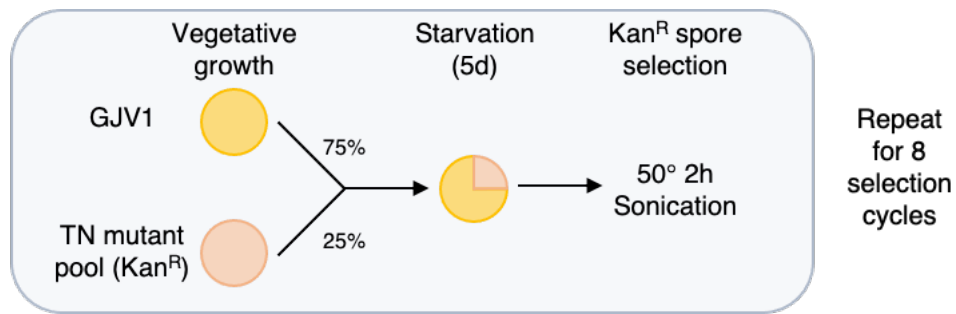
Figure S1. Selection for genotypes with increased fitness during chimeric multicellular development with a non-evolving ancestor using a nearly saturated transposon mutant library. 39 kanamycin-resistant transposon mutant pools, represented by the red circle, were grown to turbidity along with their non-evolving ancestor (yellow circle). Vegetatively grown cells were resuspended to high density and mixed for multicellular development with the mutant pools as a 25% minority. The chimeric populations competed during development for five days, followed by selection for heat-resistant spores. Only the kanamycin-resistant mutant pools were allowed to evolve and GJV1 was grown fresh from freezer stock for each selection cycle. The experiment was carried out for eight selection cycles.
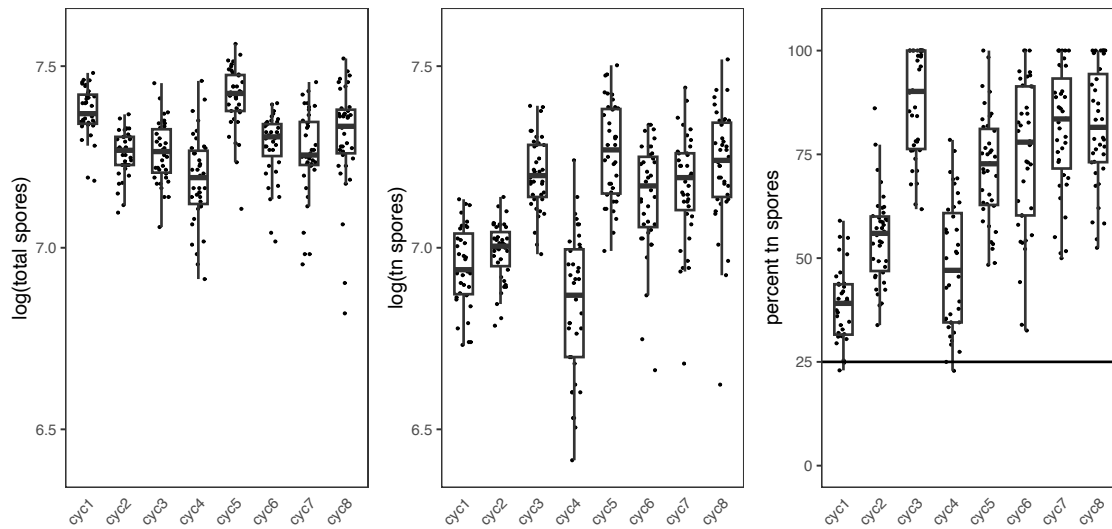
Figure S2. Selection for increased spore production during chimeric development resulted in transposon populations with increased relative fitness. Data collected while conducting the evolution experiment shows that the total spore production of the chimeric groups does not appreciably change after eight selection cycles (left). The absolute number of spores contributed by transposon mutants is higher after eight selection cycles (middle). The higher absolute number of transposon spores corresponds to an increased frequency of transposon derived spores (right). The selection cycle is shown on the *x* axis and the log-transformed spore production or percent of transposon spores in chimeric mixes is shown on the *y* axes. The horizontal black line in the right panel depicts the null expectation of no change from the initial mixing frequency.

55
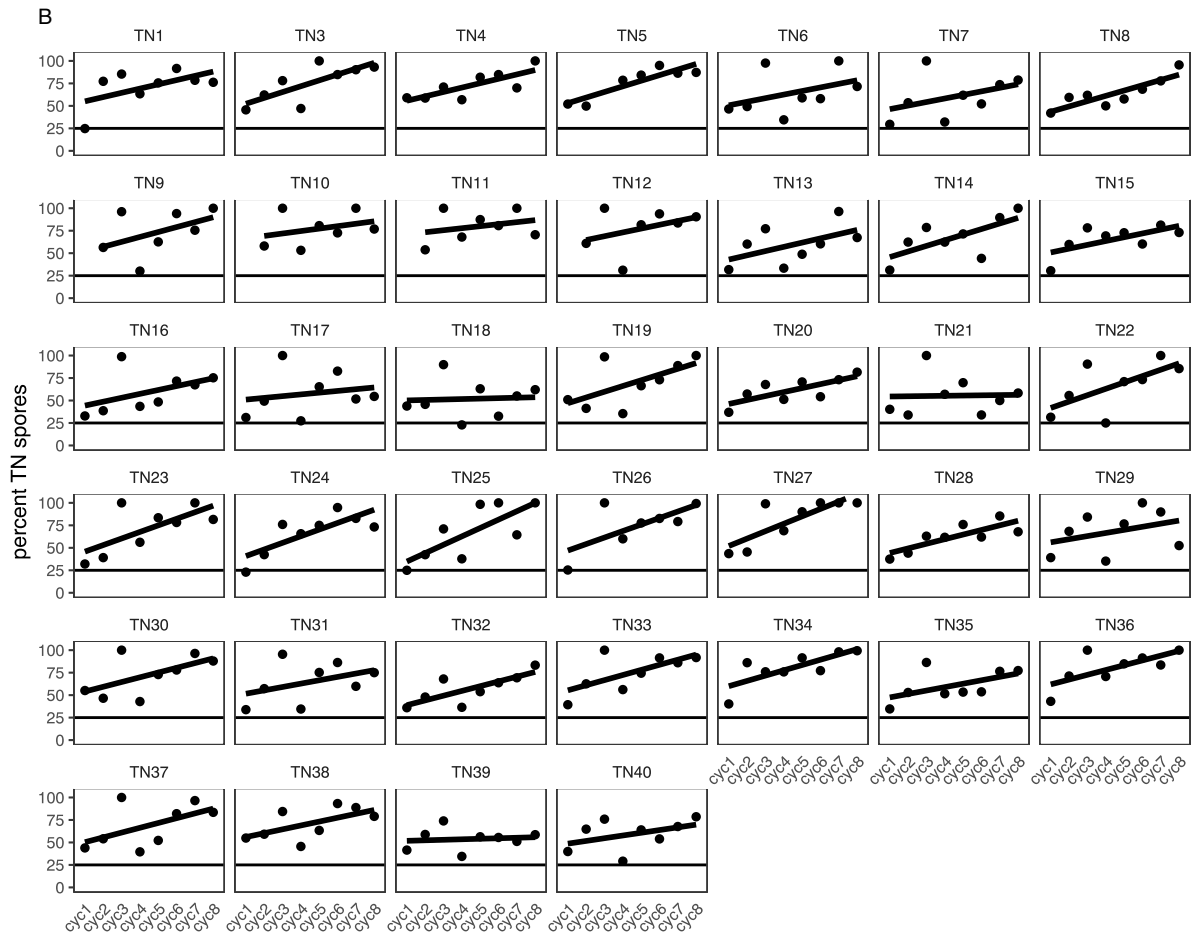
Figure S3. Transposon populations have distinct sporulation trends during evolution with GJV1. Sporulation data for each transposon population collected during the evolution experiment. **A**) The log-transformed total spore production of chimeric groups (*y* axis) over eight selection cycles (*x* axis). **B**) The percent of spores produced by the transposon-mutant populations in chimeric development with GJV1. Horizontal black lines show the null expectation of no deviation from the initial mixing frequency of 25%. Data points show the sporulation data and trend lines are linear regressions.
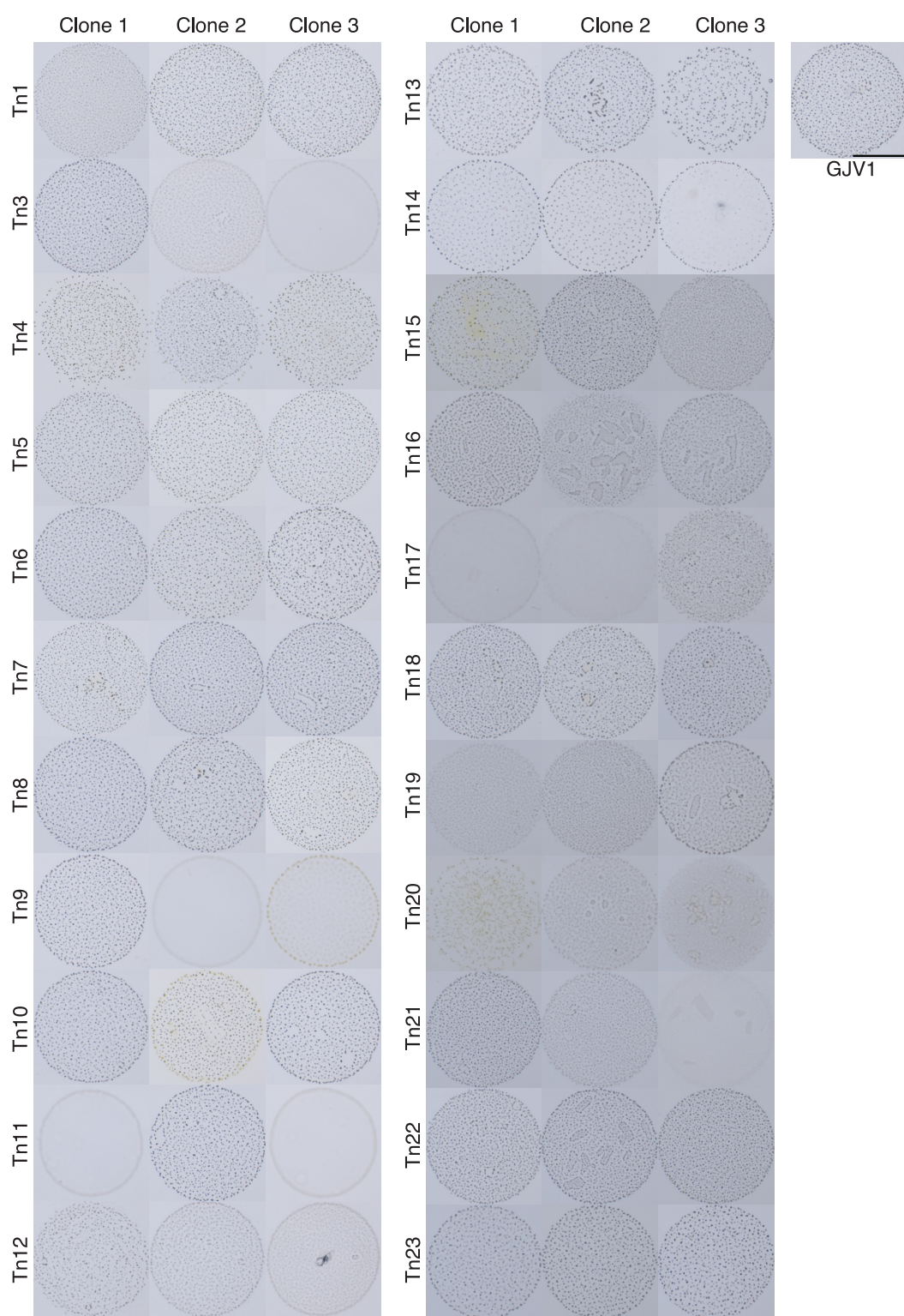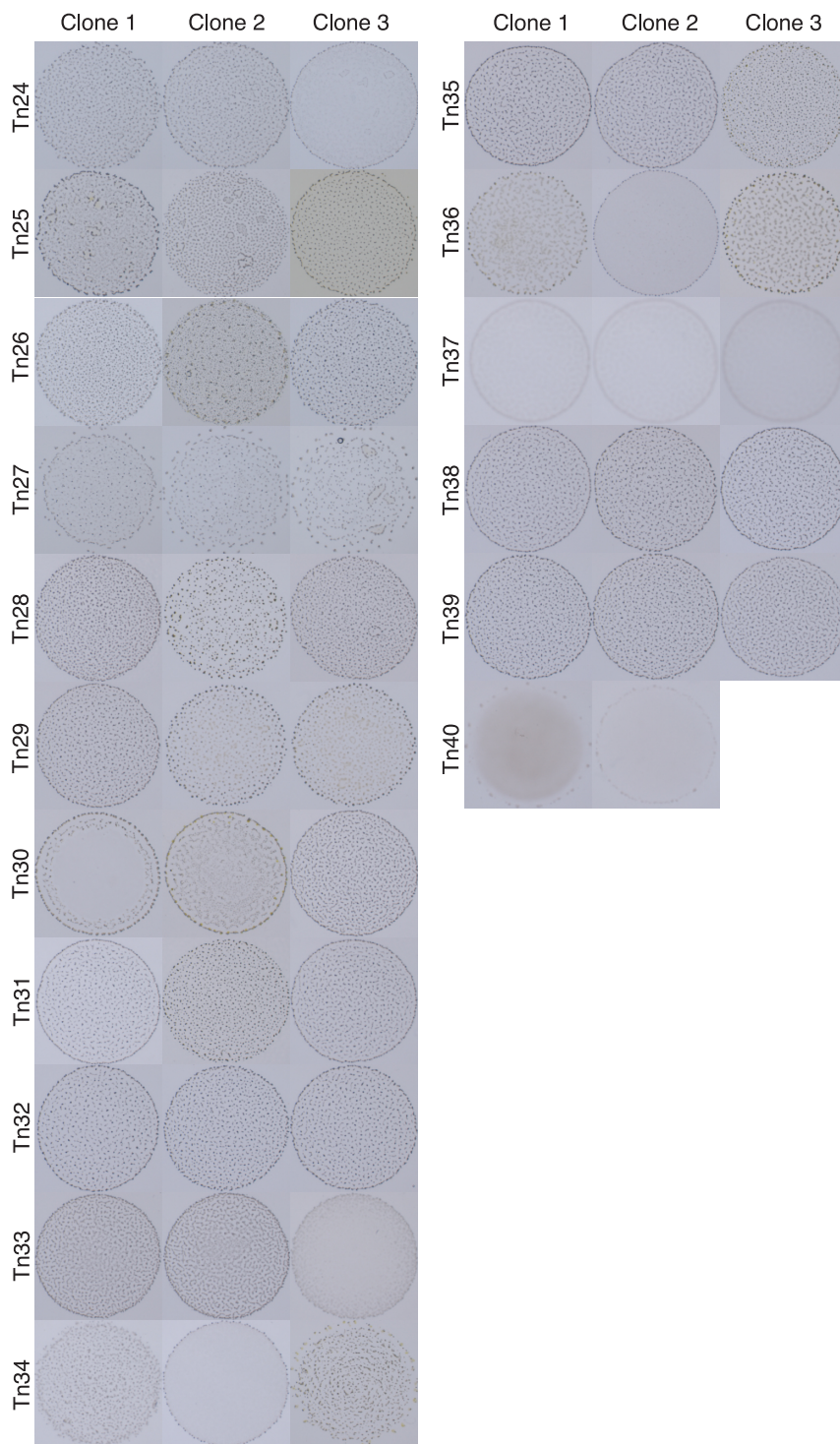
Figure S4. The evolved transposon mutant populations are composed of phenotypically distinct clones. Representative images of the phenotypes of all evolved transposon-mutant clones and the ancestor (GJV1) after five days of starvation-induced development in pure culture. Scale bar = 0.5 cm, Three biological replicates were performed for each clone, except Tn40c3 which does not grow well in liquid culture and therefore was not included.
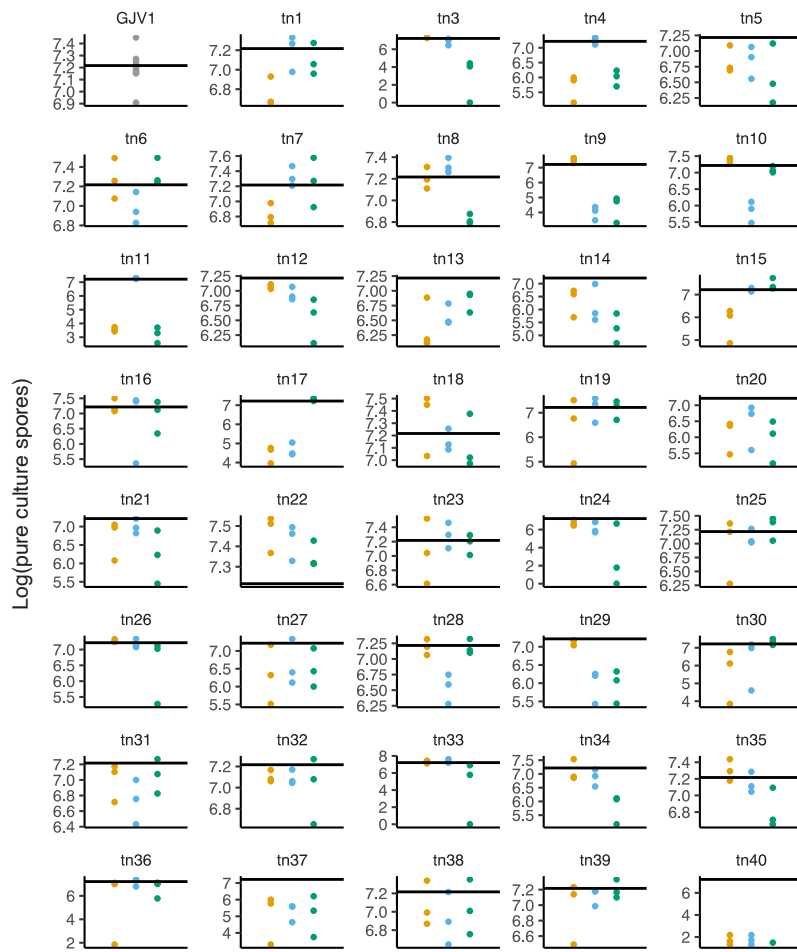
Figure S5. Evolved clones differ in their pure-culture sporulation levels. The log-transformed pure-culture spore production of all evolved transposon mutant clones as compared to their ancestor (GJV1). The horizontal black bars show the null expectation of no deviation from the average pure culture spore production of GJV1. The three clones selected from each evolved population (population number shown above each plot) are displayed in different colors. Three biological replicates were performed for each clone, except Tn40c3 which does not grow well in liquid culture and therefore was not included in subsequent analyses.

.
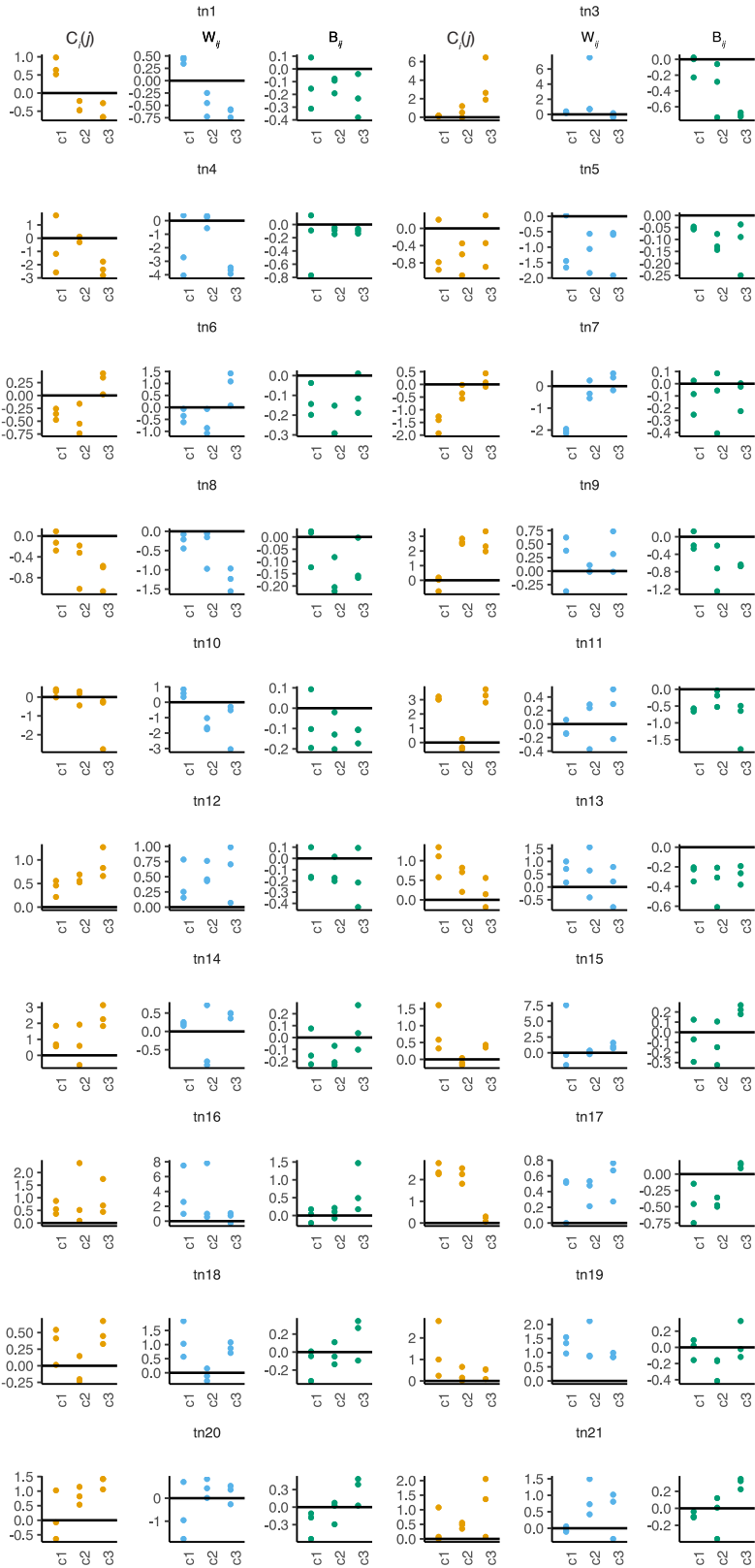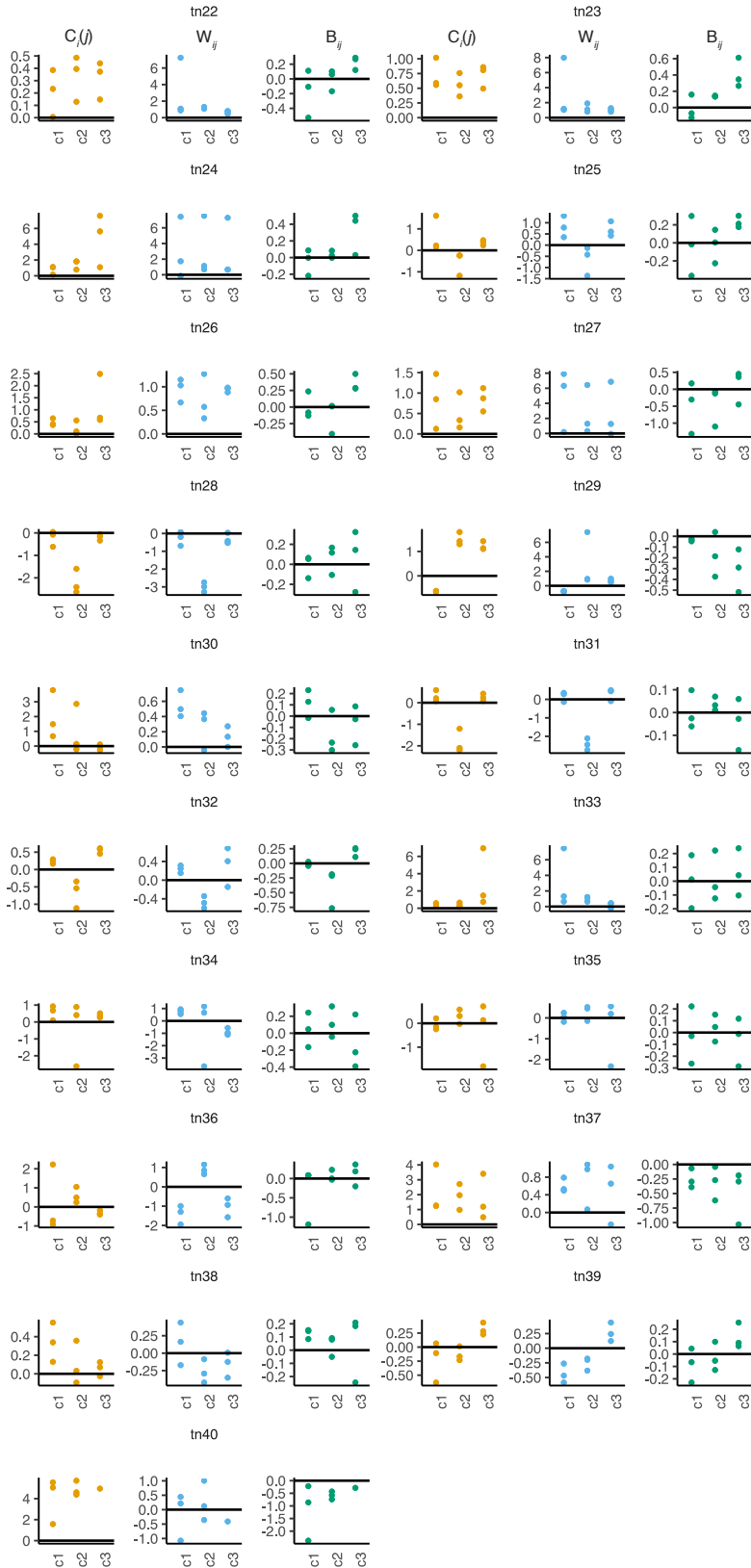
Figure S6. Evolved clones differ in their competitive interactions with GJV1. The one-way effect of mixing ($C_i(j)$) and relative fitness (W_{ij}) of the focal evolved clone during chimeric development with GJV1 and the bidirectional effect of mixing (B_{ij}) the focal clone with GJV1. Each plot shows the sporulation parameter (indicated each column of plots) for all three clones isolated from each evolved population (indicated above each set of three plots). Horizontal black lines show the null expectation of no effect of mixing on the spore production of the evolved clones ($C_i(j)$), no relative fitness difference between the mixed strains (W_{ij}), or no deviation of group productivity from that predicted by the pure culture spore performance of the mixed strains (B_{ij}). Each data point shows the calculated parameter of one biological replicate; three biological replicates were performed for each clone, except Tn40c3 which does not grow well in liquid culture and therefore was not included in subsequent analyses.

Table S2. *Classification of competitor type for all evolved clones based on their values for pure-culture sporulation, $C_i(j)$, and W_{ij} assigned as described in Table 1. Positive and negative values for pure-culture sporulation, $C_i(j)$, and W_{ij} were assigned when all biological replicates had values above or below the null expectations, respectively. Equal values were assigned when the biological replicates had values both above and below the null expectations.*

Strain	Clone	Relative fitness of clone (W_{ij})	Pure culture	One-way effect of mixing with ancestor ($C_i(j)$)	Competitor classification
tn1	c1	+	-	+	Cheater
tn1	c2	-	=	-	Disadvantaged cooperator
tn1	c3	-	=	-	Disadvantaged cooperator
tn3	c1	+	+	+	Increased pure-culture sporulator
tn3	c2	+	-	=	GJV1 sporulation suppressor
tn3	c3	=	-	+	Complemented
tn4	c1	=	-	=	Complemented
tn4	c2	=	=	=	Cooperator
tn4	c3	-	-	-	Disadvantaged defector
tn5	c1	=	-	=	Complemented
tn5	c2	-	-	-	Disadvantaged defector
tn5	c3	-	-	-	Disadvantaged defector
tn6	c1	-	=	-	Disadvantaged cooperator
tn6	c2	-	-	-	Disadvantaged defector
tn6	c3	+	+	+	Increased pure-culture sporulator
tn7	c1	-	-	-	Disadvantaged defector
tn7	c2	=	=	-	Cooperator
tn7	c3	=	=	=	Cooperator
tn8	c1	-	=	=	Disadvantaged cooperator
tn8	c2	-	+	-	Disadvantaged cooperator
tn8	c3	-	-	-	Disadvantaged defector
tn9	c1	=	+	=	Cooperator
tn9	c2	=	-	+	Complemented
tn9	c3	=	-	+	Complemented

64

tn10	c1	+	+	=	Increased pure-culture sporulator
tn10	c2	-	-	=	Disadvantaged defector
tn10	c3	-	-	-	Disadvantaged defector
tn11	c1	=	-	+	Complemented
tn11	c2	=	+	=	Cooperator
tn11	c3	=	-	+	Complemented
tn12	c1	+	-	+	Cheater
tn12	c2	+	-	+	Cheater
tn12	c3	+	-	+	Cheater
tn13	c1	+	-	+	Cheater
tn13	c2	=	-	+	Complemented
tn13	c3	=	-	=	Complemented
tn14	c1	+	-	+	Cheater
tn14	c2	+	-	=	GJV1 sporulation suppressor
tn14	c3	+	-	+	Cheater
tn15	c1	=	-	+	Complemented
tn15	c2	=	=	=	Cooperator
tn15	c3	+	+	+	Increased pure-culture sporulator
tn16	c1	+	=	+	Facultative exploiter
tn16	c2	+	=	+	Facultative exploiter
tn16	c3	=	=	+	Cooperator
tn17	c1	=	-	+	Complemented
tn17	c2	+	-	+	Cheater
tn17	c3	+	+	+	Increased pure-culture sporulator
tn18	c1	+	=	+	Facultative exploiter
tn18	c2	=	=	=	Cooperator
tn18	c3	+	=	+	Facultative exploiter
tn19	c1	+	=	+	Facultative exploiter
tn19	c2	+	=	+	Facultative exploiter
tn19	c3	+	=	+	Facultative exploiter
tn20	c1	=	-	=	Complemented
tn20	c2	+	-	+	Cheater
tn20	c3	=	-	+	Complemented
tn21	c1	=	-	=	Complemented
tn21	c2	+	-	+	Cheater
tn21	c3	=	-	+	Complemented
tn22	c1	+	+	+	Increased pure-culture sporulator

tn22	c2	+	+	+	Increased pure-culture sporulator
tn22	c3	+	+	+	Increased pure-culture sporulator
tn23	c1	+	=	+	Facultative exploiter
tn23	c2	+	=	+	Facultative exploiter
tn23	c3	+	=	+	Facultative exploiter
tn24	c1	=	-	+	Complemented
tn24	c2	+	-	+	Cheater
tn24	c3	+	-	+	Cheater
tn25	c1	+	=	+	Facultative exploiter
tn25	c2	-	=	-	Disadvantaged cooperator
tn25	c3	+	=	+	Facultative exploiter
tn26	c1	+	+	+	Increased pure-culture sporulator
tn26	c2	+	=	+	Facultative exploiter
tn26	c3	+	-	+	Cheater
tn27	c1	+	-	+	Cheater
tn27	c2	+	=	+	Facultative exploiter
tn27	c3	=	-	+	Complemented
tn28	c1	=	=	=	Cooperator
tn28	c2	-	-	-	Disadvantaged defector
tn28	c3	=	=	-	Cooperator
tn29	c1	-	-	-	Disadvantaged defector
tn29	c2	+	-	+	Cheater
tn29	c3	+	-	+	Cheater
tn30	c1	+	-	+	Cheater
tn30	c2	=	-	=	Complemented
tn30	c3	=	=	=	Cooperator
tn31	c1	=	-	+	Complemented
tn31	c2	-	-	-	Disadvantaged defector
tn31	c3	=	=	+	Cooperator
tn32	c1	+	-	+	Cheater
tn32	c2	-	-	-	Disadvantaged defector
tn32	c3	=	=	+	Cooperator
tn33	c1	+	=	+	Facultative exploiter
tn33	c2	+	=	+	Facultative exploiter
tn33	c3	=	-	+	Complemented
tn34	c1	+	=	+	Facultative exploiter

tn34	c2	=	-	=	Complemented
tn34	c3	-	-	+	Disadvantaged defector
tn35	c1	=	=	=	Cooperator
tn35	c2	=	=	=	Cooperator
tn35	c3	=	-	=	Complemented
tn36	c1	-	-	=	Disadvantaged defector
tn36	c2	+	=	+	Facultative exploiter
tn36	c3	-	-	-	Disadvantaged defector
tn37	c1	+	-	+	Cheater
tn37	c2	+	-	+	Cheater
tn37	c3	=	-	+	Complemented
tn38	c1	=	=	+	Cooperator
tn38	c2	-	=	=	Disadvantaged cooperator
tn38	c3	=	=	=	Cooperator
tn39	c1	-	=	=	Disadvantaged cooperator
tn39	c2	-	-	=	Disadvantaged defector
tn39	c3	+	=	+	Facultative exploiter
tn40	c1	=	-	+	Complemented
tn40	c2	=	-	+	Complemented

References

Basler M, Ho BT, Mekalanos JJ. Tit-for-Tat: Type VI Secretion System Counterattack during Bacterial Cell-Cell Interactions. Cell. 2013;152(4):884–94.

Bates D, Mächler M, Bolker B, Walker S. Fitting Linear Mixed-Effects Models Using lme4. J Stat Softw. 2015;67(1).

Bretscher AP, Kaiser D. Nutrition of Myxococcus xanthus, a fruiting myxobacterium. J Bacteriol. 1978;133(2):763–8.

Bruce JB, Cooper GA, Chabas H, West SA, Griffin AS. Cheating and resistance to cheating in natural populations of the bacterium Pseudomonas fluorescens. Evolution. 2017;71(10):2484–95.

Butaitė E, Baumgartner M, Wyder S, Kümmerli R. Siderophore cheating and cheating resistance shape competition for iron in soil and freshwater Pseudomonas communities. Nat Commun. 2017;8(1):414.

Buttery NJ, Rozen DE, Wolf JB, Thompson CRL. Quantification of Social Behavior in D. discoideum Reveals Complex Fixed and Facultative Strategies. Curr Biol. 2009;19(16):1373–7.

Buttery NJ, Thompson CRL, Wolf JB. Complex genotype interactions influence social fitness during the developmental phase of the social amoeba Dictyostelium discoideum. J Evol Biol. 2010;23(8):1664–71.

Chen ICK, Satinsky BM, Velicer GJ, Yu YTN. sRNA-pathway genes regulating myxobacterial development exhibit clade-specific evolution. Evol Dev. 2019;21(2):82–95.

Chuang JS, Rivoire O, Leibler S. Simpson's Paradox in a Synthetic Microbial System. Science. 2009;323(5911):272–5.

Dandekar AA, Chugani S, Greenberg EP. Bacterial Quorum Sensing and Metabolic Incentives to Cooperate. Science. 2012;338(6104):264–6.

Diggle SP, Griffin AS, Campbell GS, West SA. Cooperation and conflict in quorum-sensing bacterial populations. Nature. 2007;450(7168):411–4.

Fiegna F, Velicer GJ. Competitive fates of bacterial social parasites: persistence and self-induced extinction of Myxococcus xanthus cheaters. Proc Biol Sci. 2003;270(1523):1527–34.

Fiegna F, Velicer GJ. Exploitative and Hierarchical Antagonism in a Cooperative Bacterium. Plos Biol. 2005;3(11):e370.

Fiegna F, Yu YTN, Kadam SV, Velicer GJ. Evolution of an obligate social cheater to a superior cooperator. Nature. 2006;441(7091):310–4.

Fortezza ML, Schaal KA, Velicer GJ. The Evolution of Multicellularity. In: Herron, Conlin MD, Ratcliff WC, editors. Group Formation: On the Evolution of Aggregative Multicellularity. CRC Press; 2022. p. 89–110.

Fortezza ML, Velicer GJ. Social selection within aggregative multicellular development drives morphological evolution. Proc Biol Sci. 2021;288(1963):20211522.

Fortunato A, Queller DC, Strassmann JE. A linear dominance hierarchy among clones in chimeras of the social amoeba Dictyostelium discoideum. J Evol Biol. 2003;16(3):438–45.

Foster KR, Fortunato A, Strassmann JE, Queller DC. The costs and benefits of being a chimera. Proc Biol Sci. 2002;269(1507):2357–62.

Foster KR, Shaulsky G, Strassmann JE, Queller DC, Thompson CRL. Pleiotropy as a mechanism to stabilize cooperation. Nature. 2004;431(7009):693–6.

Fox J, Weisberg S. An R Companion to Applied Regression. Sage publications; 2019.

Frank SA. Foundations of social evolution. Vol. 2. Princeton University Press; 1998.

Freilich S, Zarecki R, Eilam O, Segal ES, Henry CS, Kupiec M, et al. Competitive and cooperative metabolic interactions in bacterial communities. Nat Commun. 2011;2(1):589.

Ghoul M, Mitri S. The Ecology and Evolution of Microbial Competition. Trends Microbiol. 2016;24(10):833–45.

Gilbert OM, Foster KR, Mehdiabadi NJ, Strassmann JE, Queller DC. High relatedness maintains multicellular cooperation in a social amoeba by controlling cheater mutants. Proc Natl Acad Sci USA. 2007;104(21):8913–7.

Griffin AS, West SA, Buckling A. Cooperation and competition in pathogenic bacteria. Nature. 2004;430(7003):1024–7.

Hamilton WD. The Evolution of Altruistic Behavior. Am Nat. 1963;97(896):354–6.

Hamilton WD. The genetical evolution of social behaviour. I. J Theor Biol. 1964a;7(1):1–16.

Hamilton WD. The genetical evolution of social behaviour. II. J Theor Biol. 1964b;7(1):17–52.

Harrison F, Paul J, Massey RC, Buckling A. Interspecific competition and siderophore-mediated cooperation in Pseudomonas aeruginosa. ISME J. 2008;2(1):49–55.

Jacobs MA, Alwood A, Thaipisuttikul I, Spencer D, Haugen E, Ernst S, et al. Comprehensive transposon mutant library of Pseudomonas aeruginosa. Proc Natl Acad Sci USA. 2003;100(24):14339–44.

Kaiser D. Social gliding is correlated with the presence of pili in Myxococcus xanthus. Proc National Acad Sci USA. 1979;76(11):5952–6.

Katzianer DS, Wang H, Carey RM, Zhu J. "Quorum Non-Sensing": Social Cheating and Deception in Vibrio cholerae. Appl Environ Microbiol. 2015;81(11):3856–62.

Kraemer SA, Toups MA, Velicer GJ. Natural variation in developmental life-history traits of the bacterium Myxococcus xanthus. FEMS Microbiol Ecol. 2010;73(2):226–33.

Kraemer SA, Velicer GJ. Endemic social diversity within natural kin groups of a cooperative bacterium. Proc National Acad Sci USA. 2011;108(supplement_2):10823–30.

Kreft JU. Biofilms promote altruism. Microbiology (Reading). 2004;150(8):2751–60.

Kümmerli R, Griffin AS, West SA, Buckling A, Harrison F. Viscous medium promotes cooperation in the pathogenic bacterium Pseudomonas aeruginosa. Proc Biol Sci. 2009a;276(1672):3531–8.

Kümmerli R, Jiricny N, Clarke LS, West SA, Griffin AS. Phenotypic plasticity of a cooperative behaviour in bacteria. J Evol Biol. 2009b;22(3):589–98.

Kuspa A, Plamann L, Kaiser D. A-signalling and the cell density requirement for Myxococcus xanthus development. J Bacteriol. 1992;174(22):7360–9.

Length R. emmeans: Estimated Marginal Means, aka Least-Squares Means. R package version 1.8.6 [Internet]. 2023. Available from: https://CRAN.R-project.org/package=emmeans

Lenz DH, Mok KC, Lilley BN, Kulkarni RV, Wingreen NS, Bassler BL. The Small RNA Chaperone Hfq and Multiple Small RNAs Control Quorum Sensing in Vibrio harveyi and Vibrio cholerae. Cell. 2004;118(1):69–82.

MacLean RC, Gudelj I. Resource competition and social conflict in experimental populations of yeast. Nature. 2006;441(7092):498–501.

Medina JM, Shreenidhi PM, Larsen TJ, Queller DC, Strassmann JE. Cooperation and conflict in the social amoeba Dictyostelium discoideum. Int J Dev Biol. 2019;63(8-9–10):371–82.

Mendes-Soares H, Chen ICK, Fitzpatrick K, Velicer GJ. Chimaeric load among sympatric social bacteria increases with genotype richness. Proc Biol Sci. 2014;281(1787):20140285.

Mitri S, Foster KR. The Genotypic View of Social Interactions in Microbial Communities. Annu Rev Genet. 2013;47(1):247–73.

Nair RR, Fiegna F, Velicer GJ. Indirect evolution of social fitness inequalities and facultative social exploitation. Proc Biol Sci. 2018;285(1875):20180054.

Ostrowski EA. Enforcing Cooperation in the Social Amoebae. Curr Biol. 2019;29(11):R474–84.

Özkaya Ö, Balbontín R, Gordo I, Xavier KB. Cheating on Cheaters Stabilizes Cooperation in Pseudomonas aeruginosa. Curr Biol. 2018;28(13):2070-2080.e6.

Palmer JD, Foster KR. Bacterial species rarely work together. Science. 2022;376(6593):581–2.

Pande S, Velicer GJ. Chimeric Synergy in Natural Social Groups of a Cooperative Microbe. Curr Biol. 2018;28(2):262-267.e3.

Pollitt EJG, West SA, Crusz SA, Burton-Chellew MN, Diggle SP. Cooperation, quorum sensing, and evolution of virulence in Staphylococcus aureus. Infect Immun. 2014;82(3):1045–51.

Rainey PB, Rainey K. Evolution of cooperation and conflict in experimental bacterial populations. Nature. 2003;425(6953):72–4.

Rendueles O, Amherd M, Velicer GJ. Positively Frequency-Dependent Interference Competition Maintains Diversity and Pervades a Natural Population of Cooperative Microbes. Curr Biol. 2015;25(13):1673–81.

Riley MA, Wertz JE. Bacteriocins: evolution, ecology, and application. Annu Rev Microbiol. 2002;56(1):117–37.

Ross-Gillespie A, Gardner A, West SA, Griffin AS. Frequency Dependence and Cooperation: Theory and a Test with Bacteria. Am Nat. 2007;170(3):331–42.

Sana TG, Flaugnatti N, Lugo KA, Lam LH, Jacobson A, Baylot V, et al. Salmonella Typhimurium utilizes a T6SS-mediated antibacterial weapon to establish in the host gut. Proc National Acad Sci USA. 2016;113(34):E5044–51.

Sandoz KM, Mitzimberg SM, Schuster M. Social cheating in Pseudomonas aeruginosa quorum sensing. Proc National Acad Sci USA. 2007;104(40):15876–81.

Santorelli LA, Thompson CRL, Villegas E, Svetz J, Dinh C, Parikh A, et al. Facultative cheater mutants reveal the genetic complexity of cooperation in social amoebae. Nature. 2008;451(7182):1107–10.

Sathe S, Kaushik S, Lalremruata A, Aggarwal RK, Cavender JC, Nanjundiah V. Genetic Heterogeneity in Wild Isolates of Cellular Slime Mold Social Groups. Microb Ecol. 2010;60(1):137–48.

Scrucca L, Fraley C, Murphy TB, Raftery AE. Model-Based Clustering, Classification, and Density Estimation Using mclust in R [Internet]. Chapman and Hall/CRC; 2023. Available from: https://mclust-org.github.io/book/

Slattery M, Rajbhandari I, Wesson K. Competition-mediated antibiotic induction in the marine bacterium Streptomyces tenjimariensis. Microb Ecol. 2001;41(2):90–6.

Smith EE, Buckley DG, Wu Z, Saenphimmachak C, Hoffman LR, D'Argenio DA, et al. Genetic adaptation by Pseudomonas aeruginosa to the airways of cystic fibrosis patients. Proc National Acad Sci USA. 2006;103(22):8487–92.

Strassmann JE, Gilbert OM, Queller DC. Kin Discrimination and Cooperation in Microbes. Annu Rev Microbiol. 2011;65(1):349–67.

Strassmann JE, Zhu Y, Queller DC. Altruism and social cheating in the social amoeba Dictyostelium discoideum. Nature. 2000;408(6815):965–7.

team P. RStudio: Integrated Development Environment for R. Posit Software, PBC, Boston, MA [Internet]. 2023. Available from: http://www.posit.co/

Team RC. R: A language and environment for statistical computing. R Foundation for Statistical Computing, Vienna, Austria [Internet]. 2023. Available from: https://www.R-project.org/

Travisano M, Velicer GJ. Strategies of microbial cheater control. Trends Microbiol. 2004;12(2):72–8.

Velicer GJ. Social strife in the microbial world. Trends Microbiol. 2003;11(7):330–7.

Velicer GJ, Kroos L, Lenski RE. Developmental cheating in the social bacterium Myxococcus xanthus. Nature. 2000;404(6778):598–601.

Velicer GJ, Raddatz G, Keller H, Deiss S, Lanz C, Dinkelacker I, et al. Comprehensive mutation identification in an evolved bacterial cooperator and its cheating ancestor. Proc National Acad Sci USA. 2006;103(21):8107–12.

Velicer GJ, Vos M. Sociobiology of the Myxobacteria. Annu Rev Microbiol. 2009;63(1):599–623.

Vos M, Velicer GJ. Social Conflict in Centimeter-and Global-Scale Populations of the Bacterium Myxococcus xanthus. Curr Biol. 2009;19(20):1763–7.

Vulić M, Kolter R. Evolutionary Cheating in Escherichia coli Stationary Phase Cultures. Genetics. 2001;158(2):519–26.

West SA, Diggle SP, Buckling A, Gardner A, Griffin AS. The Social Lives of Microbes. Annu Rev Ecol Evol Syst. 2007;38(1):53–77.

Xavier JB, Foster KR. Cooperation and conflict in microbial biofilms. Proc National Acad Sci USA. 2007;104(3):876–81.

Chapter 2

Kin discrimination and outer membrane exchange in *Myxococcus xanthus*: Experimental analysis of a natural population

Sarah M. Cossey[1]*†, Yuen-Tsu Nicco Yu[1]†, Laura Cossu[2] and Gregory J. Velicer[1], 2019,

PLOS ONE

† These authors contributed equally to the work.

*Correspondence to: sarah.cossey@env.ethz.ch

[1] Institute for Integrative Biology, Department of Environmental Systems Science, ETH Zürich,

8092 Zürich, Switzerland

[2] Department of Environmental Microbiology, Eawag, 8600 Dübendorf, Switzerland

Abstract

In some species of myxobacteria, adjacent cells sufficiently similar at the adhesin protein TraA can exchange components of their outer membranes. The primary benefits of such outer membrane exchange (OME) in natural populations are unclear, but in some OME interactions, transferred OM content can include SitA toxins that kill OME participants lacking an appropriate immunity gene. Such OME-dependent toxin transfer across *Myxococcus xanthus* strains that differ only in their *sitBAI* toxin/antitoxin cassette can mediate inter-strain killing and generate colony-merger incompatibilities (CMIs)–inter-colony border phenotypes between distinct genotypes that differ from respective self-self colony interfaces. Here we ask whether OME-dependent toxin transfer is a common cause of prevalent CMIs and antagonisms between *M. xanthus* natural isolates identical at TraA. We disrupted *traA* in eleven isolates from a cm-scale soil population and assayed whether *traA* disruption eliminated or reduced CMIs between swarming colonies or antagonisms between strains in mixed cultures. Among 33 isolate pairs identical at *traA* that form clear CMIs, in no case did functional disruption of *traA* in one partner detectably alter CMI phenotypes. Further, *traA* disruption did not alleviate strong antagonisms observed during starvation-induced fruiting body development in seven pairs of strains identical at *traA*. Collectively, our results suggest that most mechanisms of interference competition and inter-colony kin discrimination in natural populations of myxobacteria do not require OME. Finally, our experiments also indicate that several closely related laboratory reference strains kill some natural isolates by toxins delivered by a shared, OME-independent type VI secretion system (T6SS), suggesting that some antagonisms between sympatric natural isolates may also involve T6SS toxins.

Introduction

Kin discrimination among microbes can be defined phenomenologically as differential expression (or effects) of behaviour across interactants as a function of genetic relatedness [1–3]. Such behaviors include secretion of toxins to which a producer cell is genetically resistant but to which victim cells are not [4, 5] and preferential co-aggregation with genetically similar cells [1, 6]. Another form of microbial kin discrimination is boundary formation at colony interfaces that are specific to encounters between distinct genotypes, or colony-merger incompatibility (CMI, [1]). Because the evolutionary significance of social interactions hinges on the relatedness of interactants [7, 8], kin-discriminatory behaviors in both microbes [9–11] and animals [12–16] are often interpreted in the context of kin-selection theory [2]. However, because evolutionary forces other than kin selection can cause kin-discriminatory behaviors to evolve [1, 17], the ultimate causes of such behaviors among naturally-evolved microbes are often unclear.

Genetically determined CMI is a major form of microbial kin discrimination in which colonies of distinct bacterial genotypes meet through motility-driven swarming and generate a border phenotype different from the phenotypes of self-self colony borders. CMIs were first described in *Proteus mirabilis* [18] but have since been observed in other species, including *Myxococcus xanthus* [1, 19], *Bacillus subtilis* [20] and *Pseudomonas aeruginosa* [21]. CMIs are potentially important in the social evolution of motile bacteria because they can reflect the outcome of genotype x genotype interactions affecting fitness. For example, CMIs between natural isolates of *M. xanthus* are associated with reduced co-aggregation into shared fruiting-body groups at colony interfaces [1].

CMIs can be generated by a variety of mechanisms, both across and within species. In *P. mirabilis*, some inter-colony boundaries are due to effector toxins delivered by the type VI secretion system (T6SS) [22–24]. In *B. subtilis*, mechanisms include outer-membrane alterations that likely influence susceptibility to antimicrobials and mutations in contact-

dependent growth-inhibition loci such as *wapAI* [25]. Experimental populations of *M. xanthus* readily evolve CMIs by a variety of genetic mechanisms [1] and toxin delivery by both outer membrane exchange (OME) [26, 27] and a T6SS [28] can generate CMIs involving relevant mutants of this species.

Myxobacteria exhibit several complex social behaviors, including coordinated group motility [29, 30] while hunting other microbes [31] and multicellular fruiting-body development in response to starvation [30, 32]. Additionally, in the model species *M. xanthus*, experiments showing that motility-related proteins can be transferred between cells revealed a process now known as outer membrane exchange, or OME [33, 34]. Specifically, the motility defect of a mutant unable to produce the protein Tgl, which facilitates formation of an outer-membrane channel for type IV pili [35], was found to be rescued by inter-cellular transfer of Tgl from a *tgl*+ strain [33]. Tgl transfer was later found to occur by a contact-dependent mechanism requiring both of the co-operonic genes *traA* and *traB* [34]. A TraA/TraB protein complex facilitates OME by homotypic interaction between cell-surface-bound TraA, which appears to act as an adhesin [34, 36]. TraA-mediated OME causes cells to fuse their outer membranes and exchange large amounts of cellular material [34]. OME occurs on relatively solid surfaces but apparently not on soft, moist surfaces or in liquid [34, 36, 37].

The *traA/traB* operon is present in a majority of myxobacterial species examined to date but has not been found outside the myxobacteria [38]. However, genomes representing more than one third of all myxobacterial genera examined to date lack this operon. These include some species, such as *Chondromyces crocatus*, known to engage in complex fruiting-body formation [38]. Consistent with this finding, deletion of *traA* from *M. xanthus* was not found to significantly affect the major social traits of social motility or fruiting-body development in this species [34]. Thus, OME is not essential for the most prominent social behaviors of myxobacteria.

TraA has diversified into a variety of functionally distinct allotypes across the myxobacteria [38]. These include several allotypes within *M. xanthus* that are incompatible for OME due to dissimilarity in the PA14 hyper-variable domain of TraA [3, 36]. CMI patterns among natural isolates of M. xanthus [3] and experimentally-evolved strains [1] suggest that divergence at TraA does not contribute to CMIs. TraA has been hypothesized to be a greenbeard trait that preferentially directs cooperative benefits of OME between cells with functionally compatible TraA proteins [36]. It has been further speculated that a major group-level benefit might derive from reduction of physiological heterogeneity among neighboring cells (or, phrased inversely, an increase in group-level homeostasis) due to OME [39]. However, the selective forces responsible for the maintenance of the *traA/traB* operon in some myxobacterial species remain to be clarified [3, 26, 39–44].

In contrast to the possibility that OME may mediate cooperative benefits, it has become clear that, like contact-dependent growth inhibition in other species [45], OME has the potential to mediate strong antagonistic interactions. Dey *et al.* discovered that a polyploid prophage (Mx alpha) present in many *M. xanthus* strains produces SitA toxins that can transfer across cells by TraA-dependent OME and kill OME participants lacking a cognate immunity gene [46]. Wielgoss *et al.* (2016) subsequently localized this prophage to an ~150 kb region of the *M. xanthus* genome that is exceptionally polymorphic with respect to gene content among the Tübingen cm-scale isolates [47]. Patterns of gene content in this highly polymorphic region were found to correlate with CMI-allotype categories previously defined among a subset of cm-scale isolates from Tübingen, Germany [19]. It was thus proposed that distinct OME-transferrable toxins might be encoded in the highly polymorphic region by some strains and contribute to inter-strain antagonisms in local natural populations [47].

Toxin production that is asymmetric across colony borders is expected to generate CMIs. Consistent with this, Vassallo *et al.* [26] found that colonies of isogenic strains expressing distinct *sitBAI* toxin/immunity cassettes generate CMIs at colony interfaces due to

OME-mediated killing. They further presented data suggesting that mutants of a lab reference strain incapable of OME or Sit-toxin production may be less competitive against OME-compatible natural isolates than is the parental reference strain. In light of these results, it was again suggested that OME-toxin transfer may be involved in naturally evolved forms of interference competition and CMIs.

Wielgoss *et al.* (2018) examined this hypothesis in a comparative analysis of *M. xanthus* natural isolates from the Tübingen cm-scale population with respect to patterns of CMIs, antagonisms and TraA diversity among isolate pairs [3]. Almost all previously documented strong antagonisms among these cm-scale strains [19, 48] were found to occur between genotypes predicted to be incompatible for OME due to dissimilarity at TraA, implicating OME-independent mechanisms. OME-independent CMIs among these strains were also common, as all strain pairs predicted to be OME-incompatible at TraA exhibited clear CMIs. Overall, patterns of TraA variation in that focal population predict that most randomly selected isolate pairs should be incompatible for OME at TraA [3], in turn suggesting that most latent CMIs and antagonisms among all theoretically possible pairs of natural isolates do not involve OME.

Nonetheless, Wielgoss et al. (2018) also found that a large fraction of cm-scale strain pairs identical at *traA* exhibit clear CMIs that could potentially be caused by OME-delivered toxins [3]. Diversity in natural *M. xanthus* populations is highly structured, such that relatedness between strains increases with decreasing distance between them [47, 49]. Thus, genetically distinct neighbors likely to interact in the soil may often be sufficiently similar at TraA to be compatible for OME [3]. It is thus relevant to test whether CMIs or antagonisms between such TraA-similar natural isolates from the same local population generally involve OME.

Here we ask whether disruption of *traA*—and hence debilitation of OME—in cm-scale natural isolates reduces or eliminates CMI boundaries at colony interfaces with other isolates

that share the same *traA* allele. We further document several severe antagonisms between *traA*-identical strains and test whether *traA* disruption alleviates those antagonisms. Finally, having discovered in the course of our experiments that lab reference strains inhibit growth of natural isolates in an OME-independent manner, we test whether these antagonisms are caused by a T6SS carried by the reference strains.

Materials and methods

Strains and primers

The two primary lab reference strains used in this study are GJV1 and DK101 (Table 1). GJV1is a close derivative of DK1622 [50], differing by only five mutations [51]. GJV1 is highly proficient at both mechanisms of motility employed by *M. xanthus* (S-motility and A-motility, A+S+) and fruiting-body development [51, 52]. DK101 is a mutant of strain FB [29] that is defective at type IV pili-mediated S-motility but has a functional A-motility system (A+S-) [53]. DK101 has three Mx-alpha prophage repeats that encode SitA toxins transferrable by OME and corresponding antitoxins [26, 46]. DK1622 was generated from DK101 through UV mutagenesis and Mx8 phage transduction that restored functional S motility [50]. During this process DK1622 lost two Mx-alpha repeats and the associated toxin and antitoxin genes, which resulted in susceptibility to OME-mediated killing by DK101 [46]. Also, DK101 colonies expand only very slowly on a hard-agar surface compared to GJV1 and the natural isolates used in this study (S1 Fig). For these reasons, DK101 was utilized to test for loss of *traA* function in relevant mutants, as described further below.

Table 1. Strains.

Strain	Description	Reference
DK101	A+S- (proficient at A-motility, defective at S-motility)	[29]
GJV1	A+S+ DK1622 derivative	[51, 52]
GJV1*traA*	*Mxan_6895* knock-in mutant	[3]
GJV1*traA*-S	*Mxan_6895* knock-in mutant	This study
GJV1*traB*	*Mxan_6898* knock-in mutant	This study
A88	Natural isolate	[54]

A88*traA*	*Mxan_6895* knock-in mutant	This study
SA3437	DK1622 Δ*vgrG1* (*Mxan_4800*)	[55]
SA5700	DK1622 Δ*vgrG2* (*Mxan_5573*)	[55]
SA5701	DK1622 Δ*tagF* (*Mxan_4805*)	[55]
SA5707	DK1622 ΔT6SS (*Mxan_4800-Mxan_4813*)	[55]
SA5712	DK1622 Δ*vgrG1* Δ*vgrG2*	[55]
A00	Natural isolate	[54]
A23	Natural isolate	[54]
A30	Natural isolate	[54]
A31	Natural isolate	[54]
A32	Natural isolate	[54]
A44	Natural isolate	[54]
A46	Natural isolate	[54]
A60	Natural isolate	[54]
A72	Natural isolate	[54]
A93	Natural isolate	[54]
A00*traA*	*Mxan_6895* knock-in mutant	This study
A23*traA*	*Mxan_6895* knock-in mutant	This study
A44*traA*	*Mxan_6895* knock-in mutant	This study
A60*traA*	*Mxan_6895* knock-in mutant	This study
A72*traA*	*Mxan_6895* knock-in mutant	This study
A60Δ*traA*	*Mxan_6895* in-frame deletion	This study
A23rif[R]	Rifampicin resistant A23	[19]
A07	Natural isolate	[54]
A26	Natural isolate	[54]
A47	Natural isolate	[54]
A96	Natural isolate	[54]
A07*traA*	*Mxan_6895* knock-in mutant	This study
A47*traA*	*Mxan_6895* knock-in mutant	This study
A96*traA*	*Mxan_6895* knock-in mutant	This study
A47rif[R]	Rifampicin resistant A47	[19]
A96rif[R]	Rifampicin resistant A96	[19]
A17	Natural isolate	[54]
A38	Natural isolate	[54]
A65	Natural isolate	[54]
A73	Natural isolate	[54]
A38*traA*	*Mxan_6895* knock-in mutant	This study
A01	Natural isolate	[54]
A33	Natural isolate	[54]
A45	Natural isolate	[54]
A01*traA*	*Mxan_6895* knock-in mutant	This study
Top10	*E. coli* strain for plasmid construction	Invitrogen

Additional strains are natural isolates of *M. xanthus* originally isolated from a 16 x 16-cm soil patch in Tübingen, Germany [54] and *traA* disruption or deletion mutants of those isolates (Table 1). Social compatibilities and competitive abilities of some of those isolates have been characterized [3, 19, 48], as have the phylogenetic and predicted functional relationships of TraA sequences across the entire cm-scale isolate set [3]. The subset of

strains used in this study was selected to represent five of the TraA compatibility groups predicted by Wielgoss *et al.* [3]. These compatibility groups were predicted based on phylogenetic context of the relevant Tübingen cm-scale isolates relative to isolates previously tested for OME [3, 36, 40].

Primers used in this study are listed in Table 2. In a previous study, *traA*-disruption mutants defective at OME were generated by plasmid integration of a 543-bp insert [34]. Here, two primer pairs (Table 2) were used to amplify a slightly larger (788 bp) region of *traA* in GJV1 and the natural isolates. This larger region was used to disrupt *traA* because it allowed generation of the plasmid constructs for all natural isolates with common primers aligned to homologous sequence. Plasmid integration was verified using primer M13 or M13r (depending on the orientation of the plasmid used when generating the *traA* mutants) in combination with an additional primer (GV763) designed to bind upstream of the plasmid integration site.

Table 2. Plasmids and primers.

Plasmid	Description	Reference
pCR-Blunt	Cloning/integrative vector	Invitrogen
pBJ113	Allele exchange plasmid with kan^R and *galK* genes	[56]
pDP3	pCR2.1 containing *traB* insertion cassette	[34]
pCR_A88*traA*	Contains a 788-bp fragment of *Mxan_6895* amplified using primers GV751 and GV753	This study
pCR_A00*traA*	Contains a 788-bp fragment of *Mxan_6895* amplified using primers GV752 and GV755	This study
pCR_A23*traA*	Contains a 788-bp fragment of *Mxan_6895* amplified using primers GV752 and GV755	This study
pCR_A44*traA*	Contains a 788-bp fragment of *Mxan_6895* amplified using primers GV752 and GV755	This study
pCR_A60*traA*	Contains a 788-bp fragment of *Mxan_6895* amplified using primers GV752 and GV755	This study
pCR_A72*traA*	Contains a 788-bp fragment of *Mxan_6895* amplified using primers GV752 and GV755	This study
pCR_A60Δ*traA* pBJ_A60Δ*traA*	In-frame deletion of *Mxan_6895* (amino acid residues 13-695) generated using primers GV765, GV766, GV767, and GV768	This study
pCR_A07*traA*	Contains a 788-bp fragment of *Mxan_6895* amplified using primers GV752 and GV755	This study
pCR_A47*traA*	Contains a 788-bp fragment of *Mxan_6895* amplified using primers GV752 and GV755	This study
pCR_A96*traA*	Contains a 788-bp fragment of *Mxan_6895* amplified using primers GV752 and GV755	This study

pCR_A38*traA*	Contains a 788-bp fragment of *Mxan_6895* amplified using primers GV751 and GV753	This study
pCR_A01*traA*	Contains a 788-bp fragment of *Mxan_6895* amplified using primers GV752 and GV755	This study

Primer	Sequence
GV751	5' TCACTGTCTTGTCGGTGTGCCTC 3'
GV752	5' TCACTGTCCTGGCGGTGTGCCTC 3'
GV753	5' AAGAAGGTGTGCCTCCCGCCTGC 3'
GV755	5' TTGCCGTAGGAGAGGAAGCTTCC 3'
GV756	5' GCCGGTTGATGACCTGATACGG 3'
GV763	5' GTGGGAGATATCCCTCATTG 3'
GV765	5' AGCGCTACCACGTGGACCCC 3'
GV766	5' TTTCAAAGCCCCGCAACAATG 3'
GV767	5'TGTTGCGGGGCTTTGAAATTCCTGCTGCTGCTC GCCGCG 3'
GV768	5' CCTCCAGGTTGGCGCCGCCC 3'
M13	5' GTAAAACGACGGCCAG 3'
M13r	5' CAGGAAACAGCTATGAC 3'

Pre-assay culture conditions

Strains were inoculated from frozen stocks onto CTT [57] 1.5% agar plates and allowed to grow for 3–5 days at 32° C and 90% relative humidity. Strains were subsequently transferred into 8 mL of liquid CTT and grown overnight until turbid while shaking at 32° C, 300 rpm, diluted in 8 mL CTT and again grown overnight. On the day each experiment was initiated, cultures were grown to mid-log phase, centrifuged at 12,000 rpm for 5 minutes and then resuspended in TPM liquid buffer [57] to a density of ~5 x 109 cells/mL for use in assays of swarming inhibition, kin discrimination, and developmental competition.

Construction of traA/B-disruption mutants

An internal 788-bp region of *traA* was amplified from natural isolates and GJV1 with primers listed in Table 2 to generate the corresponding pCR-*traA* plasmids (Table 2). Additional primers were used to amplify an internal 543-bp fragment of the GJV1 *traA* allele to create a *traA* knock-in mutant similar to the one used by Pathak *et al.* for comparison [34]. Amplicons were gel extracted and ligated into the pCR-Blunt vector (Invitrogen), which confers resistance to kanamycin. Plasmids (pCR_*traA*) putatively including the relevant *traA* fragment

were verified by EcoRI digestion and sequencing. The plasmids constructed with the 543 and 788-bp fragments of the GJV1 *traA* allele are labelled pCR_*traA*-S and pCR_*traA*, respectively.

The natural isolates and GJV1 were transformed with the *traA* plasmids to generate corresponding *traA*-disrupted mutants. GJV1 was also transformed with pDP3, the *traB*-disruption plasmid used by Pathak *et al.* 2012 [34]. The integration of the pCR_*traA*, pCR_*traA*-S, and pDP3 plasmids results in a mero-diploid with one allele truncated at the 3'-end and the other at the 5'-end. The disrupted mutants generated by pCR_*traA* contain the complete PA14 highly variable region of TraA while the pCR_*traA*-S mutant only possesses a portion of PA14. Cell lysates of *traA* and *traB* mutants were used in colony PCR to verify transformants. Advantage GC2 polymerase was used for the verification and the standard manufacturer recommended protocol was followed.

In-frame deletion of traA

An in-frame deletion of *traA* was created in the A60 background, one of the natural isolates belonging to the largest TraA recognition group among the Tübingen isolates. Primers were designed to amplify two fragments that span approximately 500 bp upstream and downstream of *traA* in A60 that overlap by 18 bp. The two PCR products were used as the template for a sequence overlapping extension (SOE) reaction to generate a 1-kb fragment (equivalent to an in-frame deletion of TraA amino-acid residues 13–695). The in-frame deletion product was then cloned into the pCR-Blunt (Invitrogen) vector to generate pCR_*ΔtraA*. The fragment was then excised from the plasmid using EcoRV and BamHI, gel purified, and cloned to the Hin-cII-BamH1 linearized pBJ113 vector to create the plasmid pBJ_*ΔtraA*.

The A60 *traA* in-frame deletion was constructed by transformation with pBJ_*ΔtraA* and a previously described galactose-selection allele-exchange protocol [56]. Putative in-frame deletion clones were verified by PCR amplification and sequencing.

Colony-merger incompatibility assays

Compatibility or incompatibility for self-self-like colony merger was determined by spotting pairs of 10 µL cell suspensions (at ~5 x 10^9 cells/ml) at a distance of 10 (most cases) or 7.5 mm (a few cases for slow-swarming strains) on a 0.1% CTT 1.5% agar plate. Spots were allowed to dry completely and plates then were incubated at 32° C with 90% relative humidity for 5–6 days. After incubation, the presence of CMI demarcations was determined visually relative to self-self controls by previously described criteria [1, 3, 47]. Each natural isolate and the corresponding *traA* mutant were tested for CMIs with every other strain belonging to the same predicted TraA recognition group. Self-self control encounters were also done for each strain simultaneously with self-nonself assays. For this and all other assays, at least three biological replicates initiated on different days were performed.

Swarming-inhibition assay

GJV1, all natural isolates and all *traA* mutants were assayed for swarming inhibition by DK101 in experiments similar to those of Dey *et al.* [46]. Each strain was mixed at a 1:1 ratio or a 1:9 ratio with DK101 (with the latter in the majority) from cell suspensions at ~5 x 10^9 cells/ml. 10 µL aliquots of both the mixed cultures and pure cultures of each strain were spotted on a CTT 1.5% agar plate with 2 mM CaCl2. Plates were incubated at 32° C with 90% relative humidity for 5–6 days. After incubation, swarming distance was measured for all monocultures and DK101 mixes as the average distance of colony expansion along several radii from the time of inoculation to the time of measurement. The percentage-swarm expansion of each focal strain mixed with DK101 relative to its swarm expansion in pure culture was calculated as:

$$\frac{S[focal:DK101] - S[GJV1:DK101]}{S[focal] - S[GJV1:DK101]} \times 100$$

where S is the distance swarmed by a pure culture of a focal strain $S[focal]$ or a mixed culture of a focal strain or GJV1 with DK101 ($S[focal:DK101]$ or $S[GJV1:DK101]$, respectively). The percentage-relative swarm expansion was calculated within each replicate for each strain pair and averaged across replicates. Because DK101 kills GJV1, mixed cultures of these strains expand at a rate indistinguishable from pure colonies of DK101.

Killing assay

We tested whether DK101 and GJV1 kill the kanamycin-resistant strain A60*traA* in mixed cultures with an agar-flipping assay initiated in the same manner as the swarming-inhibition assays described above, except A60t*raA* was mixed with each paired strain at a 1:2 (A60*traA*: partner) ratio. After four days of incubation, the agar containing the initially mixed swarm was cut out using a scalpel and flipped upside-down onto a CTT 1.5% agar plate containing 40 μg/mL kanamycin. Killing was determined by the absence of growth on the kanamycin-containing plate. Controls of A60*traA* mixed with its parent A60, A60*traA* in pure culture and GJV1*traA* mixed with each of GJV1 and DK101 were also performed with the same assay.

Five T6SS mutants [55] that were constructed in the DK1622 background were similarly tested for their ability to kill A60*traA*. One of the mutants, SA5701, retains T6SS activity [55]. The other mutants have deletions in either *vgrG1*, *vgrG2*, both *vgrG1* and *vgrG2*, or the entire intact T6SS (*Mxan_*4800-*Mxan_*4813).

To confirm that the lack of growth by A60*traA* observed after mixing with some strains in the flipped-agar assay described above was due to killing of A60*traA* by the respective aggressor strain, we performed a colony-forming unit (CFU) recovery experiment to evaluate the survival rate of A60*traA* after 24 hours of pairwise co-incubation with strains of interest. DK101, GJV1, A60, A60*traA*, SA5701(*ΔtagF*), and SA5707(*ΔT6SS*) were cultured as described under 'Pre-assay culture conditions'. The kanamycin-resistant strain A60*traA* was

mixed in the minority (1:2 ratio) with each of the other strains (all kanamycin-sensitive) listed above. 10 µL of the mixed cell suspension were spotted onto a CTT 1.5% agar plate supplemented with 2 mM CaCl2, and incubated at 32° and 90% relative humidity for 24 hours. The entire inoculum was harvested with a sterile scalpel followed by serial dilution and plating in CTT soft agar with and without kanamycin. Colonies were counted after six days of incubation at 32°C and 90% relative humidity.

Developmental antagonism assays

Previously described rifampicin-resistant mutants of A23, A47 and A96 [19] and *traA* mutants of the same strains (Table 1) were mixed at a 1:99 ratio with other unmarked natural isolates prior to initiation of starvation-induced fruiting-body development. In all cases, the unmarked isolate in each pairing was previously predicted to belong to the same TraA-compatibility category as the parent of each focal mutant [3]. Specifically, A23rif[R] and A23*traA* were mixed in the minority with A30, A72 and A93, A47rif[R] and A47*traA* were mixed with A96 and A96rif[R] and A96*traA* with A07, A26, and A47. Additionally, A23rif[R] was mixed in the minority with A00, A32, A46 and A60 and A47rif[R] was mixed in the minority with A07 and A26. All strains also simultaneously underwent development in pure culture.

Results

Plasmid disruption of traA eliminates OME-mediated toxin transfer

To test whether TraA-mediated toxin delivery plays a major role in *M. xanthus* kin discrimination, we constructed plasmid-insertion mutants in which plasmid integration created merodiploids containing two non-functional copies of *traA*. We modified a previously described swarming assay [46] to confirm loss of *traA* or *traB* function upon integration of relevant plasmids into strain GJV1, the genome sequence of which is nearly identical to the published DK1622 sequence [51]. Both DK1622 and GJV1 derive from strain DK101 and possess a

functional S-motility system (involving type IV pili), which DK101 lacks. Both DK1622 and GJV1 lack Mx-alpha toxin/antitoxin cassettes carried by DK101 and it has been shown that DK1622 is killed in an OME-dependent manner by strains carrying the same Mx-alpha toxin cassettes as DK101 [46].

GJV1 swarms much faster than DK101 on agar surfaces due to the absence of S-motility in DK101 (S1 Fig). Thus, if there were no interaction between these strains in mixed cultures spotted onto agar, the GJV1 subpopulation would swarm outward at a rate similar that of a GJV1 monoculture. However, in such DK101:GJV1 mixes, GJV1 fails to swarm outward (Fig 1). Because i) strain DK1622 is killed by DK101 due to OME-mediated toxin delivery [46], ii) the genome sequence of GJV1 (our lab version of DK1622) is identical to the published DK1622 sequence excepting five mutations [51], and iii) disruption of both *traA* and *traB* alleviate DK101 inhibition of GJV1 swarming (Fig 1), we infer that DK101 inhibits GJV1 swarming by the same OME-delivered toxin that inhibited swarming by the version of DK1622 used by Dey *et al.* (2016) [46].
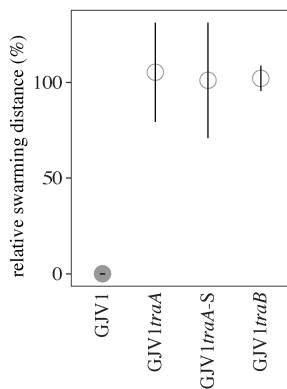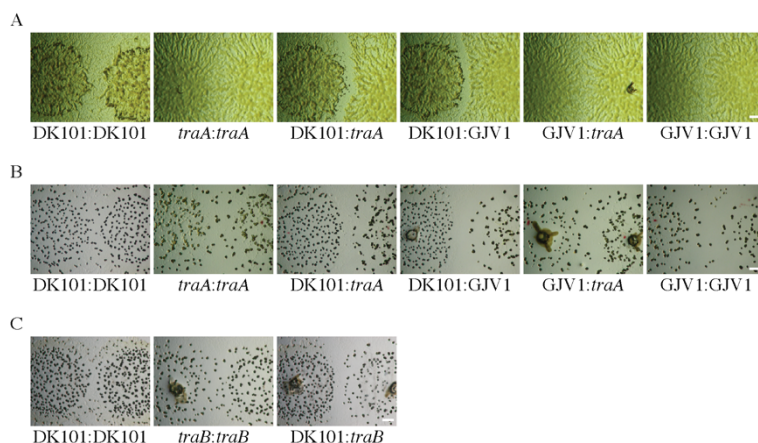

Fig 1. Disruption of *traA* and *traB* alleviates inhibition of GJV1 swarming by DK101. When mixed at a 1:1 ratio, DK101 inhibits swarming by GJV1 but not GJV1*traA*, GJV1*traA*-S or GJV1*traB*. *y* axis values indicate the percentage distance swarmed by each focal strain indicated on the *x* axis in mixture with DK101 relative to its swarming distance in pure culture (see Methods for details). Error bars are 95% confidence intervals, *n* = 3 replicates

In contrast, mutants of GJV1 in which OME has been debilitated by disruption of *traA* or *traB* survive contact with DK101 and swarm outward at the same rate as pure colonies of the respective mutants (Fig 1). Two plasmids containing 788-bp and 543-bp fragments of *traA*

(pCR_GJV1*traA* and pCR_GJV1*traA*-S, respectively, Table 2) were utilized to disrupt *traA*. The shorter fragment was used in a previous study [34] and we thus use it as a control to demonstrate elimination of OME by disruption with the longer fragment. (Allele-specific versions of the same long fragment were used to disrupt *traA* in natural isolates for the experiments reported below (Table 2).) Mutants with *traA* disrupted by both the short and long fragments were equally able to escape swarm inhibition by DK101 (Fig 1), implying that both plasmids debilitate OME.

A CMI between DK101 and GJV1 does not require functional TraA

Colonies of DK101 and GJV1 on the same agar plate form a clear CMI boundary upon encounter on both nutrient-rich and nutrient-poor agar (Fig 2A and 2B, respectively). This CMI might have been caused by the same mechanism of OME-mediated killing of GJV1 by DK101 observed when these strains are homogeneously mixed. Under this hypothesis, disruption of *traA* in either strain should eliminate (or greatly reduce) boundary formation, just as disruption of *traA* alleviates killing of GJV1*traA*. However, we observed that disruption of *traA* in GJV1 did not visibly reduce the CMI between GJV1*traA* and DK101 relative to GJV1 (Fig 2A and 2B). Thus, the CMI between these two closely related laboratory strains does not appear to involve OME-mediated toxin delivery. Disruption of *traB* also failed to eliminate the CMI between DK101 and GJV1 (Fig 2C).

A

DK101:DK101   *traA:traA*   DK101:*traA*   DK101:GJV1   GJV1:*traA*   GJV1:GJV1

B

DK101:DK101   *traA:traA*   DK101:*traA*   DK101:GJV1   GJV1:*traA*   GJV1:GJV1

C

DK101:DK101   *traB:traB*   DK101:*traB*

Fig 2. Disruption of *traA* or *traB* does not eliminate a CMI between GJV1 and DK101. Colony-encounter phenotypes in pairings of GJV1, GJV1*traA* (abbreviated to '*traA*' below images), and DK101

on 0.3% (**A**) and 0.1% (**B**) casitone media. For both **A** and **B**, colonies merge freely in self-self encounters of GJV1, GJV1*traA* and DK101 and in the non-self encounter of GJV1 and GJV1*traA*. In the left-most image of row A, the two DK101 colonies have darker center regions surrounded by distal regions that are less opaque but are nonetheless covered by cells. In this image, DK101 cells are continuous across the entire colony-interface region and do not exhibit a CMI phenotype. In contrast, strong CMI demarcations are formed in non-self encounters between DK101 and both GJV1 and GJV1*traA*. **C.** Interfaces between GJV1*traB* (abbreviated to '*traB*' below images) and DK101 colonies growing on 0.1% casitone also exhibit a clear CMI whereas self-self interfaces do not. Scale bars: 1 mm.

CMIs between TraA-homotypic natural isolates also do not require functional TraA

Eleven of the 78 Tübingen cm-scale natural isolates sampled by Vos & Velicer [54] were selected for *traA* disruption (Table 1) to test whether TraA-mediated toxin transfer is commonly responsible for kin discrimination between TraA-homotypic strains in a local natural population. These isolates tend toward antagonistic interactions in pairwise mixes [19] and represent multiple TraA "recognition groups" [3]–sets of highly similar TraA sequences that allow OME to occur when paired across adjacent cells. In a previous study, these recognition groups were not found to predict CMI kin-discrimination types [3]. Plasmids carrying the same 788-bp *traA* fragment corresponding to that in pCR_GJV1*traA* were integrated into eleven natural isolates representing five *traA* alleles, which in turn are predicted to represent five TraA PA14 OME recognition groups (Table 2 in [3] and Figs 2 and 4 in [3]). Colony encounter phenotypes were then compared for each parental natural isolate and its corresponding *traA* disruption mutant. This was done for pairings of each parent and its *traA* mutant with all other isolates examined here sharing the same *traA* allele.

None of the *traA* disruption mutants exhibited a different CMI-occurrence pattern in encounters with other natural isolates than their respective parental strains (Fig 3 and S2 Fig). This result indicates that TraA-mediated OME toxin transfer is not necessary for expression of CMI phenotypes in the examined set of strain pairs. Additionally, the CMI phenotypes involving the mutants were in no case visibly reduced relative to those of the respective parental strains (e.g. Fig 3A), suggesting that OME toxin transfer does not contribute significantly (or at all) to the observed CMIs.

The plasmid pCR_GJV1*traA* eliminates TraA function upon integration into GJV1 (Fig 1). It is expected that integration of similar plasmids that differ only in their *traA* allele debilitates *traA* function in all strains. Nonetheless, it is possible, if unlikely, that the non-disrupted 3' portion of *traA* remaining after integration of pCR_*traA* (which includes the entire PA14-encoding region) might somehow retain function and allow OME to occur only in the mutants of natural isolates and not in GJV1*traA*. To address this possibility, we generated an in-frame deletion of a large segment of *traA* in a natural isolate (A60) corresponding to removal of almost the entire gene (amino-acid residues 13–695 from the 719 aa-long TraA sequence), including the entire PA14 region [34, 36]. We then compared CMI-boundary-occurrence patterns in pairings with other natural isolates for A60, A60*traA* and A60Δ*traA*. Like plasmid disruption of *traA* in A60*traA*, deletion of almost the entire *traA* sequence in A60Δ*traA* did not eliminate or visibly reduce the CMI phenotypes exhibited by strain pairs that include A60 (Fig 3).

A
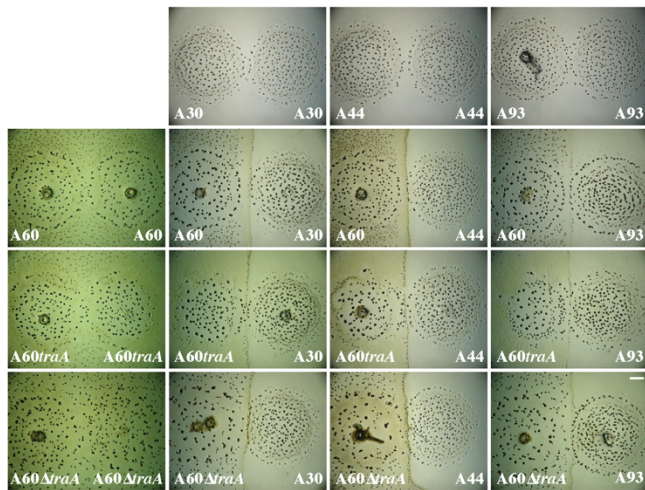
B
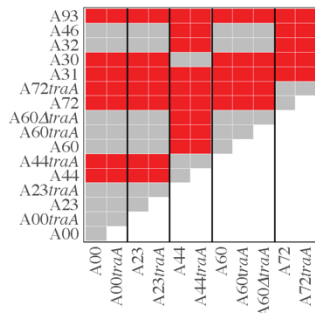
Fig 3. Disruption of *traA* does not alter CMI-occurrence patterns across pairings of *traA*-identical natural isolates. A. Examples of self-self colony-encounter phenotypes (left column and top row) and CMI phenotypes between distinct natural isolates and respective *traA* mutants (other images). Scale bar: 1 mm. **B.** All possible pairwise encounters between strains sharing the same *traA* allele for one of several alleles. (See also S2 Fig for results from other allele categories.) Red represents formation of visible CMI demarcation boundaries while grey represents the absence of such boundaries. In no case did disruption of *traA* (or deletion in the case of A60) eliminate a CMI boundary present between colonies of two natural isolates (or generate such a boundary not present between two isolates). The plasmid-integration and in-frame-deletion mutants of A60 exhibit CMIs with the same set of natural isolates as the parent strain.

Inhibition of natural-isolate swarming by DK101 is traA-independent

As shown above, DK101 inhibits swarming by GJV1 in mixed cultures in an OME-dependent manner (Fig 1). Additionally, DK101 also causes OME-independent CMI phenotypes during colony encounters with GJV1*traA* (Fig 2), even though DK101 does not kill or reduce the swarming of that mutant in mixed cultures (Fig 1). To investigate other OME-independent social incompatibilities involving DK101, we tested whether DK101 exhibits *traA*-independent antagonisms toward several of the natural isolates examined here, all but one of

90

which (A88) are predicted to be incompatible with DK101 for OME due to TraA dissimilarity [3, 36], as well as corresponding *traA* mutants. DK101 strongly inhibited swarm expansion by all of the natural isolates and corresponding *traA* mutants examined (Fig 4), demonstrating that DK101 exerts strong *traA*-independent toxicity toward all of these strains, including A88.
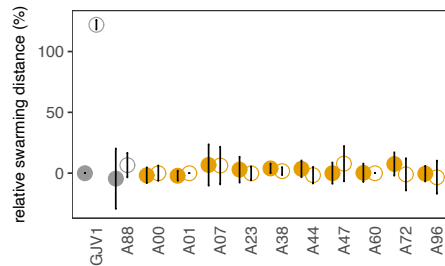

Fig 4. Disruption of *traA* does not alleviate DK101 inhibition of swarming in natural isolates. The *y* axis reflects the same relative swarming-distance parameter as in Fig 1. Two strains known (GJV1) or predicted (A88) to be compatible with DK101 for OME at *traA* are depicted in grey, whereas strains predicted to be incompatible with DK101 for OME are depicted in orange. Parental strains and their corresponding *traA* mutants are depicted by closed and open circles, respectively. All strains were mixed with DK101 at a 1:9 initial ratio. Error bars show 95% confidence intervals, *n* = 3 replicates.

DK101 and GJV1 kill a natural isolate without TraA-mediated delivery of Sit toxins

The severity of swarming inhibition exerted by DK101 on various natural isolates and their *traA* mutants suggested that the corresponding antagonisms mediated by DK101 may be lethal. To test this for one natural isolate, we spotted cultures of GJV1*traA* and A60*traA* each mixed with DK101 and its own parental strain on CTT hard agar. After four days of incubation, an agar section containing the entire colony was cut out and transferred upside down onto CTT kanamycin-agar plates. Because the *traA* mutants are kanamycin-resistant (whereas DK101 is kanamycin-sensitive), they will grow and swarm outward after placement on kanamycin plates if DK101 does not kill them. GJV1*traA* survived interaction with DK101 and swarmed outward on kanamycin agar (Fig 5), whereas A60*traA* did not exhibit detectable growth or swarming. Thus, DK101 appears to secrete toxins lethal to A60*traA* that are not transferred by OME and which are responsible for the swarming-inhibition of A60 and A60*traA* (and likely other natural isolates as well) shown in Fig 4.

Additionally, because DK101 and GJV1 are expected to be identical across most of their genomes [46, 51, 58], the two strains are likely to make most or all of the same OME-

91

independent toxins. Indeed, A60*traA* was killed by GJV1 as well as by DK101, but not by its parental strain A60 (Fig 5), implicating a killing mechanism that does not involve OME-mediated delivery of Sit toxins.

GJV1+ GJV1*traA*	A60+ A60*traA*	DK101+ GJV1*traA*
DK101+ A60*traA*	GJV1+ A60*traA*	A60*traA*
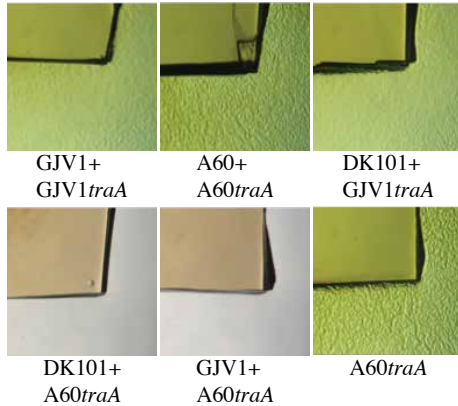
Fig 5. Inhibition of A60*traA* swarming by DK101 and GJV1 is caused by TraA-independent killing. Mixes of kanamycin-resistant *traA* mutants with kanamycin-sensitive non-mutants were incubated on CTT agar without kanamycin and subsequently transferred on onto CTT agar with kanamycin. Lack of swarming out-growth on the kanamycin plates indicates killing of the focal *traA* mutant by the focal non-mutant prior to exposure to kanamycin. None of the *traA* mutants are killed by its parental strain and GJV1*traA* is not killed by DK101 (top row). A60*traA* is killed by both DK101 and GJV1 (bottom row).

*DK101/GJV1 killing of A60traA requires a T6SS*

Many antagonistic interactions between bacteria have been attributed to the T6SS [22, 24, 59, 60]. The T6SS functions in a cell-contact dependent manner in which toxic effector proteins are transferred from donor to recipient cells and can kill recipients that do not produce an appropriate antitoxin [60, 61]. *M. xanthus* encodes the major T6SS gene cluster composed of thirteen loci [62] that include a primary *vgrG* gene (*vgrG1*), but also carries an additional orphan *vgrG* paralog (*vgrG2*) located elsewhere in the genome [55]. VgrG proteins are typically structural components required for T6SS functionality and are located at the tip of the puncturing structure which is formed by Hcp hexamers [63, 64]. Previous work has shown that T6SS-dependent killing in *M. xanthus* is abolished if either the primary or orphan *vgrG* gene is disrupted [55]. Further, deletion of a putative effector gene (*tsxE*) downstream of *vgrG2* similarly abolished T6SS-mediated antagonisms. Complementation of *tsxE* restored the killing phenotype and deletion of the associated immunity gene *tsxI* rendered the mutant susceptible to killing by its parental strain.

To test whether the observed TraA-independent killing of A60*traA* by GJV1 is mediated by its T6SS, we used five T6SS mutants created in the DK1622 background [55]. Four of these five mutants had their T6SS defect verified by Hcp secretion assays and complementation, whereas one (SA5701, *ΔtagF*) retained T6SS activity [55]. Killing was first assayed by determining the presence or absence of A60*traA* growth on kanamycin agar after co-culture with the T6SS mutants. Consistent with the results of Troselj *et al.* [55], we found that the *ΔtagF* mutant SA5701 retained the ability to kill A60*traA*, whereas the other four mutants, which each lacked one or both of the *vgrG* genes, were unable to kill A60*traA* (Fig 6A). These results are supported further by a quantitative assay of survival by A60*traA* after co-incubation with several strains, including its own parent A60. After 24 hrs of co-incubation at a 1:2 ratio, A60*traA* CFU counts were greatly reduced by DK101, GJV1 and the *ΔtagF* mutant SA5701, but not by the T6SS-deletion mutant SA5707, relative to the control mix of A60*traA* with A60 (Fig 6B).

These results implicate the DK1622/GJV1 T6SS as the mechanism by which GJV1 kills both A60 and A60*traA*. Further, from the expected overall genomic similarity of GJV1 and DK101 [46, 51], we infer that T6SS-dependent killing is most likely responsible for the TraA-independent swarming inhibition of the natural isolates by DK101 as well. A model of known and proposed interactions and relationships among DK101, DK1622 and GJV1 collectively emerging from our results and those of previous studies is presented in Fig 7.
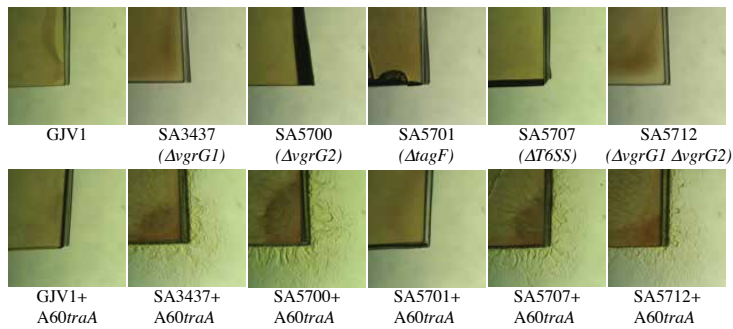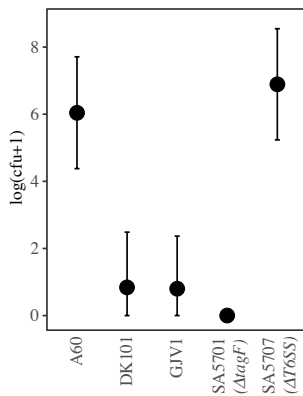
Fig 6. Deletion of T6SS genes alleviates TraA-independent killing of a natural isolate. A. Top row: Monocultures of kanamycin-sensitive GJV1 and T6SS mutants initially grown on CTT agar fail to grow when placed on CTT-kanamycin agar. Bottom row: Killing-assay phenotypes of cultures of A60*traA* mixed with GJV1 and several T6SS mutants initially grown on CTT agar and transferred to CTT-kanamycin agar. GJV1 and a *ΔtagF* mutant (SA5701) both retain T6SS activity [55] and kill A60*traA*. Mutants known to have lost T6SS activity (SA3437, SA5700, SA5707, and SA5712 [55]) do not kill A60*traA*. B. CFU counts of A60*traA* after 24 hours of co-incubation with each strain indicated on the *x* axis. Error bars represent 95% confidence intervals, *n* = 3 replicates.
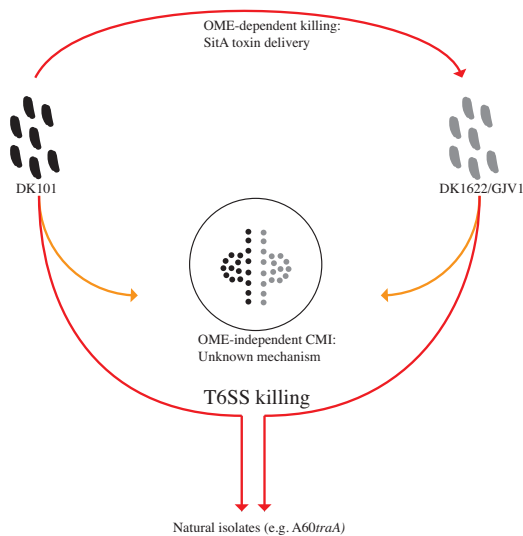
Fig 7. Model of known and proposed interactions and relationships among DK101, DK1622 and GJV1. DK101 kills DK1622 and GJV1 due to OME delivery of SitA toxins ([26, 46] and Fig 1). A CMI boundary forms between colonies of DK101 and GJV1 (and by inference DK1622) that is not caused by OME-delivered Sit toxins (Fig 2). DK101, DK1622 and GJV1 are proposed to kill (and thus inhibit swarming by) natural isolates (and *traA* mutants of such isolates) due to a shared T6SS (Fig 6).

Developmental antagonisms between TraA-identical natural isolates are also independent of OME

When *M. xanthus* natural isolates are mixed at unequal frequencies, the minority strain is often strongly antagonized by the majority type, suffering greatly reduced population size or outright extinction [48]. We tested for a possible role of OME-delivered toxins such as SitA in mediating antagonisms between TraA-compatible natural isolates during starvation-induced development. To do so, we screened for developmental antagonisms exerted against rifampicin-marked variants of strains A23, A47 and A96 when they were mixed as the minority type in 1:99 ratios with the other unmarked strains in this study sharing the same *traA* allele (A00, A23, A30, A32, A46, A60, A72 and A93 mixed with A23rifR; A07, A26, A47 and A96 mixed with A47rif[R]; and A07, A26, A47 and A96 mixed with A96rif[R]). Strain pairs were homogeneously mixed, starved on TPM agar and viable spore production after five days of starvation was quantified for the total population and both individual strains.

In pure-culture controls, all strains examined produced high levels of viable spores (S3 Fig). In control pairings of the three rifampicin-resistant mutants of A23, A47 and A96 mixed as a minority with their unmarked parent, no antagonism was observed, as spore production by the minority marked type was not reduced by the parent relative to expectations from pure-culture assays (Fig 8). Among the 13 pairings of the rifampicin-resistant mutants with other (nonparental) strains, in seven cases the majority strain eliminated spore production by the minority strain (at our limit of detection) whereas in the other six pairings no antagonism was observed (Fig 8). Strains A30, A72 and A93 in the majority eliminated spore production by A23rif[R], A96 similarly antagonized A47rif[R] and A07, A26 and A47 antagonized A96rif[R] (Fig 8).
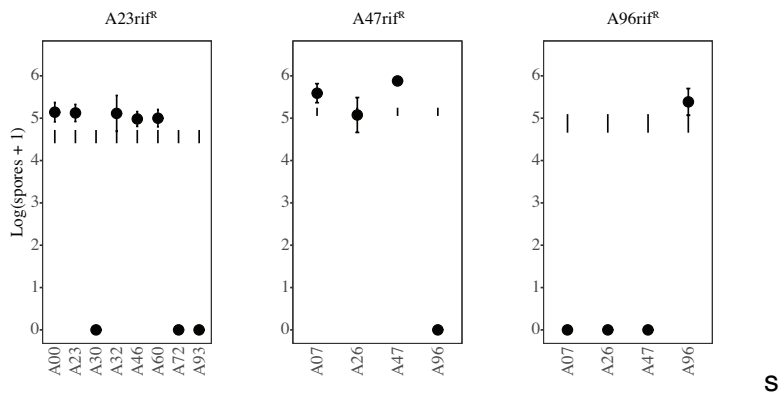
Fig 8. Antagonism patterns of focal minority strains in mixed groups during starvation-induced development. Actual spore production by marked natural isolates mixed in the minority at a 1:99 ratio with unmarked isolates (indicated on the *x* axis) prior to starvation-induced development is represented by closed circles. Expected spore production ranges of the minority strains based on pure-culture assays are depicted by error bars with no circles. Error bars represent 95% confidence intervals, $n = 3$ replicates.

To examine whether OME-transferred toxins might fully or partially cause the observed developmental antagonisms, we tested whether the antagonisms are alleviated to any degree by disruption of *traA* in the parent of the respective minority victim strain. In all seven cases of severe antagonism, spore production by the corresponding *traA* mutant of the victim minority strain was also reduced to zero (or near zero) by the antagonistic majority strain, thus implicating OME-independent mechanisms (Fig 9).
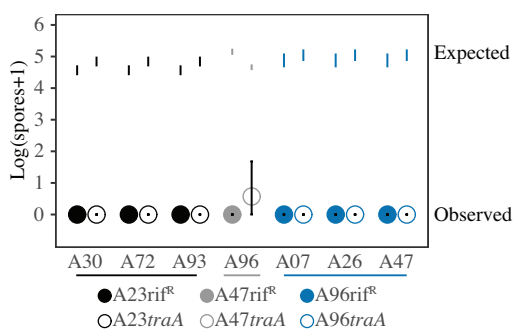
Fig 9. Severe antagonisms between TraA-identical natural isolates are independent of TraA. Antagonisms during development in which viable spore production by some natural isolates is eliminated (or nearly eliminated) in mixtures with other isolates are not alleviated by disruption of *traA*. Actual spore production by rifampicin-resistant variants of victim strains and respective kanamycin-resistant *traA* mutants in 1:99 initial mixtures with respective unmarked antagonizing isolates is represented by closed and open circles, respectively. Expected spore production of the victim strains from pure-culture assays is depicted by error bars with no circles. A23rif[R] and A23*traA* (black circles) were each mixed with A30, A72 and A93, A47rif[R] and A47*traA* (grey circles) were mixed with A96 and A96rif[R] and A96*traA* (blue circles) were mixed with A07, A26 and A47. Error bars represent 95% confidence intervals, $n = 3$ replicates.

96

Discussion

The occurrence of five predicted TraA compatibility groups in a cm-scale *M. xanthus* population [3] (with multiple isolates representing each group) suggests that a large fraction of randomly selected isolate pairs will be incompatible for OME due to functional dissimilarity at the PA14 domain of TraA. For this reason alone, a large fraction of latent CMIs and antagonisms among all possible *M. xanthus* strain pairs (e.g. [19, 48, 65]) are expected to be independent of OME. Nonetheless, *M. xanthus* natural genetic diversity is highly structured spatially [47, 49], such that strains sampled at small spatial scales across which interactions between genotypes are most likely (e.g. μm–cm) may often be compatible for OME at TraA. It is thus relevant to test whether CMIs and antagonisms among TraA-compatible natural isolates of *M. xanthus* from the same local population generally involve OME-mediated toxin transfer, as this study has done.

The *traA* gene was disrupted in eleven *M. xanthus* natural isolates and potential alleviation of CMIs by *traA* disruption was examined for 33 isolate pairs. In no case were CMI phenotypes eliminated or even visually reduced by *traA* disruption (Fig 3 and S2 Fig). Moreover, seven severe antagonisms between distinct isolates identical at TraA were also not alleviated by *traA* disruption (Fig 9). Thus, our results do not support the hypothesis that OME-dependent toxin delivery is commonly responsible for inter-strain CMIs and antagonisms among natural isolates compatible for OME at TraA [26, 47]. Rather, these findings suggest that any CMIs and/ or antagonisms among natural isolates caused primarily by OME-delivered toxins are rare relative to OME-independent mechanisms, even among strains compatible for OME at *traA*. In turn, these results do not strengthen the hypothesis that selection for resistance to newly evolved forms of OME toxin delivery is the primary evolutionary mechanism by which TraA has diversified into several types that are functionally incompatible for OME [3, 38].

Both the results of a previous study [3] and our findings here indicate that OME-independent CMIs can evolve rapidly. First, they are common among strains in the focal Tübingen cm-scale population [3] that are genomically similar yet TraA-incompatible. Second, we discovered that the very closely related lab strains GJV1 and DK101 form CMI boundaries between them, regardless of whether or not both strains have a functional copy of *traA* (Fig 2) and despite swarming inhibition of GJV1 by DK101 being alleviated by *traA* disruption (Fig1). These strains differ primarily in the absence in GJV1 of a substantial portion of a highly variable 150 kb region (localized near position 2.2 Mbp in the genome of reference strain DK1622; [47]) in which phage genes are overrepresented and homologs of contact-dependent growth inhibition genes were found [47]. Partial deletion of this region in the lineage from DK101 to DK1622 (the immediate precursor to GJV1), including deletion of two of the three Mx-alpha prophage copies present in DK101 [46], may have generated not only the OME-dependent susceptibility of DK1622 to an Mx-alpha toxin produced by DK101, but also the OME-independent CMI that we observed between these strains (Fig 2). Finally, in a previous study, TraA-independent CMIs were found to evolve indirectly between a majority of pairs of lab-evolved *M. xanthus* populations that recently diverged from a common ancestor [1].

Future identification of genes responsible for CMIs and inter-strain antagonisms will be of interest for gaining a molecular-level understanding of intra-specific social divergence in natural populations of myxobacteria. Such antagonistic compounds might be secondary metabolites [66] or proteins, including bacteriolytic enzymes [67, 68] which have been suggested to aid in predation and act as anti-competitor agents [69–71] and T6SS effector toxins [28, 55]. Some anti-competitor compounds might be delivered by outer-membrane vesicles, which have been implicated in predation by *M. xanthus* [72]. The full range of OM-vesicle contents in this species is not known, but many hydrolases and proteases have been identified [73, 74]. While the binding of *M. xanthus* outer-membrane vesicles to other *M.*

xanthus cells has not been demonstrated, it is thought that outer-membrane vesicles in general are able to fuse with other gram-negative bacteria [75, 76].

The T6SS is common among bacteria and is also found in multiple species of myxobacteria [55]. In this study, we found that T6SS-defective mutants of the lab reference strain DK1622 are unable to kill a natural isolate that is killed by both DK101 and GJV1, implicating their sharedT6SS in these lethal interactions (Fig 6). Intraspecific variation in effector/immunity gene combinations can generate many mutually toxic T6SS types within the same bacterial species [77], a possibility that may explain some of the lethal antagonisms among *M. xanthus* natural isolates [48].

Wielgoss *et al.* 2016 [47] found a correlation between gene-content patterns in the 150 kb highly variable genomic region containing the prophage Mx alpha in DK101 and DK1622 (46) and previously categorized inter-colony compatibility types (or "allorecognition types") [19].This correlation suggested that variation in toxin-gene content in this region (e.g. encoding Sit, T6SS, and Rhs/CdiA toxins) may be responsible for at least some antagonisms among the Tübingen cm-scale strains, whether by TraA-dependent or TraA-independent mechanisms [47]. Such polymorphic toxin systems, which often include T6SS and *rhs/cdiA* loci, are common among both bacteria and archaea that do not carry TraA homologs, which appear to be specific to the myxobacteria [38, 78, 79].

We observed that the pattern of severe developmental antagonisms across strain pairings demonstrated in this study (Fig 8) corresponds exactly with the pattern of colony incompatibility documented by Vos & Velicer (2009) [19] among the respective (unmarked) strains (Table 3). The combination of this correspondence and the previously noted correlation of the colony-compatibility pattern in [19] with gene-content in the highly polymorphic genomic region [47] suggests that variation in toxin/immunity gene content in this region may be largely responsible for severe antagonisms among the Tübingen cm-scale isolates. This hypothesis requires further testing, but if it is the case, the results shown in Fig 9 suggest that the relevant

toxins expressed from the 150 kb polymorphic region do not generally require TraA-dependent OME to reach and kill competing genotypes.

Table 3. Patterns of developmental antagonism and colony incompatibility.

Developmental competition strains		Antagonism of minority strain	Demarcation line between parental strains in [19]	CMI between parental strains in this study (Figs. 3B, S2A)
Minority	Majority			
A23rif[R]	A00	−	−	−
A23rif[R]	A30	+	+	+
A23rif[R]	A32	−	−	−
A23rif[R]	A46	−	−	−
A23rif[R]	A60	−	−	−
A23rif[R]	A72	+	+	+
A23rif[R]	A93	+	+	+
A47rif[R]	A07	−	−	−
A47rif[R]	A26	−	−	−
A47rif[R]	A96	+	+	+
A96rif[R]	A07	+	+	+
A96rif[R]	A26	+	+	+
A96rif[R]	A47	+	+	+

Our results do not exclude the possibility that OME-delivered Sit toxins contribute to some antagonisms and CMIs between TraA-compatible myxobacterial strains in nature. However, the finding that *traA* disruption does not alleviate any of the severe antagonisms examined this study suggests that the respective aggressor strains either do not produce toxins delivered by OME or, if they do, any effects of such TraA-dependent toxins are secondary to TraA-independent mechanisms. These results thus magnify the open question of how much fitness benefits from OME-mediated interference competition contribute to the evolutionary maintenance of the *traA/traB* operon in many species of myxobacteria [38] relative to other selective forces.

Acknowledgments

Author Contribution

References

1. Rendueles O, Zee PC, Dinkelacker I, Amherd M, Wielgoss S, Velicer GJ. Rapid and widespread de novo evolution of kin discrimination. Proc Natl Acad Sci USA. 2015; 112(29):9076–81. https://doi.org/10.1073/pnas.1502251112 PMID: 261504982.
2. Strassmann JE, Gilbert OM, Queller DC. Kin Discrimination and Cooperation in Microbes. Annu Rev Microbiol. 2011; 65:349–67. https://doi.org/10.1146/annurev.micro.112408.134109 PMID: 216826423.
3. Wielgoss S, Fiegna F, Rendueles O, Yu YN, Velicer GJ. Kin discrimination and outer membrane exchange in Myxococcus xanthus: A comparative analysis among natural isolates. Mol Ecol. 2018; 27(15):3146–58. https://doi.org/10.1111/mec.14773 PMID: 299248834.
4. Aoki SK, Pamma R, Hernday AD, Bickham JE, Braaten BA, Low DA. Contact-dependent inhibition of growth in Escherichia coli. Science. 2005; 309(5738):1245–8. https://doi.org/10.1126/science.1115109 PMID: 161098815.
5. Hawlena H, Bashey F, Mendes-Soares H, Lively CM. Spiteful Interactions in a natural population of the bacterium Xenorhabdus bovienii. Am Nat. 2010; 175(3):374–81. https://doi.org/10.1086/650375 PMID:200958266.
6. Gilbert OM, Foster KR, Mehdiabadi NJ, Strassmann JE, Queller DC. High relatedness maintains multicellular cooperation in a social amoeba by controlling cheater mutants. Proc Natl Acad Sci USA. 2007;104(21):8913–7. https://doi.org/10.1073/pnas.0702723104 PMID: 174961397.

7. Hamilton WD. The genetical evolution of social behaviour. I. J Theor Biol. 1964; 7(1):1–16. https://doi.org/10.1016/0022-5193(64)90038-4 PMID: 5875341

8. West SA, Griffin AS, Gardner A. Social semantics: altruism, cooperation, mutualism, strong reciprocity and group selection. J Evol Biol. 2007; 20(2):415–32. https://doi.org/10.1111/j.1420-9101.2006.01258. x PMID: 17305808

9. Gardner A, West SA, Buckling A. Bacteriocins, spite and virulence. Proc Biol Sci. 2004; 271 (1547):1529–35. https://doi.org/10.1098/rspb.2004.2756 PMID: 15306326

10. Ho HI, Hirose S, Kuspa A, Shaulsky G. Kin Recognition Protects Cooperators against Cheaters. Curr Biol. 2013; 23(16):1590–5. https://doi.org/10.1016/j.cub.2013.06.049 PMID: 23910661

11. Mehdiabadi NJ, Jack CN, Farnham TT, Platt TG, Kalla SE, Shaulsky G, et al. Social evolution: kin preference in a social microbe. Nature. 2006; 442(7105):881–2. https://doi.org/10.1038/442881a PMID: 16929288

12. Beecher MD, Beecher IM, Hahn S. Parent-Offspring Recognition in Bank Swallows (Riparia-Riparia) .2. Development and Acoustic Basis. Anim Beh. 1981; 29(Feb):95–101.

13. Breed MD, Williams KR, Fewell JH. Comb wax mediates the acquisition of nest-mate recognition cues in honey bees. Proc Natl Acad Sci USA. 1988; 85(22):8766–9. https://doi.org/10.1073/pnas.85.22.8766 PMID: 16593995

14. Dietemann V, Liebig J, Holldobler B, Peeters C. Changes in the cuticular hydrocarbons of incipient reproductives correlate with triggering of worker policing in the bulldog ant Myrmecia gulosa. Behav Ecol Sociobiol. 2005; 58(5):486–96.

15. Komdeur J, Hatchwell BJ. Kin recognition: function and mechanism in avian societies. Trends Ecol Evol. 1999; 14(6):237–41. https://doi.org/10.1016/s0169-5347(98)01573-0 PMID: 10354628

16. Peeters C, Monnin T, Malosse C. Cuticular hydrocarbons correlated with reproductive status in a queenless ant. Proc R Soc Lond B. 1999; 266(1426):1323–7.

17. Nair RR, Fiegna F, Velicer GJ. Indirect evolution of social fitness inequalities and facultative social exploitation. Proc R Soc B. 2018; 285(1875).

18. Dienes L. Reproductive Processes in Proteus Cultures. Proc Soc Exp Biol Med. 1946; 63(2):265–70. https://doi.org/10.3181/00379727-63-15570 PMID: 20277719

19. Vos M, Velicer GJ. Social Conflict in Centimeter and Global-Scale Populations of the Bacterium Myxococcus xanthus. Curr Biol. 2009; 19(20):1763–7. https://doi.org/10.1016/j.cub.2009.08.061 PMID: 19879146

20. Stefanic P, Kraigher B, Lyons NA, Kolter R, Mandic-Mulec I. Kin discrimination between sympatric Bacillus subtilis isolates. Proc Natl Acad Sci USA. 2015; 112(45):14042–7. https://doi.org/10.1073/ pnas.1512671112 PMID: 26438858

21. Munson EL, Pfaller MA, Doern GV. Modification of dienes mutual inhibition test for epidemiological characterization of Pseudomonas aeruginosa isolates. J Clin Microbiol. 2002; 40(11):4285–8. https:// doi.org/10.1128/JCM.40.11.4285-4288.2002 PMID: 12409411

22. Alteri CJ, Himpsl SD, Pickens SR, Lindner JR, Zora JS, Miller JE, et al. Multicellular Bacteria Deploy the Type VI Secretion System to Preemptively Strike Neighboring Cells. PLoS Pathog. 2013; 9(9).

23. Gibbs KA, Urbanowski ML, Greenberg EP. Genetic determinants of self identity and social recognition in bacteria. Science. 2008; 321(5886):256–9. https://doi.org/10.1126/science.1160033 PMID: 18621670

24. Wenren LM, Sullivan NL, Cardarelli L, Septer AN, Gibbs KA. Two independent pathways for self-recognition in Proteus mirabilis are linked by type VI-dependent export. MBio. 2013; 4(4).

25. Lyons NA, Kraigher B, Stefanic P, Mandic-Mulec I, Kolter R. A Combinatorial Kin Discrimination System in Bacillus subtilis. Curr Biol. 2016; 26(6):733–42. https://doi.org/10.1016/j.cub.2016.01.032 PMID: 26923784

26. Vassallo CN, Cao PB, Conklin A, Finkelstein H, Heyer CS, Wall D. Infectious polymorphic toxins delivered by outer membrane exchange discriminate kin in myxobacteria. Elife. 2017; 6.

27. Patra P, Vassallo CN, Wall D, Igoshin OA. Mechanism of Kin-Discriminatory Demarcation Line Formation between Colonies of Swarming Bacteria. Biophys J. 2017; 113(11):2477–2486. https://doi.org/10. 1016/j.bpj.2017.09.020 PMID: 29212001

28. Gong Y, Zhang Z, Liu Y, Zhou XW, Anwar MN, Li ZS, et al. A nuclease-toxin and immunity system for kin discrimination in Myxococcus xanthus. Environ Microbiol. 2018; 20(7):2552–67. https://doi.org/10.1111/1462-2920.14282 PMID: 29806725

29. Hodgkin J, Kaiser D. Genetics of Gliding Motility in Myxococcus xanthus (Myxobacterales) - 2 Gene Systems Control Movement. Mol Gen Genet. 1979; 171(2):177–91.

30. Kaiser D. Signaling in myxobacteria. Annu Rev Microbiol. 2004; 58:75–98. https://doi.org/10.1146/annurev.micro.58.030603.123620 PMID: 15487930

31. Berleman JE, Kirby JR. Deciphering the hunting strategy of a bacterial wolfpack. FEMS Microbiol Rev. 2009; 33(5):942–57. https://doi.org/10.1111/j.1574-6976.2009.00185.x PMID: 19519767

32. Wireman JW, Dworkin M. Developmentally Induced Autolysis during Fruiting Body Formation by Myxococcus xanthus. J Bacteriol. 1977; 129(2):796–802.

33. Nudleman E, Wall D, Kaiser D. Cell-to-cell transfer of bacterial outer membrane lipoproteins. Science. 2005; 309(5731):125–7. https://doi.org/10.1126/science.1112440 PMID: 15994555

34. Pathak DT, Wei XM, Bucuvalas A, Haft DH, Gerloff DL, Wall D. Cell Contact-Dependent Outer Membrane Exchange in Myxobacteria: Genetic Determinants and Mechanism. PLoS Genet. 2012; 8 (4):160–71.

35. Nudleman E, Wall D, Kaiser D. Polar assembly of the type IV pilus secretin in Myxococcus xanthus. Mol Microbiol. 2006; 60(1):16–29. https://doi.org/10.1111/j.1365-2958.2006.05095.x PMID: 16556217

36. Pathak DT, Wei XM, Dey A, Wall D. Molecular Recognition by a Polymorphic Cell Surface Receptor Governs Cooperative Behaviors in Bacteria. PLoS Genet. 2013; 9(11).

37. Wei X, Pathak DT, Wall D. Heterologous protein transfer within structured myxobacteria biofilms. Mol Microbiol. 2011; 81(2):315–26. https://doi.org/10.1111/j.1365-2958.2011.07710.x PMID: 21635581

38. Cao P, Wei X, Awal RP, Muller R, Wall D. A Highly Polymorphic Receptor Governs Many Distinct Self-Recognition Types within the Myxococcales Order. MBio. 2019; 10(1).

39. Vassallo C, Pathak DT, Cao PB, Zuckerman DM, Hoiczyk E, Wall D. Cell rejuvenation and social behaviors promoted by LPS exchange in myxobacteria. Proc Natl Acad Sci USA. 2015; 112(22):E2939–E46. https://doi.org/10.1073/pnas.1503553112 PMID: 26038568

40. Cao P, Wall D. Self-identity reprogrammed by a single residue switch in a cell surface receptor of a social bacterium. Proc Natl Acad Sci USA. 2017; 114(14):3732–7. https://doi.org/10.1073/pnas. 1700315114 PMID: 28320967

41. Cao PB, Dey A, Vassallo CN, Wall D. How Myxobacteria Cooperate. J Mol Biol. 2015; 427(23):3709– 21. https://doi.org/10.1016/j.jmb.2015.07.022 PMID: 26254571

42. Vassallo CN, Wall D. Tissue repair in myxobacteria: A cooperative strategy to heal cellular damage. Bioessays. 2016; 38(4):306–15. https://doi.org/10.1002/bies.201500132 PMID: 26898360

43. Wall D. Molecular recognition in myxobacterial outer membrane exchange: functional, social and evolutionary implications. Mol Microbiol. 2014; 91(2):209–20. https://doi.org/10.1111/mmi.12450 PMID: 24261719

44. Wall D. Kin Recognition in Bacteria. Annu Rev Microbiol. 2016; 70:143–60. https://doi.org/10.1146/ annurev-micro-102215-095325 PMID: 27359217

45. Ruhe ZC, Low DA, Hayes CS. Bacterial contact-dependent growth inhibition. Trends Microbiol. 2013; 21(5):230–7. https://doi.org/10.1016/j.tim.2013.02.003 PMID: 23473845

46. Dey A, Vassallo CN, Conklin AC, Pathak DT, Troselj V, Wall D. Sibling Rivalry in Myxococcus xanthus Is Mediated by Kin Recognition and a Polyploid Prophage. J Bacteriol. 2016; 198(6):994–1004. https:// doi.org/10.1128/JB.00964-15 PMID: 26787762

47. Wielgoss S, Didelot X, Chaudhuri RR, Liu X, Weedall GD, Velicer GJ, et al. A barrier to homologous recombination between sympatric strains of the cooperative soil bacterium Myxococcus xanthus. ISME J. 2016; 10(10):2468–77. https://doi.org/10.1038/ismej.2016.34 PMID: 27046334

48. Rendueles O, Amherd M, Velicer GJ. Positively Frequency-Dependent Interference Competition Maintains Diversity and Pervades a Natural Population of Cooperative Microbes. Curr Biol. 2015; 25 (13):1673–81. https://doi.org/10.1016/j.cub.2015.04.057 PMID: 26051889

49. Vos M, Velicer GJ. Isolation by distance in the spore-forming soil bacterium Myxococcus xanthus. Curr Biol. 2008; 18(5):386–391. https://doi.org/10.1016/j.cub.2008.02.050 PMID: 18328701

50. Kaiser D. Social Gliding Is Correlated with the Presence of Pili in Myxococcus xanthus. Proc Natl Acad Sci USA. 1979; 76(11):5952–6. https://doi.org/10.1073/pnas.76.11.5952 PMID: 42906

51. Velicer GJ, Raddatz G, Keller H, Deiss S, Lanz C, Dinkelacker I, et al. Comprehensive mutation identification in an evolved bacterial cooperator and its cheating ancestor. Proc Natl Acad Sci USA. 2006; 103 (21):8107–12. https://doi.org/10.1073/pnas.0510740103 PMID: 16707573

52. Velicer GJ, Kroos L, Lenski RE. Loss of social behaviors by Myxococcus xanthus during evolution in an unstructured habitat. Proc Natl Acad Sci USA. 1998; 95(21):12376–80. https://doi.org/10.1073/pnas. 95.21.12376 PMID: 9770494

53. Wall D, Kolenbrander PE, Kaiser D. The Myxococcus xanthus pilQ (sglA) gene encodes a secretin homolog required for type IV pilus biogenesis, social motility, and development. J Bacteriol. 1999; 181

54. Vos M, Velicer GJ. Genetic population structure of the soil bacterium Myxococcus xanthus at the centimeter scale. Appl Environ Microbiol. 2006; 72(5):3615–25. https://doi.org/10.1128/AEM.72.5.36153625.2006 PMID: 16672510

55. Troselj V, Treuner-Lange A, Sogaard-Andersen L, Wall D. Physiological Heterogeneity Triggers Sibling Conflict Mediated by the Type VI Secretion System in an Aggregative Multicellular Bacterium. MBio. 2018; 9(1).

56. Rodriguez AM, Spormann AM. Genetic and molecular analysis of cglB, a gene essential for single-cell gliding in Myxococcus xanthus. J Bacteriol. 1999; 181(14):4381–90. PMID: 10400597

57. Bretscher AP, Kaiser D. Nutrition of Myxococcus xanthus, a fruiting myxobacterium. J Bacteriol. 1978; 133(2):763–8. PMID: 415048

58. Muller S, Willett JW, Bahr SM, Scott JC, Wilson JM, Darnell CL, et al. Draft Genome of a Type 4 Pilus Defective Myxococcus xanthus Strain, DZF1. Genome Announc. 2013; 1(3).

59. Hood RD, Singh P, Hsu F, Guvener T, Carl MA, Trinidad RR, et al. A type VI secretion system of Pseudomonas aeruginosa targets a toxin to bacteria. Cell Host Microbe. 2010; 7(1):25–37. https://doi.org/10. 1016/j.chom.2009.12.007 PMID: 20114026

60. Russell AB, Hood RD, Bui NK, LeRoux M, Vollmer W, Mougous JD. Type VI secretion delivers bacteriolytic effectors to target cells. Nature. 2011; 475(7356):343–7. https://doi.org/10.1038/nature10244 PMID: 21776080

61. Russell AB, Peterson SB, Mougous JD. Type VI secretion system effectors: poisons with a purpose. Nat Rev Microbiol. 2014; 12(2):137–48. https://doi.org/10.1038/nrmicro3185 PMID: 24384601

62. Konovalova A, Petters T, Sogaard-Andersen L. Extracellular biology of Myxococcus xanthus. FEMS Microbiol Rev. 2010; 34(2):89–106. https://doi.org/10.1111/j.1574-6976.2009.00194.x PMID: 19895646

63. Cianfanelli FR, Monlezun L, Coulthurst SJ. Aim, load, fire: The Type VI secretion system, a bacterial nanoweapon. Trends Microbiol. 2016; 24(1):51–62. https://doi.org/10.1016/j.tim.2015.10.005 PMID: 26549582

64. Zoued A, Brunet YR, Durand E, Aschtgen MS, Logger L, Douzi B, et al. Architecture and assembly of the Type VI secretion system. Biochim Biophys Acta. 2014; 1843(8):1664–73. https://doi.org/10.1016/j. bbamcr.2014.03.018 PMID: 24681160

65. Kraemer SA, Wielgoss S, Fiegna F, Velicer GJ. The biogeography of kin discrimination across microbial neighbourhoods. Mol Ecol. 2016; 25(19):4875–88. https://doi.org/10.1111/mec.13803 PMID: 27540705

66. Krug D, Zurek G, Revermann O, Vos M, Velicer GJ, Muller R. Discovering the hidden secondary metabolome of Myxococcus xanthus: a study of intraspecific diversity. Appl Environ Microbiol. 2008; 74 (10):3058–68. https://doi.org/10.1128/AEM.02863-07 PMID: 18378661

67. McCurdy HD Jr., MacRae TH. Xanthacin. A bacteriocin of Myxococcus xanthus fb. Can J Microbiol. 1974; 20(2):131–5. https://doi.org/10.1139/m74-021 PMID: 4132608

68. Sudo S, Dworkin M. Bacteriolytic Enzymes Produced by Myxococcus xanthus. J Bacteriol. 1972; 110 (1):236–245. PMID: 4622898

69. Davies J, Spiegelman GB, Yim G. The world of subinhibitory antibiotic concentrations. Curr Opin Microbiol. 2006; 9(5):445–53. https://doi.org/10.1016/j.mib.2006.08.006 PMID: 16942902

70. Keane R, Berleman J. The predatory life cycle of Myxococcus xanthus. Microbiology. 2016; 162(1):1– 11. https://doi.org/10.1099/mic.0.000208 PMID: 26518442

71. Smith DR, Dworkin M. Territorial interactions between two Myxococcus Species. J Bacteriol. 1994; 176 (4):1201–5. https://doi.org/10.1128/jb.176.4.1201-1205.1994 PMID: 8106334

72. Evans AGL, Davey HM, Cookson A, Currinn H, Cooke-Fox G, Stanczyk PJ, et al. Predatory activity of Myxococcus xanthus outer-membrane vesicles and properties of their hydrolase cargo. Microbiology. 2012; 158:2742–52. https://doi.org/10.1099/mic.0.060343-0 PMID: 22977088

73. Berleman JE, Allen S, Danielewicz MA, Remis JP, Gorur A, Cunha J, et al. The lethal cargo of Myxococcus xanthus outer membrane vesicles. Front Microbiol. 2014; 5:474. https://doi.org/10.3389/fmicb. 2014.00474 PMID: 25250022

74. Kahnt J, Aguiluz K, Koch J, Treuner-Lange A, Konovalova A, Huntley S, et al. Profiling the Outer Membrane Proteome during Growth and Development of the Social Bacterium Myxococcus xanthus by Selective Biotinylation and Analyses of Outer Membrane Vesicles. J Proteome Res. 2010; 9(10):5197– 208. https://doi.org/10.1021/pr1004983 PMID: 20687614

75. Kadurugamuwa JL, Beveridge TJ. Bacteriolytic effect of membrane vesicles from Pseudomonas aeruginosa on other bacteria including pathogens: Conceptually new

antibiotics. J Bacteriol. 1996; 178 (10):2767–74. https://doi.org/10.1128/jb.178.10.2767-2774.1996 PMID: 8631663

76. Kulp A, Kuehn MJ. Biological Functions and Biogenesis of Secreted Bacterial Outer Membrane Vesicles. Ann Rev Microbiol. 2010; 64:163–84.

77. Unterweger D, Miyata ST, Bachmann V, Brooks TM, Mullins T, Kostiuk B, et al. The Vibrio cholerae type VI secretion system employs diverse effector modules for intraspecific competition. Nat Commun. 2014; 5:3549. https://doi.org/10.1038/ncomms4549 PMID: 24686479

78. Jamet A, Nassif X. New Players in the Toxin Field: Polymorphic Toxin Systems in Bacteria. MBio. 2015; 6(3).

79. Makarova K, Wolf Y, Karamycheva S, Zhang D, Aravind L, Koonin E. Antimicrobial Peptides, Polymorphic Toxins, and Self-Nonself Recognition Systems in Archaea: an Untapped Armory for Intermicrobial Conflicts. MBio. 2019; 10(3).

Supporting information
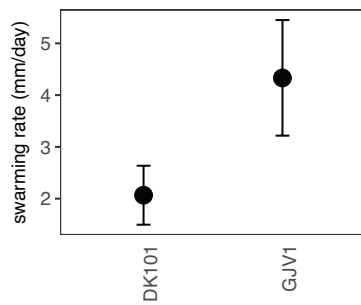
S1 Fig. GJV1 and DK101 differ in their monoculture swarming rates. In monoculture, GJV1 swarms faster than DK101 due to the motility defect of DK101. *y* axis values indicate the swarming rate (mm/day) for each strain indicated on the *x* axis. Error bars are 95% confidence intervals, *n* = 3 temporally independent replicates.
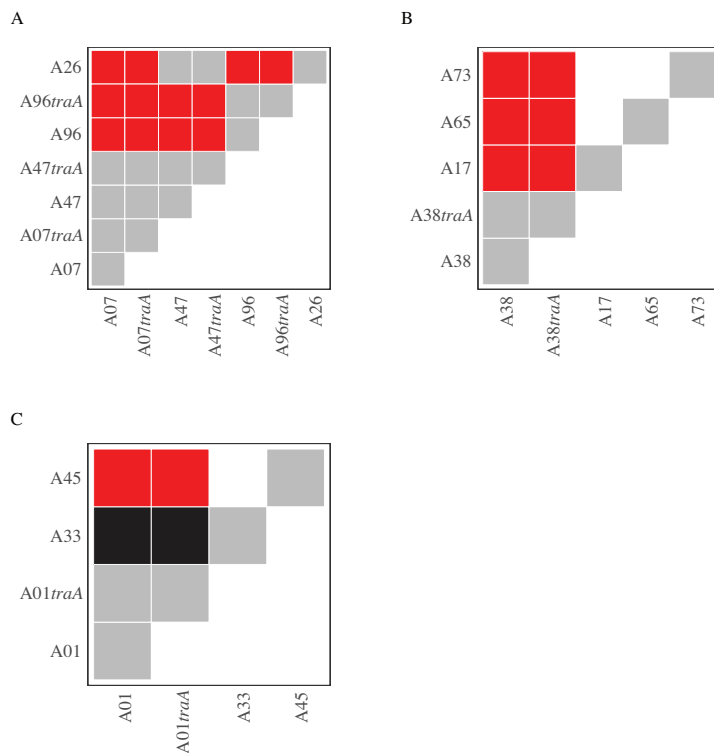
S2 Fig. Disruption of *traA* does not alter CMI-occurrence patterns across pairings of *traA*-identical natural isolates. All possible pairwise encounters between strains sharing the same *traA* allele for three different alleles representing three predicted TraA compatibility groups (A, B, and C, respectively) (3). Red represents formation of visible CMI demarcation boundaries, grey represents the absence of such boundaries, and black represents inconsistent results between replicates. In no case did disruption of *traA* eliminate a CMI boundary present between colonies of two natural isolates (or generate such a boundary not present between two isolates).
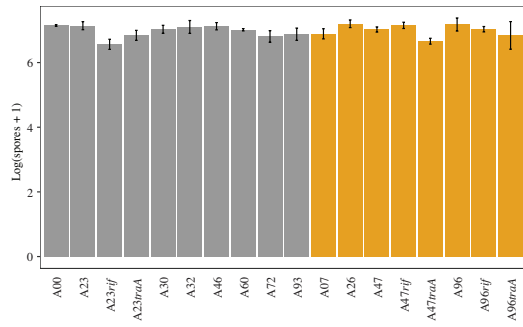
S3 Fig. Monoculture spore production values of a subset of natural isolates. Viable spore production of A23, A47, A96, their respective rifampicin-resistant variants and kanamycin-resistant *traA* mutants, and all other isolates mixed with A23, A47 or A96 during co-development (Fig 8). *y* axis values show the log-transformed spore production of each isolate indicated on the *x* axis. Bars are colored either orange or grey to indicated predicted TraA compatibility. Error bars are 95% confidence intervals, *n* = 3 replicates.

Chapter 3

Shorter starvation favors non-sporulating cell types during *Myxococcus xanthus* multicellular development

Sarah M. Cossey, Marie Vasse, Yuen-Tsu Nicco Yu, Gregory Velicer

Abstract

Genetically identical individuals in a microbial population can be phenotypically distinct. Such heterogeneity can help a population cope with environmental fluctuations and allows for the division of labor in clonal groups, such as in the multicellular-development program of the bacterium *Myxococcus xanthus*. Upon depletion of growth resources, *M. xanthus* initiates its development program in which many cells contribute to fruiting-body formation while only a minority become stress-resistant spores. Non-spore cells are thought to mostly die, whereas spores can survive extended starvation to germinate when conditions become favorable. An additional cell type present during development – peripheral rods – neither form spores nor enter fruiting bodies but remain metabolically active and motile. We asked whether genotypes that commit fewer cells to the spore fate would have an advantage over genotypes that convert more cells into spores when conditions allowing growth are encountered sooner rather than later after initiation of development. During an evolution experiment designed to address this question, for two of three ancestral genotypes used, populations that starved for a short period (two days) before resuming growth in each evolutionary life-cycle evolved to commit fewer cells to the spore fate than populations that starved longer (ten days). This outcome supports the hypothesis that cell-type differentiation during aggregative development is an evolutionary bet-hedging strategy that is responsive to selection by variable degrees of starvation-induced stress in natural populations.

Introduction

Fluctuations in abiotic and biotic environments are ubiquitous and living organisms must be able to cope with these changes. Sensing and responding to environmental fluctuations using dedicated sensory systems is common, but maintaining these systems can be energetically expensive, especially if environmental insults occur infrequently or unpredictably (Kussell and Leibler 2005). The cost of maintaining multiple sensory systems is even higher, making it impractical to have a distinct system for each of many different environmental stressors (Kashiwagi et al. 2006). Microbes can dodge some of these costs through a phenomenon called phenotypic heterogeneity (Wolf et al. 2005; Acar et al. 2008), in which a genetically identical population is phenotypically diverse (Ackermann 2015). Phenotypic heterogeneity can result in populations being better able to survive heat stress (Levy et al. 2012), antibiotic exposure (Balaban et al. 2004), or being able to continue growth after nutrient shifts (Solopova et al. 2014)

Phenotypic heterogeneity can be determined randomly at the single-cell level, such as during the transition to competence in *Bacillus subtilis* (Maamar et al. 2007; Chastanet et al. 2010) or becoming an antibiotic tolerant persister cell during *Escherichia coli* growth (Balaban et al. 2004). It can also occur at the group level, such as in variation of fruiting-body group size in *M. xanthus* (Amherd et al. 2018). There are also coordinated mechanisms for generating heterogeneity such as the cell-cell signaling that happens during nitrogen-fixing heterocyst formation (Flores and Herrero 2010). Phenotypic heterogeneity need not be advantageous in all environments to be net-beneficial, but might often be advantageous over a phenotypically homogenous population when environmental conditions fluctuate extensively (Ackermann 2015). Non-genetic phenotypic diversity can play a key role in a microbe's ability to cope with rapidly changing environments and provides an opportunity for division of labor to arise in clonal groups.

Division of labor is characterized by cooperative individuals specializing and working as a collective to complete tasks in a more efficient manner (West and Cooper 2016). In microbes, division of labor is important during complex behaviors such as host infection in *Salmonella,* where a subset of the population expresses the Type-III secretion system (T3SS). T3SS-expressing cells generate inflammation in the host which benefits the non-expressing subset of the population by allowing them to outcompete the native host microbiota (Stecher et al. 2007; Ackermann et al. 2008). Biofilms, which rely on cells specializing in functions such as adhesion or extracellular matrix production, can also be considered in the context of division of labor (Gestel et al. 2015; Dragoš et al. 2018). The cooperative formation of multicellular fruiting-body structures is also characterized by cells adopting specific cell fates such as sterile stalk cells that prop up and aid in the dispersal of stress-resistant spores (Miguélez et al. 1999; Strassmann et al. 2000). Division of labor is thought to be more robust when relatedness is high due to the reduced potential for conflict between individuals during the expression of cooperative behaviors (West and Cooper 2016).

Some cell fates involve performing costly behaviors that benefit other cells in the population, as occurs during starvation-induced multicellular development in the dictyostelids and myxobacteria*,* where some cells die while forming multicellular fruiting-body structures that are presumed to benefit another cell type in the group, namely spores (Wireman and Dworkin 1977; Strassmann et al. 2000). Processes like multicellular development and sporulation are beneficial under harsh environmental conditions, especially when those conditions are long-lasting (Lennon and Jones 2011). However, if environmental conditions improve relatively quickly, cells already committed to the spore fate might resume growth less quickly than any non-spores that remain viable. Therefore, allocating some cells in a population to a cell fate that can respond more quickly to improved environmental conditions and other cells to another fate better at enduring longer stress could be a bet-hedging strategy in some microbial species (Simons 2011). Illustrating this hypothesis, theoretical studies of

developing *Dictyostelium discoideum* populations predict that a non-sporulating, non-aggregating cell type, which is at a disadvantage during starvation-induced development, can be favored over spores if nutrients replenish quickly after the initiation of development (Dubravcic et al. 2014; Tarnita et al. 2015).

The social soil bacterium *Myxococcus xanthus* responds to nutrient deprivation by entering a starvation-induced development program. The initiation of development requires a cascade of intra and intercellular signaling events – some of which are density dependent – that coordinate the aggregation of single cells, culminating in the formation of multicellular, spore-bearing fruiting bodies (Shimkets 1999). *M. xanthus* cells differentiate into three cell types present during starvation-induced multicellular development: spores, aggregative non-spores and non-aggregating, non-sporulating cells known as peripheral rods (O'Connor and Zusman 1991b; Lee et al. 2012).

Before fruiting-body formation occurs, aggregation is triggered by nutrient deprivation, and during this process a large fraction of the population lyses (Wireman and Dworkin 1977; Nariya and Inouye 2008; Lee et al. 2012), leaving the remaining cells to differentiate between spores and peripheral rods. The aggregative cells that do not differentiate into spores contribute to the cooperative formation of fruiting bodies and their lysis may provide an energy source for development and be important for spore formation (Wireman and Dworkin 1977; Shimkets 1999), although the extent of cell lysis may differ by strain and experimental handling techniques (Wireman and Dworkin 1977; O'Connor and Zusman 1988; Nariya and Inouye 2008; Lee et al. 2012). Peripheral rods do not join aggregates, instead they remain metabolically active and motile at the periphery of aggregates and eventually fruiting bodies. They also have gene-expression and protein-accumulation profiles that are distinct from those of both vegetative cells and spores (O'Connor and Zusman 1991b; Lee et al. 2012). The mechanisms of cell-fate determination in *M. xanthus* remain largely unknown and it is still unclear whether and in what manner peripheral rod cells contribute to group-level fitness.

However, it seems likely that they serve as a type of persister cell, ready to take advantage of rapidly improving environmental conditions (Kroos 2017).

Here, we aimed to understand the evolutionary significance of the peripheral-rod fate during *M. xanthus* development. Using an experimental-evolution approach, we asked whether initially isogenic populations that repeatedly experience cycles of starvation and growth tend to evolve larger fractions of non-spores during development when starvation is shorter rather than longer, under the premise that living non-spores are expected to have an advantage over spores during the transition from starvation to growth. We sought to manipulate the degree of selection on becoming spores in two ways (Figure 1). In one manipulation, we either killed all surviving non-spores at the end of starvation by heat (maximum selection for spore formation) or not. In a second manipulation, we varied how long populations starved in each evolutionary cycle prior to resuming growth (2 days, 10 days or stochastically alternating between 2 and 10 days), predicting that the strength of selection favoring the spore fate would correlate positively with starvation duration. Specifically, we sought to test whether populations regularly given nutrients to resume growth after shorter starvation would evolve higher fractions of non-spores than populations that starve longer (10 days). Such a result would provide evidence that peripheral rod cells are an evolutionarily important cell type that likely function as an insurance policy against the rapid return of nutrients. We performed the experiment with three distinct ancestral genotypes to test whether responses to selection would be independent of or rather contingent on prior evolutionary histories.
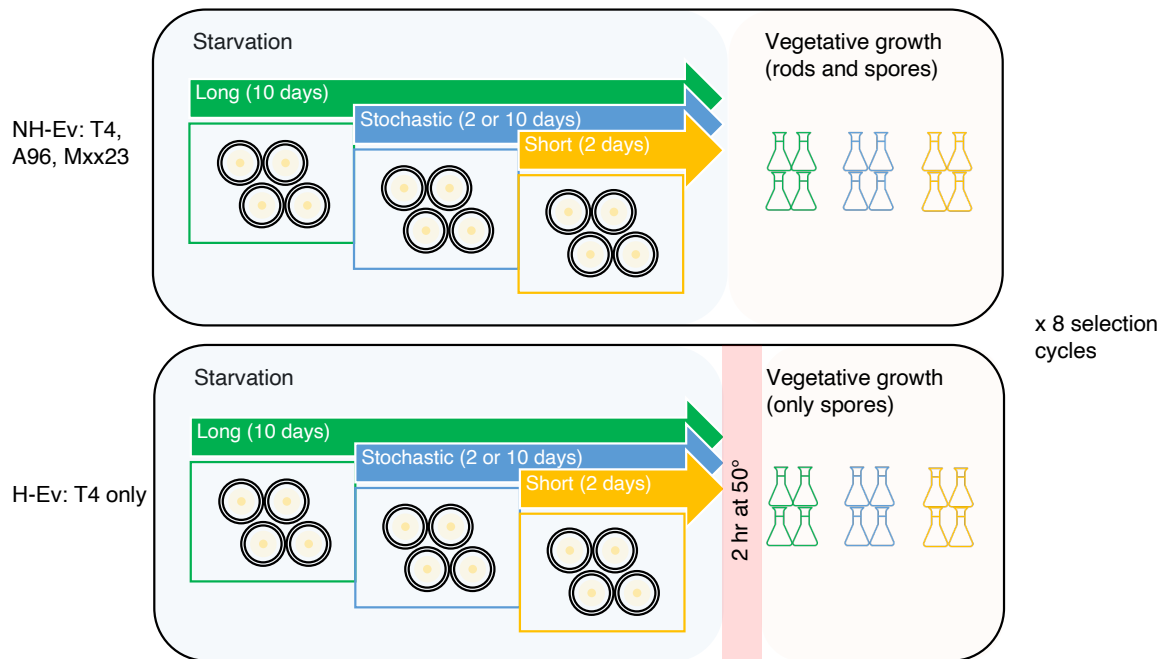
Figure 1. Experimental design. We designed this selection experiment to investigate the potential fitness consequences of different cell fates during *M. xanthus* multicellular development. The selective regimes in which peripheral rod cells are allowed to survive after starvation-induced development are collectively referred to as NH-Ev; evolution in these environments was initiated with three distinct *M. xanthus* genetic backgrounds (T4, A96, and Mxx23) (top). The presumed growth advantage of peripheral rods compared to spores may result in the evolution of altered cell-type partitioning. Four clones were isolated from each genetic background to seed four replicate populations that evolved in each of three starvation-duration treatments. After the defined starvation period, all cells were transferred to liquid growth medium for the vegetative growth phase. Starvation followed by a growth phase comprise one selection cycle, and the experiment was repeated for eight selection cycles. To understand how the developmental phenotypes would evolve when only spores were transferred between selection cycles, an additional set of the four replicate populations of the T4 genetic background were evolved with the same three starvation-duration treatments but all non-spore cells were killed with a heat treatment prior to vegetative growth at the end of each cycle.

Materials and methods

Development and sporulation assays

All cultures were grown to an OD_{595} of 0.2-0.8 in liquid CTT medium (Bretscher and Kaiser 1978) incubated at 32 °C with 300 rpm shaking. To initiate multicellular development, cultures were centrifuged and resuspended in TPM liquid medium (Bretscher and Kaiser 1978) to a density of ~5 x 10^9 cells/mL and then 50 μL of the cell suspension was spotted on TPM 1.5% agar plates. The plates were dried for ~1 hr and then incubated at 32 °C and 90% relative humidity for either 2, 5, or 10 days. To estimate spore production after starvation, cell populations were harvested from the starvation plates using a sterile scalpel, resuspended in

1 mL of sterile double-distilled water, incubated at 50 °C for 2 hours, and then sonicated and dilution-plated in CTT 0.5% agar. Dilution plates were incubated at 32 °C and 90% relative humidity for 5-6 days before colonies were counted.

Experimental evolution

Three *M. xanthus* genetic backgrounds were selected as the ancestors for an evolution experiment with three treatments that differed in the duration of starvation experienced each experimental cycle. The three strains – T4, A96 (Vos and Velicer 2009) and Mxx23 (Fiegna and Velicer 2005) – were selected for being relatively distantly related (Vos and Velicer 2009), being developmentally proficient in pure culture, and carrying a plasmid conferring kanamycin resistance. Two of the strains (A96 and Mxx23) derived from recent natural isolates. The strain 'T4' used here descends from strain GJV1 (Velicer *et al.* 2006) and was transformed with a plasmid derived from pGVTu1 (Zee et al. 2017) in which the GFP gene of pGVTu1 was exchanged with the dTomato gene (Shaner et al. 2004).

The selection experiment was established with 4 replicate populations from each genetic background within each evolutionary treatment; each replicate population was seeded from separately isolated clones of each genotype that had been stored frozen. To initiate the evolution experiment, all replicate populations were inoculated from freezer stock directly into CTT liquid medium and grown as described above until reaching mid-log phase. Each population was then resuspended to $\sim 5 \times 10^9$ cells/mL and 50 μL of the cell suspension ($\sim 2.5 \times 10^8$ cells) was spotted onto three separate TPM 1.5% agar plates corresponding to the three starvation-duration treatments: 2 days (short), 2 or 10 days (stochastic), and 10 days (long).

After the defined starvation period, cell populations were harvested from the starvation plates using a sterile scalpel, transferred to CTT liquid, and incubated as described above until they reached mid-log phase. After harvesting, cells were not incubated at 50 °C or dispersed by sonication – as is often done in *M. xanthus* developmental assays – in order to keep all

non-spore cells alive. These evolved populations are referred to as NH-Ev (no heat evolved). Growth and starvation were alternated as described for 8 selection cycles, where one cycle includes both development and vegetative growth.

For the T4 genetic background we repeated the same growth and development cycles but killed off all non-spore cells with a 50 °C heat treatment for 2 hours before beginning the growth phase. These evolved populations are referred to as H-Ev (heated evolved) . In this way we can distinguish the effects of varying starvation lengths alone on spore productivity and fruiting-body formation versus the effects of growth-phase competition between rods and spores.

Image analysis to estimate fruiting-body parameters

Prior to harvesting the fruiting bodies, images of all plates were captured using an Olympus SXZ16 microscope with an Olympus DP80 camera system. Images were captured with exposure time = 1 ms, lens = Olympus 0.5 x PF, zoom = 1.25x, ISO = 400, illumination = BF built-in system. These images were imported into F_{IJI} image-analysis software (Schindelin et al. 2012) and processed as described previously (Fortezza and Velicer 2021). Fruiting-body metrics, including fruiting-body count, size, and grey value, were collected using threshold values optimized for the ancestral strains. For strains where the image analysis pipeline did not recognize any fruiting bodies, a zero value was manually entered.

Statistical methods

Analyses were performed using R version 4.3.0 and Rstudio version 2023.03.1+446 (Team 2023; team 2023). We fitted two separate mixed linear models to the sporulation data from the T4 genetic background using the lmer() function from the lme4 R package (Bates et al. 2015). The first model included all sporulation data, including from the ancestor, and the interaction between evolution treatment and assay length as a fixed effect and replicates

nested into strain identity as random effects. The second model focused on evolved populations and we model the interaction between sporulation treatment, heat treatment , and assay length as a fixed effect with replicates nested into population identity as a random effect. We further used the first model to analyze the sporulation data of Mxx23 and A96. All models were followed by type III ANOVA using the car R package (Fox and Weisberg 2019) and pairwise comparisons of the marginal means (with Tukey correction for multiple testing) using the emmeans R package (Length 2023). The same approach was used for the fruiting body formation data sets of Mxx23 and A96. For the T4 fruiting body data we excluded the data from the NH-Ev-T4 population due to a complete separation of data in the dataset where the NH-EV-T4 populations produced either zero or very few fruiting bodies. We therefore fitted a model to the fruiting body data of the H-Ev-T4 populations and the ancestor with the interaction between evolution treatment and assay length as a fixed effect and replicate nested into strain identity as a random effect.

Results

Selection regimes

One potential advantage of maintaining a non-aggregating cell population is the potential to respond quickly upon rapid return of nutrients (Tarnita et al. 2015). Myxospores, for example, require 8-12 hours to germinate before they can resume growth and division (O'Connor and Zusman 1991a; Pande et al. 2020) while the time needed for peripheral rod cells to achieve their first division appears to be shorter (O'Connor and Zusman 1991a) although it has not been precisely measured. Further evidence supporting a growth advantage for peripheral rod cells shows that purified rods and vegetative cells have indistinguishable growth rates, as measured by swarming distance after being provided prey cells, while purified spores swarm more slowly than vegetative cells but do eventually catch up (O'Connor and Zusman 1991a). The apparent growth advantage of peripheral rod cells over spores after

nutrient replenishment led us to design an evolution experiment to ask whether the relative degree of differentiation into spores vs non-spores during *M. xanthus* development is evolutionarily responsive to differences in how long cell populations repeatedly starve before again experiencing growth-inducing resource levels (Figure 1). Our main goal in varying the duration of starvation was to vary the level of benefit derived from differentiating into a mature spore vs a viable rod cell.

We designed an experiment that involved simply growing cell cultures from three distinct genetic backgrounds to mid-log phase in liquid growth medium, plating them at high cell density on starvation agar plates to initiate multicellular development, transferring all cells back to liquid-growth medium after a defined period of starvation, and allowing the rods and spores to grow until the cultures reached mid-log phase. The putative reduced lag time of peripheral rod cells should allow them and their descendants to complete more cell divisions than lineages derived from spores. In an additional set of treatments involving one of the ancestors, rod cells were killed by heat before surviving spores were transferred into growth medium.

Starvation without heat selection favors non-sporulating cells

After 8 selection cycles we found that all of the populations that evolved under conditions of maximum selection for spores (H-Ev-T4) appear ancestral in their sporulation phenotypes (Figure 2A, linear mixed model: evolution treatment x assay length interaction, $Chi^2 = 118.6856$, $p < 0.0001$; Tukey contrasts on H-Ev-T4 vs ancestral marginal means, see Table S1), indicating that starvation-duration during evolution did not impose selection on sporulation levels when only spores were transferred across evolutionary cycles. Post-evolution assay duration did, however, have a significant effect on spore production within all H-Ev-T4 evolutionary treatments, but not on the ancestor, with spore counts after 10 days of starvation for the former being significantly lower than after 2 or 5 days (Table S2). In contrast, we found that regardless of the starvation-duration during evolution, all NH-Ev-T4 populations, in which surviving non-spores were not experimentally killed, showed reduced levels or rates of spore

118

formation compared to their ancestor (Figure 2A and Table S1, linear mixed model: evolution treatment x assay length interaction, Chi^2 = 118.6856, $p < 0.0001$; Tukey contrasts on NH-Ev-T4 vs ancestral marginal means). Non-heated T4 populations that experienced 2-day or stochastic starvation durations during evolution – 'NH-Ev2-T4' and 'NH-EvStoch-T4' populations, respectively – produced significantly fewer spores than their ancestor at all assay lengths, while the NH-Ev10-T4 populations had significantly lower spore counts after two and five days of starvation but recovered to ancestral levels after ten days of starvation. It is unclear why selection with long starvation resulted in populations with reduced spore production during shorter starvation assays. Overall, the reduced investment in spores in the NH-Ev-T4 populations, particularly in the NH-Ev2-T4 populations, shows that non-sporulating peripheral rod cells had a selective advantage during the vegetative growth phase following starvation and that the degree of cell-type heterogeneity during *M. xanthus* development is responsive to selection imposed by both heat stress and starvation duration.
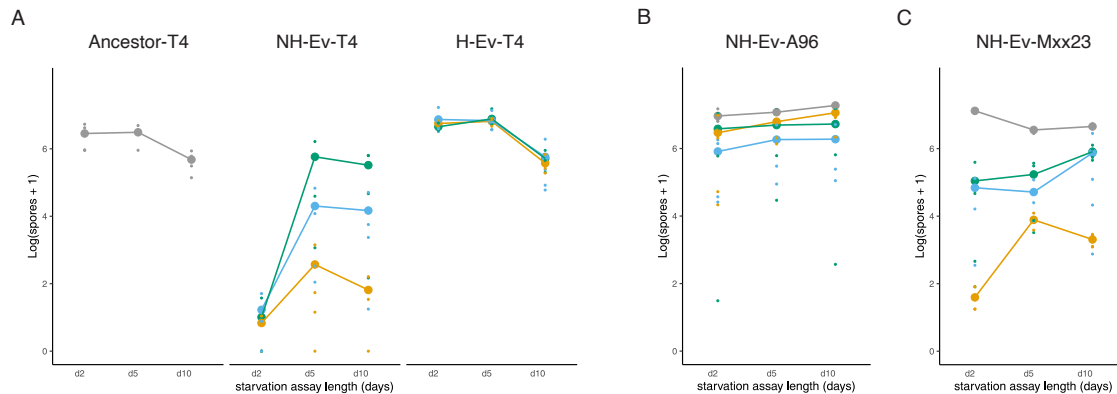
Figure 2. Heat stress and longer starvation select for higher levels of sporulation than benign temperature and short starvation, respectively, in populations descended from a lab reference strain. Patterns of spore-production evolution are highly variable across ancestral genotypes. Log-transformed spore counts are shown on the *y* axis and the length of starvation in days (assay length) is on *x* axis. Ancestor spore counts are shown in grey, short (2-day) evolution in orange, stochastic in blue, and long (10-day) in green. **A**) The T4 ancestor (grey) sporulates similarly at all assay lengths (2, 5 and 10 days). After 2 days of starvation in the post-evolution assays, all NH-Ev-T4 populations have significantly reduced spore production compared to the ancestor. After 10 days of starvation, the NH-Ev2-T4 and NH-Evstoch-T4 but not the NH-Ev10-T4 populations produced fewer spores than the ancestor (Table S1). All of the H-Ev-T4 populations sporulated as well as the ancestor at all assay lengths; spore counts were similarly high after two and five days of starvation but then decreased by ten days post-starvation (Table S1, S2). **B**) NH-Ev-A96 populations have distinct patterns of sporulation loss that the other two genetic backgrounds. The marginal means of each evolution treatment are significantly lower than that of the ancestor (Table S5). **C**) Spore production in the NH-Ev-Mxx23 populations was more similar to the T4 populations, with all evolution treatments

producing fewer spores than the ancestor at all assay lengths, but with NH-Ev2-Mxx23 producing the fewest spores (Table S4). The larger circles represent mean values across all replicate populations for a given evolution treatment while the smaller circles show the mean values of the three biological replicates of each evolved population (or the ancestor).

Short starvation selects for greater loss of spore formation than long starvation

In accordance with mathematical modeling of *D. discoideum* (Tarnita et al. 2015), we predicted that shorter starvation periods would favor non-sporulating cells, while fewer non-spores would survive longer starvation periods, resulting in higher spore production being favored. Our results show that populations evolved with short-term starvation (NH-Ev2) tended to have lower levels of spore production compared to both their ancestors and those populations that evolved with long-term starvation (NH-Ev10 or NH-Evstoch) (Figure 2; Tables S1, S3, S4) in two of the three genetic backgrounds tested (T4 and Mxx23). This suggests a greater benefit of spore production when starvation times are longer. Additionally, NH-Ev-T4 and NH-Ev-Mxx23 populations that experienced only short starvation during evolution produced significantly fewer spores than their ancestor even after being challenged with longer starvation times in the post-evolution assays. This result confirms that the short-starvation evolution treatment did not simply select for cells with delayed entry into the developmental program, but imposed the strongest selection for altered cell-type partitioning.

We found that the response to selection varied greatly as a function of ancestral genotype (Figure 2). In the A96 genetic background, for example, we did not see the same degree of reduction of spore production in the evolved populations, although overall sporulation was significantly reduced to some degree in all evolution treatments (linear mixed model: evolution treatment, $Chi^2 = 29.8288$, $p < 0.0001$, Table S5). Interestingly, we found that NH-Ev2-A96 populations produced significantly more spores than the NH-Ev10-A96 and NH-EvStoch-A96 populations. If A96 proceeds through development more quickly than the other genotypes, then two days of starvation may not be short enough of a starvation period to favor greater allocation to non-spore cells, which could explain why the NH-Ev2-A96 populations

did not show reduced spore production. The reduction in spore production for the NH-Ev10/Stoch populations has no clear relation to the selective conditions.

Selection for heat-resistant spores promotes the maintenance of fruiting-body formation

In addition to spore production, we measured the number of fruiting bodies formed by the ancestral and evolved populations. We found that selecting for heat-resistant spores promoted the maintenance of fruiting-body formation in populations descended from T4; all heat-treated populations retained relatively high fruiting-body numbers while all unheated evolved populations produced zero or very few fruiting bodies (Figure 3). The complete separation in our dataset between NH-Ev (all or mostly 0 values) and H-Ev (all non-zero values) prevented us from fitting a model. We therefore opted to test for an effect of length of starvation during evolution (Figure 3A, linear mixed model: evolution treatment, $Chi^2 = 23.658$, $p < 0.0001$) and assay length (Figure 3A, linear mixed model: assay length, $Chi^2 = 11.023$, $p = 0.004$) on only the ancestral and H-Ev fruiting-body counts. Comparison of the marginal means between length of starvation during evolution revealed that H-Ev10-T4 produced ancestral levels of fruiting bodies while the 2-day and stochastic evolutionary treatments produced significantly fewer fruiting bodies than their ancestor (Table S6). Despite the difference from the ancestor, the maintenance of fruiting-body formation in the H-Ev populations versus the almost-complete loss of fruiting-body formation in the NH-Ev populations implies that genes important for sporulation are also important for fruiting-body formation. However, we only added the H-Ev treatment for the T4 (laboratory reference) genetic background so it is unclear if this trend would hold in other genetic backgrounds as well. It does appear to make sense in the context of *M. xanthus* biology however, because fruiting-body development relies on intercellular signaling that is important to coordinate developmental gene expression (Kaiser 2004). One of those signals, the C signal, is thought to be transmitted by cell-cell contact (Kim and Kaiser 1990), and high levels of C-signal

expression are required for sporulation. The density and proximity of cells within aggregates and fruiting bodies promotes high levels of C signaling ensuring that spores are formed in the fruiting body (Søgaard-Andersen 2004).
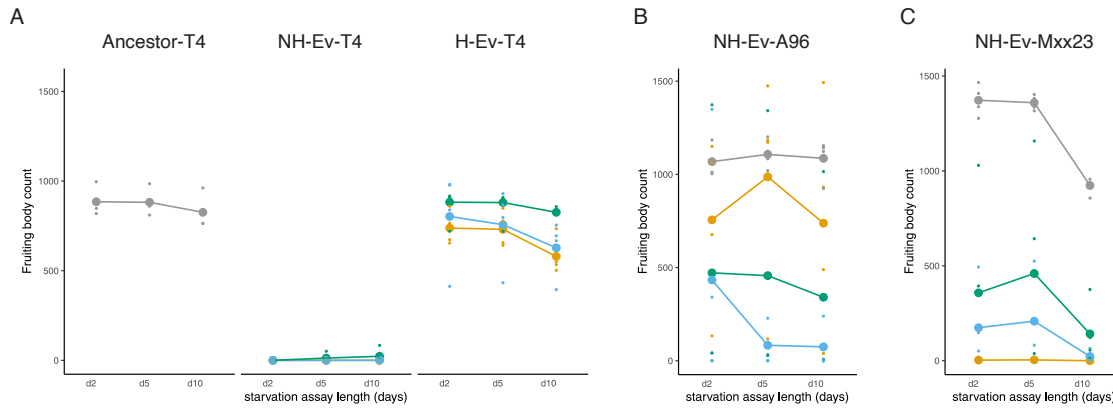
Figure 3. Heat stress promotes the maintenance of fruiting-body formation in populations descended from a laboratory reference strain. Evolution without heat selection has different effects on fruiting-body formation in different genetic backgrounds. Fruiting-body counts are shown on the *y* axis for each starvation assay length (in days) on the *x* axis. Ancestor fruiting-body counts are shown in grey, short (2d) evolution in orange, stochastic in blue, and long (10d) in green. **A**) Heat treatment during evolution had a significant effect on the fruiting-body count at all assay lengths in the T4 genetic background (Table S6). Fruiting-body counts of the NH-Ev-T4 populations are significantly lower than both the ancestor and the H-Ev-T4 populations. H-Ev10-T4 populations produce ancestral numbers of fruiting bodies, but H-Ev2-T4 and H-Evstoch-T4 populations produce significantly fewer. **B**) and **C**) All NH-Ev-A96 and NH-Ev-Mxx23 populations produced significantly fewer fruiting bodies than the ancestor overall, but patterns of evolutionary reduction differ between the ancestral genotypes (also compared to NH-Ev-T4, panel A). The larger circles represent mean values across all replicate populations for a given evolution treatment while the smaller circles show the mean values of the three biological replicates of each evolved population (or the ancestor).

The significant decrease in fruiting-body number between the ancestor and NH-Ev2-T4 and NH-EvStoch-T4 populations is intriguing. It seems likely that most of the overall difference between the ancestor vs evolved populations comes from the 10-day assay, in which the NH-Ev2-T4 and NH-EvStoch-T4 populations appear to show greater decreases in fruiting-body number than the NH-Ev10-T4 populations (Figure 3A). The reduced longevity of fruiting bodies in those treatments could be indicative of antagonistic pleiotropic effects of mutations that have opposing effects of fruiting-body formation and spore production when starvation times are short vs fruiting-body longevity.

Fruiting-body degradation during selection without heat-treatment varies as a function of ancestral genotype

As noted above, the NH-Ev-T4 populations produced zero or very few mature fruiting bodies in all evolution treatments and at all assay lengths (Figure 3A, 4A). The NH-Ev10-T4 populations were the only ones in the T4 genetic background that formed mature fruiting bodies, and only after longer starvation periods (5 or 10 days). The NH-Ev-Mxx23 populations also formed fewer fruiting bodies than their ancestors, with the degree of fruiting-body loss being highest in populations evolved with short starvation (Figure 3C, 4B). Compared to the ancestor, the number of fruiting bodies produced by all NH-Ev-Mxx23 populations was significantly reduced for all evolutionary treatments at all assay lengths (Figure 3C, linear mixed model: evolution treatment x assay length, Chi^2 = 13.999, p = 0.03; Tukey contrasts on marginal means, Table S7). The NH-Ev-A96 populations showed significantly reduced fruiting-body formation compared to their ancestor for the long and stochastic starvation-duration treatments but not for the short-starvation treatment (Figure 3B, linear mixed model: evolution treatment, Chi^2 = 15.2126, p = 0.002; Tukey contrasts on marginal means, Table S8). This pattern of fruiting-body loss is distinct from that of populations descended from the other two genotypes, where in both cases the short-starvation treatment produced fewer fruiting bodies than the other treatments. The higher fruiting-body counts for the NH-Ev2-A96 populations are consistent with the higher spore production measured for those populations. Overall, the degree of loss of fruiting-body formation varied dramatically as a function of ancestral genotype.
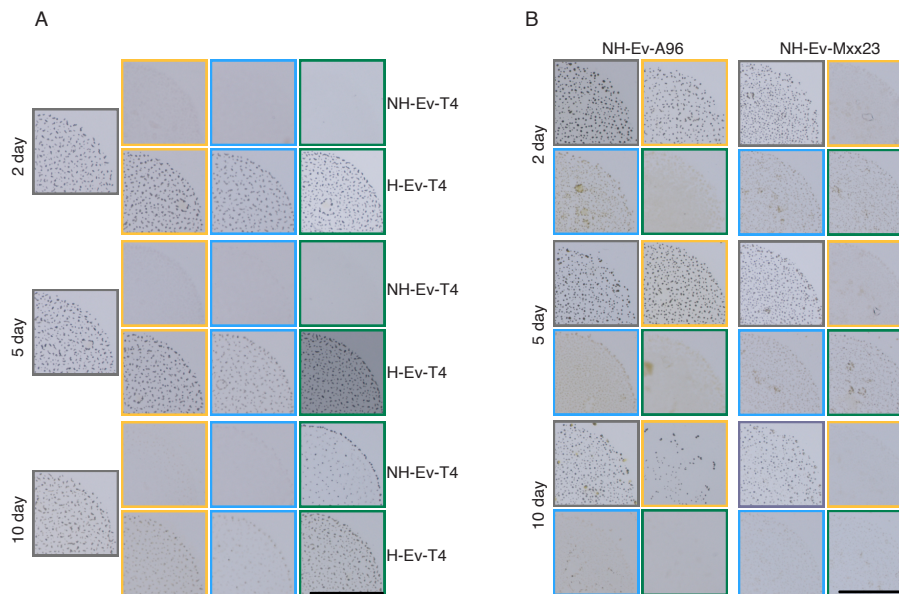
Figure 4. Starving non-heated evolved populations (NH-Ev) from all three genetic backgrounds are morphologically distinct from their ancestor and from the heated evolved (H-EV) populations for the T4 genetic background. Images of the developmental phenotypes of the ancestor versus evolved populations. Post-evolution starvation-assay length is indicated at the left of the images. Ancestor phenotypes are depicted with a grey border, short (2-day) starvation-duration during evolution with orange, stochastic starvation-duration with blue, and long starvation-duration (10-day) with green. Dark spots are mature fruiting bodies and the space between fruiting bodies is populated by peripheral rod cells that are not visible at the low magnifications used here. **A**) The ancestor T4 compared to the NH-Ev-T4 and H-Ev-T4 populations after 2, 5, and 10 days of starvation. **B**) The ancestors A96 (left column) and Mxx23 (right column) compared to their respective NH-Ev populations after 2, 5, and 10 days of starvation. Scale bar is 0.5 cm.

Discussion

We used experimental evolution to examine how cell-type heterogeneity during *M. xanthus* development differentially responds to selection imposed by different lengths of starvation and by the presence vs absence of heat stress. Consistent with the bet-hedging tradeoff hypothesis, for populations descended from two of three ancestor genotypes used, populations evolved with only short starvation produced more non-sporulating cells while populations evolved with long starvation periods tended to produce more spores. How cell-type heterogeneity evolved in response to our selection treatment differed across ancestral genotypes, with the A96 natural-isolate populations differing from populations descended from the other two ancestors by maintaining high levels of spore production regardless of starvation duration during evolution.

Our results are consistent with predictions from mathematical models of *D. discoideum* development predicting that shorter starvation periods selectively favor higher proportions of non-aggregating 'loner' cells while longer starvation periods favor higher spore production (Tarnita et al. 2015). For two of three ancestral genotypes, we observed greater decreases in spore production among populations evolved with short starvation than those with long starvation, although we did not inversely observe increased spore production – relative to the ancestor – in populations that experienced long starvation (10 days). It would be interesting to test whether selection imposed by even longer starvation periods, during which a larger fraction of non-spores might die off, would lead to absolute increases in spore production.

Although the mechanisms of cell-fate determination are not well understood in *M. xanthus*, there are a number of well-characterized developmental signaling mutants that arrest the developmental program at different temporal and morphological stages (Shimkets 1999). One of these developmental signals, the A signal, functions as a quorum-sensing system (Kuspa et al. 1992). The combination of starvation sensing and assessing population density (A-signal levels) initiates the expression of developmentally regulated genes (Kaiser 2004). It is possible then that peripheral rods are cells that either did not receive sufficient A signaling to initiate aggregation or have a different nutrient threshold at which they respond to starvation. Modeling work in *D. discoideum* supports a role of quorum sensing in cell-type partitioning, where cells that responded more slowly to quorum sensing molecules were more likely to be loners (Rossine et al. 2020). If this is the case, heritable differences in starvation sensing and sensitivity to intercellular signaling molecules could be a mechanism resulting in the increased proportion of non-aggregating cells in the NH-Ev populations. The developmental defects of *M. xanthus* signaling mutants can be complemented extracellularly, so mixing the NH-Ev populations with defined signaling mutants could identify if the phenotypes are due to signaling deficiencies that can be complemented. Further, through genome sequencing of the evolved

populations from this study we may be able to shed light on the mechanisms of cell-fate determination during *M. xanthus* development.

In combination with the reduced spore production observed for two of the tested genotypes during evolution without heat, we also observed a reduction in cooperative fruiting-body formation. The reduction was variable across genotypes with (almost) complete abolishment in the T4 genetic background, a significant reduction that was inversely related to the length of starvation during evolution in the Mxx23 genetic background, and no clear pattern in the A96 background. This may be because many of the genes important for sporulation are also likely to be important for fruiting-body formation. Further, developmentally induced cell lysis may aid in the sporulation process (Wireman and Dworkin 1977; Shimkets 1999). The liquid-growth phases of our selection experiment favored viable cells that could respond quickly to nutrient replenishment, which may have resulted in decreased developmental cell lysis. Fruiting-body morphogenesis and sporulation may be less efficient when nutrients released from lysed cells are reduced. It would therefore be interesting to compare the degree of cell lysis in the NH-Ev populations versus that of their ancestors.

During cooperative behaviors like multicellular development, fitness asymmetries between genotypes result in within-group conflict (Velicer 2003; Velicer and Vos 2009). In many studies of both *M. xanthus* and *D. discoideum* development, spore production is the only component of developmental fitness examined. Tarnita *et al.* proposed that a spore-centric view may be an over-simplification because differences in cell-type partitioning between genotypes could explain asymmetries in spore production during chimeric development in the absence of interactions between genotypes. Our results provide empirical support for this perspective by showing that relative investment in spores versus non-spores can evolve in response to selection imposed by variable duration of starvation stress. Further experiments testing whether the NH-Ev populations produce fewer spores during chimeric development with their

ancestor would provide support for the investment strategy of a given genotype impacting its

spore production in chimera.

Table S1. Linear mixed model: evolution treatment x assay length interaction, Chi^2 = 118.6856, p < 0.0001; Tukey contrasts on ancestral versus evolved marginal means at the specified assay length. Sporulation in T4 genetic background.

contrast (evolution treatment)	assay length	Estimate	SE	df	t.ratio	p.value
10d - ancestor	d10	-1.209487	0.465360	211.0176	-2.599033	0.131519
10d_heat - ancestor	d10	-0.188469	0.503825	212.8578	-0.374076	0.999781
2d - ancestor	d10	-4.494825	0.465360	211.0176	-9.658804	0.000000
2d_heat - ancestor	d10	-0.033227	0.465360	211.0176	-0.071400	1.000000
ancestor - stochastic	d10	2.787168	0.465360	211.0176	5.989267	0.000000
ancestor - stochastic_heat	d10	0.103728	0.465360	211.0176	0.222899	0.999990
10d - ancestor	d2	-5.820199	0.465360	211.0176	-12.506863	0.000000
10d_heat - ancestor	d2	0.447240	0.503825	212.8578	0.887690	0.974101
2d - ancestor	d2	-5.777503	0.465360	211.0176	-12.415115	0.000000
2d_heat - ancestor	d2	0.544918	0.465360	211.0176	1.170959	0.904287
ancestor - stochastic	d2	5.678540	0.465360	211.0176	12.202455	0.000000
ancestor - stochastic_heat	d2	-0.560320	0.465360	211.0176	-1.204057	0.892012
10d - ancestor	d5	-2.768926	0.465360	211.0176	-5.950067	0.000000
10d_heat - ancestor	d5	0.569885	0.503825	212.8578	1.131117	0.917871
2d - ancestor	d5	-5.361856	0.465360	211.0176	-11.521943	0.000000
2d_heat - ancestor	d5	0.512989	0.465360	211.0176	1.102347	0.926861
ancestor - stochastic	d5	3.937751	0.465360	211.0176	8.461724	0.000000
ancestor - stochastic_heat	d5	-0.536883	0.465360	211.0176	-1.153692	0.910331

Table S2. Linear mixed model: evolution treatment x assay length interaction, Chi^2 = 118.6856, p < 0.0001; Tukey contrasts on marginal means between assays lengths within each evolution treatment. Sporulation in T4 genetic background.

contrast (assay length)	evolution treatment	estimate	SE	df	t.ratio	p.value
d10 - d2	10d	3.757129	0.465360	211.0176	8.073589	0.000000
d10 - d5	10d	0.691726	0.465360	211.0176	1.486430	0.299478
d2 - d5	10d	-3.065403	0.465360	211.0176	-6.587159	0.000000
d10 - d2	10d_heat	-1.489292	0.537352	211.0176	-2.771539	0.016669
d10 - d5	10d_heat	-1.626066	0.537352	211.0176	-3.026073	0.007813
d2 - d5	10d_heat	-0.136774	0.537352	211.0176	-0.254534	0.964922
d10 - d2	2d	0.429095	0.465360	211.0176	0.922069	0.626959
d10 - d5	2d	-0.000682	0.465360	211.0176	-0.001465	0.999999
d2 - d5	2d	-0.429776	0.465360	211.0176	-0.923535	0.626032
d10 - d2	2d_heat	-1.431728	0.465360	211.0176	-3.076599	0.006676
d10 - d5	2d_heat	-1.413928	0.465360	211.0176	-3.038350	0.007522
d2 - d5	2d_heat	0.017800	0.465360	211.0176	0.038249	0.999194
d10 - d2	ancestor	-0.853583	0.465360	211.0176	-1.834241	0.160978
d10 - d5	ancestor	-0.867713	0.465360	211.0176	-1.864604	0.151599
d2 - d5	ancestor	-0.014130	0.465360	211.0176	-0.030363	0.999492
d10 - d2	stochastic	2.037789	0.465360	211.0176	4.378947	0.000056
d10 - d5	stochastic	0.282871	0.465360	211.0176	0.607853	0.815990
d2 - d5	stochastic	-1.754918	0.465360	211.0176	-3.771093	0.000616
d10 - d2	stochastic_heat	-1.517632	0.465360	211.0176	-3.261197	0.003688
d10 - d5	stochastic_heat	-1.508324	0.465360	211.0176	-3.241195	0.003938
d2 - d5	stochastic_heat	0.009308	0.465360	211.0176	0.020002	0.999779

Table S3. Linear mixed model: evolution treatment x heat x assay length interaction, Chi^2 = 11.8482, p = 0.019; Tukey contrasts on marginal means between evolution treatments at the specified assay length. Sporulation in T4 genetic background.

contrast (evolution treatment)	assay length	heat	estimate	SE	df	t.ratio	p.value
10d - 2d	d2	no	-0.042696	0.490177	178.0245	-0.087104	0.995826
10d - stochastic	d2	no	-0.141660	0.490177	178.0245	-0.288997	0.955017
2d - stochastic	d2	no	-0.098964	0.490177	178.0245	-0.201894	0.977783
10d - 2d	d5	no	2.592931	0.490177	178.0245	5.289787	0.000001
10d - stochastic	d5	no	1.168826	0.490177	178.0245	2.384499	0.047462
2d - stochastic	d5	no	-1.424105	0.490177	178.0245	-2.905288	0.011468
10d - 2d	d10	no	3.285338	0.490177	178.0245	6.702355	0.000000
10d - stochastic	d10	no	1.577681	0.490177	178.0245	3.218596	0.004347
2d - stochastic	d10	no	-1.707657	0.490177	178.0245	-3.483759	0.001794
10d - 2d	d2	yes	-0.101084	0.530923	179.8781	-0.190393	0.980217
10d - stochastic	d2	yes	-0.116487	0.530923	179.8781	-0.219404	0.973816
2d - stochastic	d2	yes	-0.015403	0.490177	178.0245	-0.031423	0.999456
10d - 2d	d5	yes	0.053490	0.530923	179.8781	0.100749	0.994420
10d - stochastic	d5	yes	0.029596	0.530923	179.8781	0.055744	0.998288
2d - stochastic	d5	yes	-0.023894	0.490177	178.0245	-0.048746	0.998691
10d - 2d	d10	yes	-0.158648	0.530923	179.8781	-0.298816	0.951985
10d - stochastic	d10	yes	-0.088147	0.530923	179.8781	-0.166025	0.984920
2d - stochastic	d10	yes	0.070502	0.490177	178.0245	0.143829	0.988661

Table S4. Linear mixed model: evolution treatment x assay length interaction, Chi^2 = 77.008, p < 0.0001; Tukey contrasts on marginal means of between evolution treatments at the specified assay length. Sporulation in Mxx23 genetic background.

contrast (evolution treatment)	assay length	estimate	SE	df	t.ratio	p.value
10d - 2d	d10	2.504632	0.32646	121	7.672102	0.000000
10d - ancestor	d10	-0.911799	0.32646	121	-2.792991	0.030511
10d - stochastic	d10	1.148081	0.32646	121	3.516761	0.003407
2d - ancestor	d10	-3.416432	0.32646	121	-10.465093	0.000000
2d - stochastic	d10	-1.356552	0.32646	121	-4.155341	0.000351
ancestor - stochastic	d10	2.059880	0.32646	121	6.309752	0.000000
10d - 2d	d2	2.285841	0.32646	121	7.001906	0.000000
10d - ancestor	d2	-3.636197	0.32646	121	-11.138271	0.000000
10d - stochastic	d2	-0.639593	0.32646	121	-1.959179	0.209336
2d - ancestor	d2	-5.922038	0.32646	121	-18.140177	0.000000
2d - stochastic	d2	-2.925434	0.32646	121	-8.961086	0.000000
ancestor - stochastic	d2	2.996604	0.32646	121	9.179091	0.000000
10d - 2d	d5	0.622945	0.32646	121	1.908183	0.230054
10d - ancestor	d5	-2.123126	0.32646	121	-6.503486	0.000000
10d - stochastic	d5	0.007952	0.32646	121	0.024358	0.999995
2d - ancestor	d5	-2.746072	0.32646	121	-8.411670	0.000000
2d - stochastic	d5	-0.614993	0.32646	121	-1.883826	0.240418
ancestor - stochastic	d5	2.131078	0.32646	121	6.527844	0.000000

Table S5. Linear mixed model: evolution treatment, Chi^2 = 29.8288, p < 0.0001; Tukey contrasts on marginal means between evolution treatments. Sporulation in A96 genetic background. One of the NH-Ev10-A96 populations went extinct and is not included in the analysis.

contrast	estimate	SE	df	t.ratio	p.value
10d - 2d	-1.792159	0.370139	116.5630	-4.841858	0.000023
10d - ancestor	-2.709542	0.370139	116.5630	-7.320340	0.000000
10d - stochastic	-1.106483	0.370139	116.5630	-2.989373	0.017699
2d - ancestor	-0.917382	0.337573	112.0411	-2.717582	0.037677
2d - stochastic	0.685677	0.337573	112.0411	2.031195	0.182795
ancestor - stochastic	1.603059	0.337573	112.0411	4.748776	0.000036

Table S6. Linear mixed model: evolution treatment, Chi² = 23.658, p < 0.0001; Tukey contrasts on marginal means between H-Ev treatments and their ancestor. Fruiting-body formation in T4 genetic background.

contrast	estimate	SE	df	t.ratio	p.value
10d - 2d	158.97939	47.19406	119.9137	3.368631	0.005540
10d - ancestor	-22.27061	47.19406	119.9137	-0.471894	0.965107
10d - stochastic	112.72939	47.19406	119.9137	2.388635	0.084753
2d - ancestor	-181.25000	42.80474	118.0050	-4.234344	0.000264
2d - stochastic	-46.25000	42.80474	118.0050	-1.080488	0.702096
ancestor - stochastic	135.00000	42.80474	118.0050	3.153856	0.010860

Table S7. Linear mixed model: evolution treatment x harvest, Chi^2 = 13.999, p = 0.03; Tukey contrasts on marginal means between evolution treatments at a given assay length. Fruiting-body formation in Mxx23 genetic background.

contrast	harvest	estimate	SE	df	t.ratio	p.value
10d - 2d	d2	354.5000	100.9443	121	3.511837	0.003463
10d - ancestor	d2	-1014.4167	100.9443	121	-10.049271	0.000000
10d - stochastic	d2	183.7500	100.9443	121	1.820311	0.268860
2d - ancestor	d2	-1368.9167	100.9443	121	-13.561108	0.000000
2d - stochastic	d2	-170.7500	100.9443	121	-1.691527	0.332614
ancestor - stochastic	d2	1198.1667	100.9443	121	11.869581	0.000000
10d - 2d	d5	455.0833	100.9443	121	4.508262	0.000089
10d - ancestor	d5	-899.7500	100.9443	121	-8.913331	0.000000
10d - stochastic	d5	251.1667	100.9443	121	2.488171	0.066850
2d - ancestor	d5	-1354.8333	100.9443	121	-13.421592	0.000000
2d - stochastic	d5	-203.9167	100.9443	121	-2.020091	0.186325
ancestor - stochastic	d5	1150.9167	100.9443	121	11.401502	0.000000
10d - 2d	d10	141.5000	100.9443	121	1.401763	0.500713
10d - ancestor	d10	-781.6667	100.9443	121	-7.743544	0.000000
10d - stochastic	d10	119.0000	100.9443	121	1.178868	0.641321
2d - ancestor	d10	-923.1667	100.9443	121	-9.145307	0.000000
2d - stochastic	d10	-22.5000	100.9443	121	-0.222895	0.996073
ancestor - stochastic	d10	900.6667	100.9443	121	8.922412	0.000000

Table S8. Linear mixed model: evolution treatment, Chi^2 = 15.2126, p = 0.002; Tukey contrasts on marginal means between evolution treatments. Fruiting-body formation in A96 genetic background. One of the NH-Ev10-A96 populations went extinct and is not included in the analysis.

contrast	estimate	SE	df	t.ratio	p.value
10d - 2d	-420.7726	116.2225	114.4476	-3.620405	0.002451
10d - ancestor	-681.0781	116.2225	114.4476	-5.860123	0.000000
10d - stochastic	209.2274	116.2225	114.4476	1.800232	0.278561
2d - ancestor	-260.3056	105.5262	112.0095	-2.466739	0.070821
2d - stochastic	630.0000	105.5262	112.0095	5.970083	0.000000
ancestor - stochastic	890.3056	105.5262	112.0095	8.436822	0.000000

References

Acar M, Mettetal JT, Oudenaarden A van. Stochastic switching as a survival strategy in fluctuating environments. Nat Genet. 2008;40(4):471–5.

Ackermann M. A functional perspective on phenotypic heterogeneity in microorganisms. Nat Rev Microbiol. 2015;13(8):497–508.

Ackermann M, Stecher B, Freed NE, Songhet P, Hardt WD, Doebeli M. Self-destructive cooperation mediated by phenotypic noise. Nature. 2008;454(7207):987–90.

Amherd M, Velicer GJ, Rendueles O. Spontaneous nongenetic variation of group size creates cheater-free groups of social microbes. Behav Ecol. 2018;29(2):393–403.

Balaban NQ, Merrin J, Chait R, Kowalik L, Leibler S. Bacterial Persistence as a Phenotypic Switch. Science. 2004;305(5690):1622–5.

Bates D, Mächler M, Bolker B, Walker S. Fitting Linear Mixed-Effects Models Using lme4. J Stat Softw. 2015;67(1).

Bretscher AP, Kaiser D. Nutrition of Myxococcus xanthus, a fruiting myxobacterium. J Bacteriol. 1978;133(2):763–8.

Chastanet A, Vitkup D, Yuan GC, Norman TM, Liu JS, Losick RM. Broadly heterogeneous activation of the master regulator for sporulation in Bacillus subtilis. Proc Natl Acad Sci USA. 2010;107(18):8486–91.

Dragoš A, Kiesewalter H, Martin M, Hsu CY, Hartmann R, Wechsler T, et al. Division of Labor during Biofilm Matrix Production. Curr Biol. 2018;28(12):1903-1913.e5.

Dubravcic D, Baalen M van, Nizak C. An evolutionarily significant unicellular strategy in response to starvation in Dictyostelium social amoebae. F1000Res. 2014;3:133.

Fiegna F, Velicer GJ. Exploitative and Hierarchical Antagonism in a Cooperative Bacterium. Plos Biol. 2005;3(11):e370.

Flores E, Herrero A. Compartmentalized function through cell differentiation in filamentous cyanobacteria. Nat Rev Microbiol. 2010;8(1):39–50.

Fortezza ML, Velicer GJ. Social selection within aggregative multicellular development drives morphological evolution. Proc Biol Sci. 2021;288(1963):20211522.

Fox J, Weisberg S. An R Companion to Applied Regression. Sage publications; 2019.

Gestel J van, Vlamakis H, Kolter R. Division of Labor in Biofilms: the Ecology of Cell Differentiation. Microbiol Spectr. 2015;3(2):MB-0002-2014.

Kaiser D. Signaling in Myxobacteria. Annu Rev Microbiol. 2004;58(1):75–98.

Kashiwagi A, Urabe I, Kaneko K, Yomo T. Adaptive Response of a Gene Network to Environmental Changes by Fitness-Induced Attractor Selection. PLoS ONE. 2006;1(1):e49.

Kim SK, Kaiser D. Cell Alignment Required in Differentiation of Myxococcus xanthus. Science. 1990;249(4971):926–8.

Kroos L. Highly Signal-Responsive Gene Regulatory Network Governing Myxococcus Development. Trends Genet. 2017;33(1):3–15.

Kuspa A, Plamann L, Kaiser D. A-signalling and the cell density requirement for Myxococcus xanthus development. J Bacteriol. 1992;174(22):7360–9.

Kussell E, Leibler S. Phenotypic Diversity, Population Growth, and Information in Fluctuating Environments. Science. 2005;309(5743):2075–8.

Lee B, Holkenbrink C, Treuner-Lange A, Higgs PI. Myxococcus xanthus Developmental Cell Fate Production: Heterogeneous Accumulation of Developmental Regulatory Proteins and Reexamination of the Role of MazF in Developmental Lysis. J Bacteriol. 2012;194(12):3058–68.

Length R. emmeans: Estimated Marginal Means, aka Least-Squares Means. R package version 1.8.6 [Internet]. 2023. Available from: https://CRAN.R-project.org/package=emmeans

Lennon JT, Jones SE. Microbial seed banks: the ecological and evolutionary implications of dormancy. Nat Rev Microbiol. 2011;9(2):119–30.

Levy SF, Ziv N, Siegal ML. Bet Hedging in Yeast by Heterogeneous, Age-Correlated Expression of a Stress Protectant. PLoS Biology. 2012;10(5):e1001325.

Maamar H, Raj A, Dubnau D. Noise in Gene Expression Determines Cell Fate in Bacillus subtilis. Science. 2007;317(5837):526–9.

Miguélez EM, Hardisson C, Manzanal MB. Hyphal Death during Colony Development in Streptomyces antibioticus: Morphological Evidence for the Existence of a Process of Cell Deletion in a Multicellular Prokaryote. J Cell Biol. 1999;145(3):515–25.

Nariya H, Inouye M. MazF, an mRNA Interferase, Mediates Programmed Cell Death during Multicellular Myxococcus Development. Cell. 2008;132(1):55–66.

O'Connor KA, Zusman DR. Reexamination of the role of autolysis in the development of Myxococcus xanthus. J Bacteriol. 1988;170(9):4103–12.

O'Connor KA, Zusman DR. Behavior of peripheral rods and their role in the life cycle of Myxococcus xanthus. J Bacteriol. 1991a;173(11):3342–55.

O'Connor KA, Zusman DR. Development in Myxococcus xanthus involves differentiation into two cell types, peripheral rods and spores. J Bacteriol. 1991b;173(11):3318–33.

Pande S, Escriva PP, Yu YTN, Sauer U, Velicer GJ. Cooperation and Cheating among Germinating Spores. Curr Biol. 2020;30(23):4745-4752.e4.

Rossine FW, Martinez-Garcia R, Sgro AE, Gregor T, Tarnita CE. Eco-evolutionary significance of "loners." Plos Biol. 2020;18(3):e3000642.

Schindelin J, Arganda-Carreras I, Frise E, Kaynig V, Longair M, Pietzsch T, et al. Fiji: an open-source platform for biological-image analysis. Nat Methods. 2012;9(7):676–82.

Shaner NC, Campbell RE, Steinbach PA, Giepmans BNG, Palmer AE, Tsien RY. Improved monomeric red, orange and yellow fluorescent proteins derived from Discosoma sp. red fluorescent protein. Nat Biotechnol. 2004;22(12):1567–72.

Shimkets LJ. Intercellular signaling during fruiting-body development of Myxococcus xanthus. Annu Rev Microbiol. 1999;53(1):525–49.

Simons AM. Modes of response to environmental change and the elusive empirical evidence for bet hedging. Proc Biol Sci. 2011;278(1712):1601–9.

Søgaard-Andersen L. Cell polarity, intercellular signalling and morphogenetic cell movements in Myxococcus xanthus. Curr Opin Microbiol. 2004;7(6):587–93.

Solopova A, Gestel J van, Weissing FJ, Bachmann H, Teusink B, Kok J, et al. Bet-hedging during bacterial diauxic shift. Proc National Acad Sci USA. 2014;111(20):7427–32.

Stecher B, Robbiani R, Walker AW, Westendorf AM, Barthel M, Kremer M, et al. Salmonella enterica Serovar Typhimurium Exploits Inflammation to Compete with the Intestinal Microbiota. PLoS Biol. 2007;5(10):e244.

Strassmann JE, Zhu Y, Queller DC. Altruism and social cheating in the social amoeba Dictyostelium discoideum. Nature. 2000;408(6815):965–7.

Tarnita CE, Washburne A, Martinez-Garcia R, Sgro AE, Levin SA. Fitness tradeoffs between spores and nonaggregating cells can explain the coexistence of diverse genotypes in cellular slime molds. Proc Natl Acad Sci USA. 2015;112(9):2776–81.

team P. RStudio: Integrated Development Environment for R. Posit Software, PBC, Boston, MA [Internet]. 2023. Available from: http://www.posit.co/

Team RC. R: A language and environment for statistical computing. R Foundation for Statistical Computing, Vienna, Austria [Internet]. 2023. Available from: https://www.R-project.org/

Velicer GJ. Social strife in the microbial world. Trends Microbiol. 2003;11(7):330–7.

Velicer GJ, Vos M. Sociobiology of the Myxobacteria. Annu Rev Microbiol. 2009;63(1):599–623.

Vos M, Velicer GJ. Social Conflict in Centimeter-and Global-Scale Populations of the Bacterium Myxococcus xanthus. Curr Biol. 2009;19(20):1763–7.

West SA, Cooper GA. Division of labour in microorganisms: an evolutionary perspective. Nat Rev Microbiol. 2016;14(11):716–23.

Wireman JW, Dworkin M. Developmentally induced autolysis during fruiting body formation by Myxococcus xanthus. J Bacteriol. 1977;129(2):798–802.

Wolf DM, Vazirani VV, Arkin AP. Diversity in times of adversity: probabilistic strategies in microbial survival games. J Theor Biol. 2005;234(2):227–53.

Zee PC, Liu J, Velicer GJ. Pervasive, yet idiosyncratic, epistatic pleiotropy during adaptation in a behaviourally complex microbe. J Evol Biol. 2017;30(2):257–69.

Outlook

Experimental evolution is a powerful tool that allows researchers to manipulate one or a few variables and observe the effect during evolution (Kawecki et al. 2012). Microbes are particularly suited to these types of studies due to their short generation times, genetic manipulability and relative ease of handling (Kawecki et al. 2012). Experimental evolution using microbes can be used to understand a variety of phenomenon from the emergence of multicellularity (Ratcliff et al. 2012) to the evolution of antibiotic resistance (Chevereau et al. 2015). The importance of microbes in ecosystem functioning (Crowther et al. 2019) and human health (Belkaid and Hand 2014; Sanz-García et al. 2023) makes understanding how they adapt to changes in the environment of particular interest. In this thesis, I presented two experimental evolution experiments aimed at understanding the ways in which fitness increases can be gained during the aggregative multicellular development program of *Myxococcus xanthus*.

In the first chapter, I described an evolution experiment aimed at uncovering the strategies used to gain a relative fitness advantage during an aggregative multicellular form of cooperation. The results suggest that multiple strategies including cheating, facultative exploitation and increased intrinsic sporulation are frequently favored by selection during chimeric development. These results are complementary to a similar study of *Dictyostelium discoideum*, which also engages in aggregative multicellular cooperation, where cheating and facultative cheating mutants were favored during chimeric development (Santorelli et al. 2008). This agreement across different systems suggest that these mechanisms may be used by aggregative multicellular organism in general.

These results also raise the question of how common is cheating and exploitation in natural populations of *M. xanthus*? Studies characterizing clones isolated from a single fruiting body show variation in social traits, such as fruiting body formation and sporulation as well as

swarming, with some clones being proficient and others being defective (Kraemer and Velicer 2011). Some of the socially defective clones could be complemented by other clones isolated from the same fruiting body, however, none of the defective clones have been characterized as cheaters (Kraemer and Velicer 2014). More studies are needed to understand the role of social cheating in natural populations. Facultative exploitation may be common but can be easily overlooked due to the lack of an obvious group-level defect and the proficiency of facultative exploiters in pure culture (Santorelli et al. 2008).

We also isolated many clones with apparent fitness disadvantages during pairwise interactions with the cooperator suggesting that competition between mutant clones was also important in determining which genotypes rose in frequency. More experiments are needed to determine whether these developmental losers have a fitness advantage during chimeric development with other mutants from their respective evolved populations. If not, then it is likely that further selection cycles would have resulted in their purge from the population. The molecular mechanisms responsible for the evolved phenotypes are also of interest, therefore whole genome sequencing and transposon mapping followed by molecular verification of candidate loci will be an important next step.

Fitness asymmetries between interacting strains result in conflict (Velicer and Vos 2009). One mechanism that can help reduce social conflict is kin discrimination (Strassmann et al. 2011). The second chapter explored the potential role of TraA-mediated outermembrane exchange (OME) in generating colony merger incompatibilities (CMIs) during swarming and antagonisms during chimeric development. We found that interference competition during development and swarming as well as the generation of CMIs could not be explained by TraA-mediated toxin transfer among *M. xanthus* natural isolates. However, antagonisms during swarming were reduced in mixture with Type 6 Secretion System (T6SS) mutants. Overall, patterns of interference competition and inter-colony kin discrimination are complex and likely

multifactorial. Further work is needed to understand the adaptive benefit of exchanging large amounts of outermembrane material.

Fitness during multicellular development in *M. xanthus* is often considered in the context of spore production. However, both spores and viable rod cells (peripheral rods) have the potential to contribute to group-level fitness, although the benefits of producing viable non-spore cells has not been experimentally demonstrated. In the final chapter of this thesis, I investigated the potential for developmental cell-type partitioning to evolve in response to variation in the speed of nutrient replenishment after starvation initiation. Our results show that one cell type (spores) is favored when starvation times are longer, and another cell type (viable rods) is favored when starvation times are shorter. It therefore seems likely that that the presence of these two developmental cell types represent a bet-hedging strategy that evolved in response to an environment with unpredictable cycles of nutrient availability. This work along with theoretical studies in *D. discoideum* (Dubravcic et al. 2014; Tarnita et al. 2015) suggest that non-aggregating cell types are important fitness components of aggregative multicellular organisms in general.

References

Belkaid Y, Hand TW. Role of the Microbiota in Immunity and Inflammation. Cell. 2014;157(1):121–41.

Chevereau G, Dravecká M, Batur T, Guvenek A, Ayhan DH, Toprak E, et al. Quantifying the Determinants of Evolutionary Dynamics Leading to Drug Resistance. PLoS Biol. 2015;13(11):e1002299.

Crowther TW, Hoogen J van den, Wan J, Mayes MA, Keiser AD, Mo L, et al. The global soil community and its influence on biogeochemistry. Science. 2019;365(6455).

Dubravcic D, Baalen M van, Nizak C. An evolutionarily significant unicellular strategy in response to starvation in Dictyostelium social amoebae. F1000Res. 2014;3:133.

Kawecki TJ, Lenski RE, Ebert D, Hollis B, Olivieri I, Whitlock MC. Experimental evolution. Trends Ecol Evol. 2012;27(10):547–60.

Kraemer SA, Velicer GJ. Endemic social diversity within natural kin groups of a cooperative bacterium. Proc National Acad Sci USA. 2011;108(supplement_2):10823–30.

Kraemer SA, Velicer GJ. Social complementation and growth advantages promote socially defective bacterial isolates. Proc Biol Sci. 2014;281(1781):20140036.

Ratcliff WC, Denison RF, Borrello M, Travisano M. Experimental evolution of multicellularity. Proc Natl Acad Sci USA. 2012;109(5):1595–600.

Santorelli LA, Thompson CRL, Villegas E, Svetz J, Dinh C, Parikh A, et al. Facultative cheater mutants reveal the genetic complexity of cooperation in social amoebae. Nature. 2008;451(7182):1107–10.

Sanz-García F, Gil-Gil T, Laborda P, Blanco P, Ochoa-Sánchez LE, Baquero F, et al. Translating eco-evolutionary biology into therapy to tackle antibiotic resistance. Nat Rev Microbiol. 2023;21(10):671–85.

Strassmann JE, Gilbert OM, Queller DC. Kin Discrimination and Cooperation in Microbes. Annu Rev Microbiol. 2011;65(1):349–67.

Tarnita CE, Washburne A, Martinez-Garcia R, Sgro AE, Levin SA. Fitness tradeoffs between spores and nonaggregating cells can explain the coexistence of diverse genotypes in cellular slime molds. Proc Natl Acad Sci USA. 2015;112(9):2776–81.

Velicer GJ, Vos M. Sociobiology of the Myxobacteria. Annu Rev Microbiol. 2009;63(1):599–623.